LEE, Fu Chu, 1932-
RADIATIVE HEAT TRANSFER IN AN EMITTING ABSORBING AND SCATTERING BOUNDARY LAYER.

The University of Oklahoma, Ph.D., 1967
Engineering, mechanical

University Microfilms, Inc., Ann Arbor, Michigan

THE UNIVERSITY OF OKLAHOMA

GRADUATE COLLEGE

RADIATIVE HEAT TRANSFER IN AN EMITTING ABSORBING AND SCATTERING BOUNDARY LAYER

A DISSERTATION

SUBMITTED TO THE GRADUATE FACULTY

in partial fulfillment of the requirements for the

degree of

DOCTOR OF PHILOSOPHY

BY

FU CHU LEE

Norman, Oklahoma

1967

RADIATIVE HEAT TRANSFER IN AN EMITTING

ABSORBING AND SCATTERING BOUNDARY LAYER

APPROVED BY

DISSERTATION COMMITTEE

ACKNOWLEDGEMENT

The author would like to express his deep appreciation to Dr. Tom J. Love, Jr., Director of the Department of Aerospace and Mechanical Engineering for his inspiration and guidance throughout the progress of this study. The other members of the Doctoral Committee who gave their time and advice also have the writer's appreciation and thanks.

The research was sponsored by Aerospace Research Laboratories, United States Air Force (Contract AF 33(657)8859). This financial support is gratefully acknowledged.

The writer wants, also, to acknowledge all the help offered by the Computer Laboratory of the University of Oklahoma. Their cooperation in granting access to the Osage Computer saved much time in the development of the computer programs for this study.

Finally, the author wishes to thank his family, especially his wife Diana, for her limitless patience and constant encouragement which made this work possible.

ABSTRACT

The effect of scattering on radiant heat transfer is considered. The basic model utilized is the radiant heat transfer between two diffusely reflecting and emitting plane walls with an isothermal separating medium which scatters, absorbs and emits thermal energy. The Gaussian Quadrature Formula is used for integral terms, and the integrodifferential equation of transfer is thus reduced to a system of linear differential equations. As a result, a set of dimensionless parameters which are continuous functions of optical depth and are independent of temperature, may be obtained for isothermal media. These parameters may be used for radiant heat transfer calculations.

Experimental scattering functions for aluminum, iron, carbon, silica and glass were reduced to a discrete form corresponding to Gaussian Quadrature coordinates of a third order approximation. Through the comparison of dimensionless parameters, it was concluded that the data computed from isotropic scattering, may be utilized for radiant heat transfer prediction for real media.

The problem of coupled radiation and convection in boundary layer flow over a flat plate was formulated. The fluid was an emitting, absorbing and scattering medium. The plate was assumed to be nongrey and diffusely reflecting and emitting. The properties of the medium are assumed constant. The approximate Pohlhausen technique was used for the boundary layer computations. The solutions for both radiant flux and conductive flux were obtained.

Solutions for a non-radiating medium and for a non-scattering medium were also obtained. Comparisons of the results were made for all media. The effect of wall reflectance on the heat transfer was studied. Results are presented in graphic form. The computer programs for this study are also listed.

TABLE OF CONTENTS

LIST OF TABLES

TABLE OF ILLUSTRATIONS

RADIATIVE HEAT TRANSFER IN AN EMITTING ABSORBING AND SCATTERING BOUNDARY LAYER

CHAPTER I

INTRODUCTION

The study of radiative heat transfer has been stimulated by modern technological developments such as the study of the earth environment, high speed atmospheric flight, space flight and the development of high temperature energy sources. Also, the availability of high speed computers now makes it possible to perform complicated calculations required for detailed analyses.

The present study is concerned with radiative heat transfer in plane parallel emitting, absorbing and scattering media[1] such as semi-transparent solids or mixtures of gas and solid particles.

The radiant heat transfer within an emitting and absorbing medium has been studied by astrophysicists for quite a number of years. Engineering's early interest in the subject involved furnace studies where high temperatures

[1]The terms emitting, absorbing and scattering will be abbreviated collectively by EAS throughout remainder of this work.

could be reached and where the dust and ash caused the gaseous medium to absorb thermal radiation. A semi-transparent medium may scatter energy due to local inhomogeneities. In such a scattering medium the energy is deflected from its original direction and its intensity may be changed. Scattering may consist of reflection, refraction and diffraction. Scattering media may be found in liquid particles suspended in the atmosphere, in solid fuel rocket exhausts, in fluidized beds, in ablative cooling of space vehicles, etc. Energy which is scattered, may have a different wavelength than the incident energy. If the scattered energy has the same wavelength as the incident energy the scattering is called coherent.

The nature of the scattering depends on conditions of the inhomogeneous particles such as shape, size, refractive index and the relative position of the particles. The distance between particles effects scattering. If the scattering is done by a single particle it is called single scattering. If, in a volume element, relatively few particles exist, it may be treated as a single scattering medium with the scattered energy being directly proportional to the number of particles. If the number of particles is increased in such a volume the energy scattered by each particle is also influenced by the other particles, hence multiple scattering must be taken into account. If the radiation is scattered by particles much smaller than the wavelength of the radiation, it is called Rayleigh scattering. Van de Hulst (1) discusses Mie scattering by small spherical particles in detail and presents a review of the research in this field. Love (2,3,4) reviews the works involving scattering in heat transfer prior to 1962.

Thermal radiation between parallel plates separated by an absorbing-emitting non-isothermal gas was considered by Usiskin and Sparrow (5), who utilized numerical integration to solve the integral equation. Deissler (6) used temperature jump boundary conditions at the surfaces and the diffusion approximation for the radiation in the gas to solve the same problem. A Monte Carlo solution has been obtained for the same problem by Howell and Perlmuter (7). They also solved the radiant transfer through a grey gas between concentric cylinders of infinite length by the Monte Carlo method (8).

In "Radiative Transfer", Chandrasekhar (9) reduced an integro-differential equation to a set of simultaneous differential equations by using a Gaussian Quadrature method. Love (2) utilized the Gaussian Quadrature Formula to reduce the equation of transfer for the same problem with an isothermal medium to a set of simultaneous, linear, nonhomogeneous first order differential equations. He solved these simultaneous equations by solving the matrix of the coefficients. The Gaussian Quadrature method gives good accuracy with a small number of ordinates. Consequently, the size of the matrix is reduced. Hsia (10) solved the same problem in non-isothermal media. He considered both linear and parabolic temperature profiles. One of the conclusions in reference (10) was that the heat transfer with a linear temperature distribution could be predicted by assuming an isothermal medium with a temperature equal to the average of the wall temperatures. This conclusion was utilized in this work.

In the above mentioned literature only the radiant mode of energy transfer was considered. In most practical cases the other modes of heat transfer may take place at the same time. A number of studies have been done recently of "coupled" or simultaneous heat transfer problems. Applications are found in gas-cooled nuclear reactors, chemical rockets, fluidized beds and ablative cooling of space vehicles. Cess (11) presents a good review of this field of heat transfer.

Goulard and Goulard (12) in one of the early studies extended the equations of one-dimensional radiative energy transfer to include the wall effect. An application was made to a steady low-speed high-temperature boundary layer flow over a flat plate. The optically thin approximation for the boundary layer was used to simplify the problem. An iteration method was used for the solution. Viskanta and Grosh (13) considered the problem of simultaneous conduction and radiation in a one-dimensional system consisting of two diffuse, non-black, infinite isothermal parallel plates separated by a finite space filled with an absorbing and emitting medium. In their study the non-linear integro-differential equation of transfer was reduced to a nonlinear integral equation. Again an iteration method was applied to obtain numerical results.

Lick (15) also studied the transfer of energy by simultaneous conduction and radiation. The exponential kernel approximation was used. Because too many parameters were involved, alternate numerical approximations were developed by Lick. These were an optically thick approximation for optical thickness larger than unity, a truncated power series solution and a singular perturbation solution.

Many works have also been done for a participating flowing medium in which the convective mode of transfer is coupled with thermal radiation. In some cases all three heat transfer modes were combined. Effects of the radiant transfer interaction with the other modes were investigated. External flow and boundary layer flow for absorbing media were presented by Cess (16), Sidorov (17), Koh and Desilva (18).

As has been mentioned, due to the radiation terms, the energy equation becomes an integro-differential equation and does not have a ready solution. Some of the works solve this integro-differential energy equation exactly but introduce assumptions for simplification. Others solved it by using approximate methods along with simplifications. Optically thin and optically thick approximations were used for radiant terms in the energy equation. The temperature distribution between boundary surfaces was the usual object sought. If the temperature difference between the plates or across the boundary layer is not great, a linearized function of temperature is usually applied. Other methods such as radiation slip solution, exponential kernel solution and series solution were utilized. Cess (16) studied the radiation effects upon boundary layer flow of an absorbing gas. He assumed that thermal conduction within the fluid took place only in a thin thermal boundary layer adjacent to the plate. This layer is so thin optically that radiant energy will suffer almost no attenuation in traversing it. An additional layer adjacent to it is optically thick and is called the radiation layer. In the radiation layer the temperature gradient is small and the conduction effects may be neglected. If the temperature profile could be determined in the optically thin layer, then the temperature at the edge of the boundary layer, also considered as the temperature of the radiation layer, could be known. Cess noted that there was a direct analogy between the present radiation problem and a velocity boundary layer, with the radiation layer corresponding to the potential flow outside of the velocity boundary layer.

Substantially different results were obtained in his study for the grey and non-grey medium assumptions. Because of the tedious work required to solve the problem for the optically thin case, only a first order interaction effect between convection and radiation was considered.

Oliver and McFadden (19) studied the same problem but achieved a third order approximation of the interaction effects by starting with non-interacting radiation to obtain a first approximation of temperature profile. They then used this temperature profile for second and subsequently third order approximations. Taitel and Hartnell (20) investigated the equilibrium temperature in a boundary layer flow of an absorbing and emitting gas over a flat plate. In their work the optically thin assumption was used for areas near the leading edge of the plate and the optically thick approximations for the downstream area. These cases are governed by pre-determined values of the radiation-conduction interaction parameters.

The effects of grey radiation and non-grey radiation on boundary layers at low Eckert number were studied by Smith and Hassan (21). It was found that non-grey convective heat flux was greater than grey convective heat flux while the reverse was true for radiative heat flux. The total non-grey heat flux was greater than the total grey heat flux for low wall emittance while the reverse was true for the higher wall emittance.

The above review covers some of the recent works of radiative heat transfer coupled with the conductive and/or convective modes of heat transfer. In the field of flowing media, most investigations were made only for absorbing media. The scattering effect was excluded in most cases. Chen (42) mentioned in his finding of a slug flow of EAS medium that the effects of radiative scattering may be more important than that of radiant absorption and emission.

The present work has been divided into two parts:

(1). A study of the experimental scattering function (definition will be presented later) and the calculation of dimensionless parameters.

In this study, the method of dimensionless parameters developed by Love (2) was utilized for radiant heat transfer computations. Scattering functions are required before the dimensionless parameter can be computed. Wheasler (29) and Beattie (30) measured scattering functions experimentally. Beattie's data were used for this work. These data have to be transformed by numerical integration to a specific form. The dimensionless parameters M, N and Q are independent of temperature. A comparison of data was made between the results using isotropic scattering and using the experimentally determined scattering functions. It was concluded that the isotropic approximation may be used to predict radiant heat transfer for most engineering purposes.

(2). The heat transfer problem of simultaneous convection and radiation in the boundary layer flow of an EAS medium over a flat plate was studied. The plate is considered diffusely reflecting and the edge of thermal boundary is assumed to be a black surface. The medium is assumed to have constant properties. This is an ideal approach, especially at higher temperatures. Hence the results should only be considered as qualitative solutions.

The Pohlhausen technique was used to treat the temperature and the velocity profiles in the energy equation. For the radiant heat flux prediction, a linear temperature distribution was assumed. The energy equation was iterated numerically over the thickness of thermal boundary layer, δ_t using a digital computer. The results are in terms of radiative heat flux, conductive heat flux and the ratio of the two. The thermal boundary layer thickness and the velocity boundary layer thickness are also presented.

The following cases were studied:

i). Thermal radiation involving an EAS medium.

ii). Thermal radiation involving an absorbing and emitting but non-scattering medium.

iii). No radiation terms involved.

CHAPTER II

A REVIEW OF THE ANALYSIS OF THE DIMENSIONLESS PARAMETERS SOLUTION OF RADIANT HEAT TRANSFER

The problem is to determine the radiant heat transfer between two infinite parallel and diffusely reflecting walls separated by EAS media. The physical model is shown in Figure 1. The walls are isothermal but at different temperatures and may have different reflectances. The medium is stationary and is assumed to have a constant temperature, T_a. The medium contains particles which scatter thermal radiation. If the temperature of wall 1, T_1, is greater than the temperature of wall 2, T_2, then the net heat flux from wall 1 is the result sought.

The intensity of a pencil of rays traversing an EAS medium will be diminished according to the distance traversed. This attenuation of the ray is called extinction and includes scattering and absorption by the mass encountered.

The transfer equation has to be established for the above conditions. Beer's law says that when a ray of light or energy traverses such a medium, the rate of reduction of the intensity along this ray is proportional to the local intensity. In the EAS medium, the local intensity

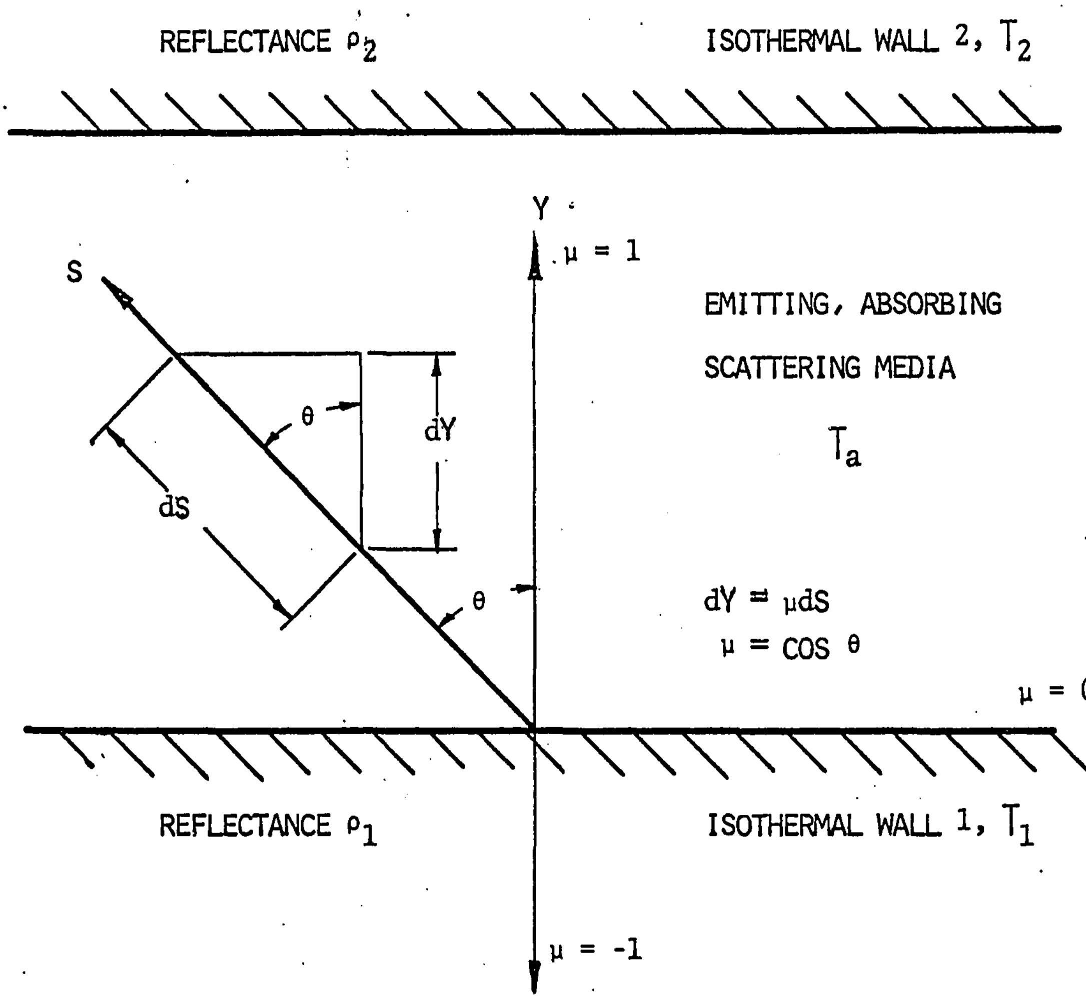

COORDINATE SCHEME FOR AXIALLY SYMMETRIC SYSTEM

Figure 1

is also enforced by energy scattered into the direction of this ray and by the energy emitted into this direction from the particles. The equation would be as follows:

$$\frac{dI_\nu(s)}{ds} = -\rho\beta_\nu I_\nu + J_{\nu,s} + J_{\nu,e} \qquad (1)$$

where I_ν = monochromatic intensity of radiation at any point along the ray. The subscript ν denotes frequency.

β_ν = monochromatic mass extinction coefficient.

ρ = mass of the scattering matter per unit volume of the mixture.

The terms on the right hand side of the equation are explained as follows:

(1). $-\rho\beta_\nu I_\nu$: β_ν, the monochromatic mass extinction coefficient, consists of two parts: $\beta_\nu = \kappa_\nu + \sigma_\nu$. κ_ν is the absorption coefficient and σ_ν is the scattering coefficient. Both are factors in the attenuation of the intensity of the ray of energy. β_ν has dimensions of ft^2/lb_m. The negative sign indicates decreasing intensity in the positive direction of s.

(2). $J_{\nu,s}$ represents the strength of the energy added to the direction s by scattering. According to reference (2)

$$J_{\nu,s}(\mu,\phi) = \frac{\rho}{4\pi} \int_0^{2\pi} \int_0^1 I_\nu(\mu',\phi') S_\nu^*(\mu',\phi';\mu,\phi)\, d\mu' d\phi' \qquad (2)$$

where $I(\mu',\phi')$ is the intensity of the incident ray, μ is the cosine value of polar angle θ, $\mu = \cos\theta$, ϕ is the azimuthal angle, $S^*_\nu(\mu',\phi',\mu,\phi)$ is the monochromatic scattering function which relates the scattering effect to the intensity of the incident rays. $J_{\nu,s}$ may be looked upon as the fraction of energy incident on a differential element of mass from all the directions which is scattered into the solid angle $d\mu d\phi$.

(3). $J_{\nu,e}$ represents an addition of intensity along the same ray by emission of the mass. Its mathematical form would be

$$J_{\nu,e} = \rho\kappa_\nu I_{b\nu}(T) \tag{3}$$

Hence equation (1) may be rewritten as:

$$\frac{dI_\nu(S)}{ds} = -\rho\beta_\nu I_\nu(S) + \frac{\rho}{4\pi}\int_0^{2\pi}\int_0^1 I_\nu(\mu',\theta')S^*_\nu(\mu',\phi';\mu,\phi)d\mu' d\phi' + \rho\kappa_\nu I_{b\nu}(T) \tag{4}$$

To simplify equation (4), the following definitions should be noted:

(1). The normalized scattering function would be

$$S_\nu(\mu',\phi';\mu,\phi) = \frac{S^*_\nu(\mu',\phi';\mu,\phi)}{\sigma_\nu} \tag{5}$$

where σ_ν is the monochromatic mass scattering coefficient of the isotropic medium.

$$\sigma_\nu = \frac{1}{4\pi}\int_0^{2\pi}\int_0^1 S^*_\nu(\mu',\phi';\mu,\phi)d\mu' d\phi' \tag{6}$$

(2). Referring to Figure 1, the optical depth or optical thickness is defined as

$$\tau = \int_0^y \rho \beta_\nu dy \tag{7}$$

(3). Axially symmetric in this investigation is defined as independence from azimuthal angle. In other words, around a normal direction, there is no change of radiative properties if θ, the polar angle, is the same.

With the above definitions, equation (4) becomes

$$\mu \frac{dI(\tau,\mu)}{d\tau} = - I_\nu(\tau,\mu) + \frac{\sigma_\nu}{4\pi\beta_\nu} \int_{-1}^{+1} I_\nu(\tau,\mu) \int_0^{2\pi} S(\theta_{ij}) d\mu' d\phi' + \frac{\kappa_\nu}{\beta_\nu} I_{bb,\nu}(\tau) \tag{8}$$

where Θ_{ij} is the angle between the incident and leaving rays, $S(\Theta_{ij})$ is the axially symmetric scattering function of the medium. $S(\Theta_{ij})$ may be written in terms of μ_i and μ_j the cosine values of the incident and leaving angles respectively. The final equation of transfer is written as follows:

$$\mu \frac{dI(\mu,\tau)}{d\tau} = - I(\mu,\tau) + \frac{\sigma}{2\beta} \int_{-1}^{+1} I(\mu,\tau) S(\mu_i,\mu_j) d\mu' + \frac{\kappa}{\beta} I_{bb,\nu}(\tau) \tag{9}$$

It should be noted here that the intensity, $I(\mu,\tau)$, within a medium is contributed by the radiation from both the positive direction and the negative direction. Hence the equation of transfer could be written as two separate equations:

$$+\mu \frac{dI^{+}(\mu,\tau)}{d\tau} = -I^{+}(\mu,\tau) + \frac{\sigma}{2\beta}\int_0^1 [\, I^{+}(\mu',\tau)S(+\mu,+\mu') +$$

$$I^{-}(\mu',\tau)S(+\mu,-\mu')]d\mu' + \frac{\kappa}{\beta} I_{bb,\nu}(\tau)$$

$$-\mu \frac{dI^{-}(\mu,\tau)}{d\tau} = -I^{-}(\mu,\tau) + \frac{\sigma}{2\beta}\int_0^1 [\, I^{+}(\mu',\tau)S(-\mu,+\mu') +$$

$$I^{-}(\mu',\tau)S(-\mu,+\mu')]d\mu' + \frac{\kappa}{\beta} I_{bb,\nu}(\tau) \qquad (10)$$

The above equations (10) are integro-differential equations. Usually they are not easily solved. Various methods of solution were studied. Kunz (22), Scarbrough (23) and Hildebrand (24) among others have good discussions of this subject. Pai (25) summerized various methods of solution in his thermal radiation field. Chandrasehkar (9) and Love (2,3,4) used a numerical quadrature formula to take the place of the integral in the equation of transfer. Following Love's analysis in which the Gaussian Quadrature Formula was used, equation (10) becomes

$$+\mu_i \frac{dI(\tau,+\mu_i)}{d\tau} = -I(\tau,+\mu_i) + \frac{\sigma}{2\beta}\sum_{j=1}^{n} a_j S(+\mu_i,+\mu_j)I(\tau,+\mu_j)$$

$$+\frac{\sigma}{2\beta}\sum_{j=1}^{n} a_j S(+\mu_i,-\mu_j)I(\tau,-\mu_j) + \frac{\kappa}{\beta} I_{bb,\nu}(\tau) \qquad (11)$$

$$-\mu_i \frac{dI(\tau,-\mu_i)}{d\tau} = -I(\tau,-\mu_i) + \frac{\sigma}{2\beta}\sum_{j=1}^{n} a_j S(-\mu_i,+\mu_j) I(\tau,+\mu_j)$$

$$+ \frac{\sigma}{2\beta}\sum_{j=1}^{n} a_j S(-\mu_i,-\mu_j) I(\tau,-\mu_j) + \frac{\kappa}{\beta} I_{bb,\nu}(\tau) \qquad (11)$$

The above equations (11) are 2n simultaneous equations. These simultaneous equations in matrix form would be

$$\frac{dI_\nu^*(\mu,\tau)}{d\tau} - M^* I_\nu^*(\mu,\tau) = \frac{\kappa}{\beta} I_{bb,\nu}(T(\tau))\left(\frac{1}{\mu}\right)^*. \qquad (12)$$

where n = 1,2,....n and also n = -1,-2,...-n. The development of equation (12) could be found in reference (10). The superscript * indicates a matrix. $T(\tau)$ is the temperature profile. Love (2,3,4) solved these simultaneous equations for isothermal medium.

$$I(\tau,+\mu_i) = \sum_{\alpha=1}^{2n} C_\alpha X_{i,\alpha} e^{\gamma_\alpha,\tau} + I_{bb,\nu}(T_a)$$

$$(13)$$

$$I(\tau,-\mu_i) = \sum_{\alpha=1}^{2n} C_\alpha X_{(i+n),\alpha} e^{\gamma_\alpha,\tau} + I_{bb,\nu}(T_a)$$

where the γ_α are eigenvalues of the coefficient matrix, the X's are the eigenvectors corresponding to each eigenvalue and the C_α's are the constants which would be determined by the given boundary conditions. In the problem of the plane-parallel diffuse walls the boundary conditions would be

$$I^{+}(0,\mu_i) = (1-\rho_1)I_{bb,\nu}(T_1) + 2\rho_1 \sum_{j=1}^{n} a_j\mu_j I^{-}(0,\mu_j)$$

$$I^{-}(\tau_o,\mu_i) = (1-\rho_2)I_{bb,\nu}(T_2) + 2\rho_2 \sum_{j=1}^{n} a_j\mu_j I^{+}(\tau,\mu_j) \tag{14}$$

Substituting equation (14) into equation (13) and collecting terms, the constant C_α may be determined. It was found that the C_α are linear combinations of $I_{bb,\nu}(T_1)$, $I_{bb,\nu}(T_2)$ and $I_{bb,\nu}(T_a)$. In this way the intensity of the medium is finally determined.

With the intensity just obtained in the direction of the specified ordinates of the quadrature formula, the net monochromatic flux may be determined, since

$$F_{net,\nu}(\tau_1) = 2\pi \int_{-1}^{+1} \mu I(\tau,\mu)d\mu \tag{15}$$

Utilizing the quadrature formula again and re-arranging the terms, one has

$$F_{net,\nu}(\tau_1) = MI_{bb,\nu}(T_1) - NI_{bb,\nu}(T_2) - QI_{bb,\nu}(T_a) \tag{16}$$

where M, N and Q are dimensionless parameters and are independent of all the temperatures. These dimensionless parameters are continuous functions of optical depth and vary with wall emittances.

$I_{bb,\nu}(\tau)$ is Plank's function.

$$I_{bb,\nu}(\tau) = \frac{2h\nu^3[\exp(-\frac{h\nu}{KT})]}{C^2[1 - \exp(-\frac{h\nu}{KT})]} \tag{17}$$

Hence $F_\nu(\tau_1)$ must be integrated over all wavelengths to obtain an equation for total heat transfer. This equation is

$$q_{net} = \int_0^\infty F_\nu d\nu \tag{18}$$

Utilizing the Reiz quadrature the final expression for the net heat transfer at τ_1 is formulated as follows:

$$q_{net} = (10^{-11}) \; [T_1^4 \sum_{j=1}^{n} A_j M_j - T_2^4 \sum_{j=1}^{n} A_j N_j - T_a^4 \sum_{j=1}^{n} A_j Q_j] \tag{19}$$

where

$$A_j = \frac{2k^4 a_j (\frac{\nu h}{KT})^3}{h^3 C^2 (1 - \exp(-\frac{\nu h}{KT}))}$$

The A_j need be calculated only once for a given order of approximation of Reiz Quadrature. For the fifth order approximation, the A_j's are:

$$A_1 = 0.347 \quad Btu\text{-}hr^{-1}\text{-}ft^{-2}\text{-}R^{-4}$$

$$A_2 = 12.460$$

$$A_3 = 30.420$$

$$A_4 = 10.780$$

$$A_5 = 0.396.$$

CHAPTER III

THE SCATTERING FUNCTION

In the previous chapters the term scattering function, $S(\theta,\phi;\theta',\phi')$, was mentioned. Scattering function relates the intensity of the scattered energy at a certain direction (θ,ϕ) to the intensities of all the incident directions on an element of mass. The scattering function used here is a normalized function corresponding to the case of pure scattering. In the calculation of the transfer equation, the scattering function should be known before hand. Many works have been done in the effort to find scattering properties of particles, but most are in the fields of astrophysics and optics. The interest of thermal scattering has been raised only in recent years. This is due to the lack of information of scattering particles and due to the difficult mathematics involved. A good review of this subject is presented by Love (2) and by Wheasler (29). The electromagnetic wave theory of the angular distribution of the intensity of light scattered by single small isotropic spherical particles was carried out by Gustav Mie. Chu, Clark and Churchill (28) extended Mie's work by computing the angular distribution coefficients, a_n, for different particle size parameters and refractive indexes.

Using these coefficients to expand a Lagendre polynomial, the scattering function can be obtained. For engineering applications of this kind, one may not expect that the particles are in perfect spherical shape with a uniform size or are distributed evenly. Most practical cases involve a distribution of size and shape of particles. Mathematically speaking, even with simplification, it is very difficult to find a solution and the results may not be accurate, for there is no practical way to describe the size, shape and refractive index etc. of the real particles. Because of these difficulties, Love (2) suggested that the scattering function be determined experimentally for the real particles. Wheasler (29) and Beattie (30) developed the apparatus and performed the experiments. Details of the design and the experimental methods used will not be mentioned here. The general principles for this experiment are listed below:

(1). Sample medium should contact the radiative thermal energy directly in order to avoid reflective and refractive effect of the particle container.

(2). Heat source was a "glow bar" which radiated energy.

(3). A monochromator was used to detect scattered radiation.

(4). The extinction coefficients should be measured directly by determining the decrease of intensity of radiation as it traverses a known depth of mass.

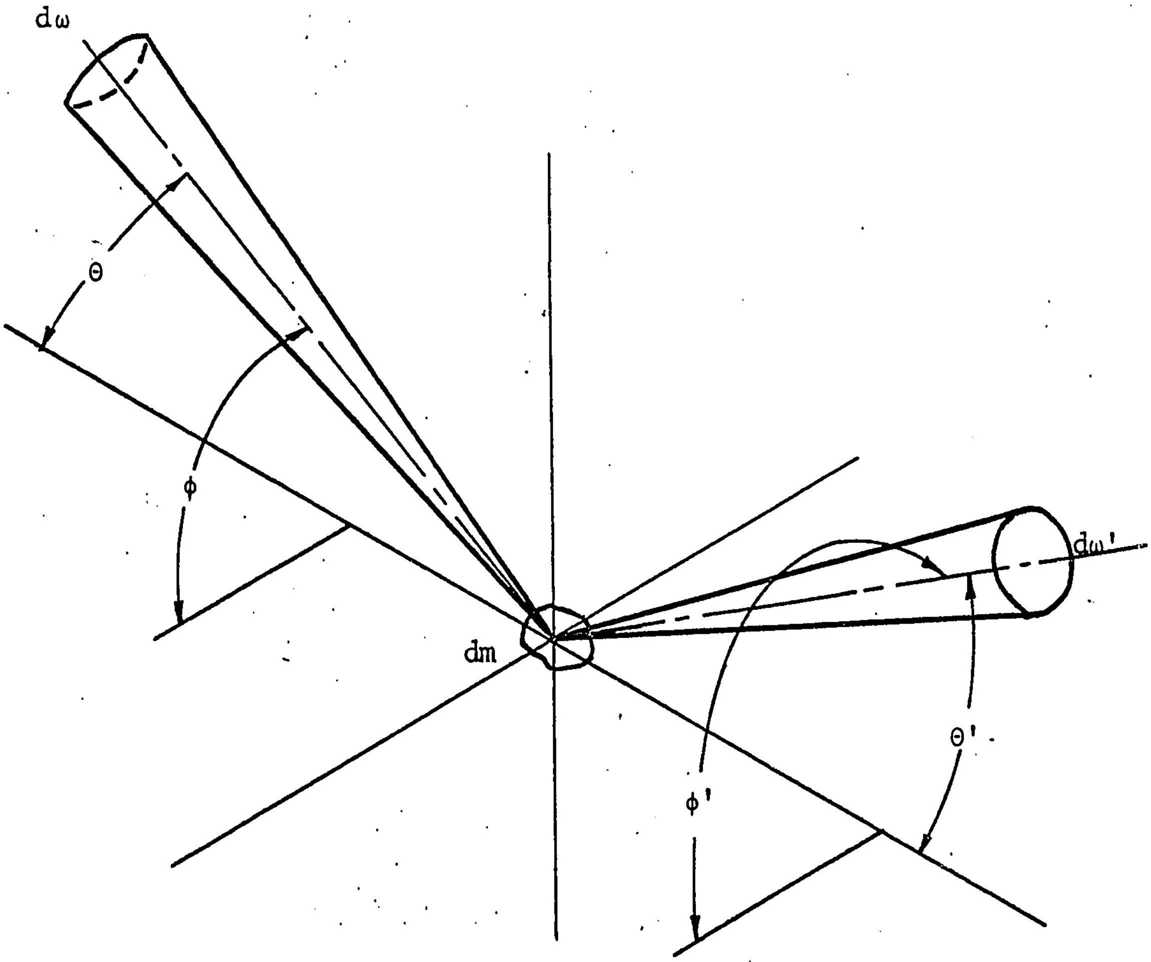

COORDINATE SCHEME FOR SCATTERING FUNCTION

Figure 2.

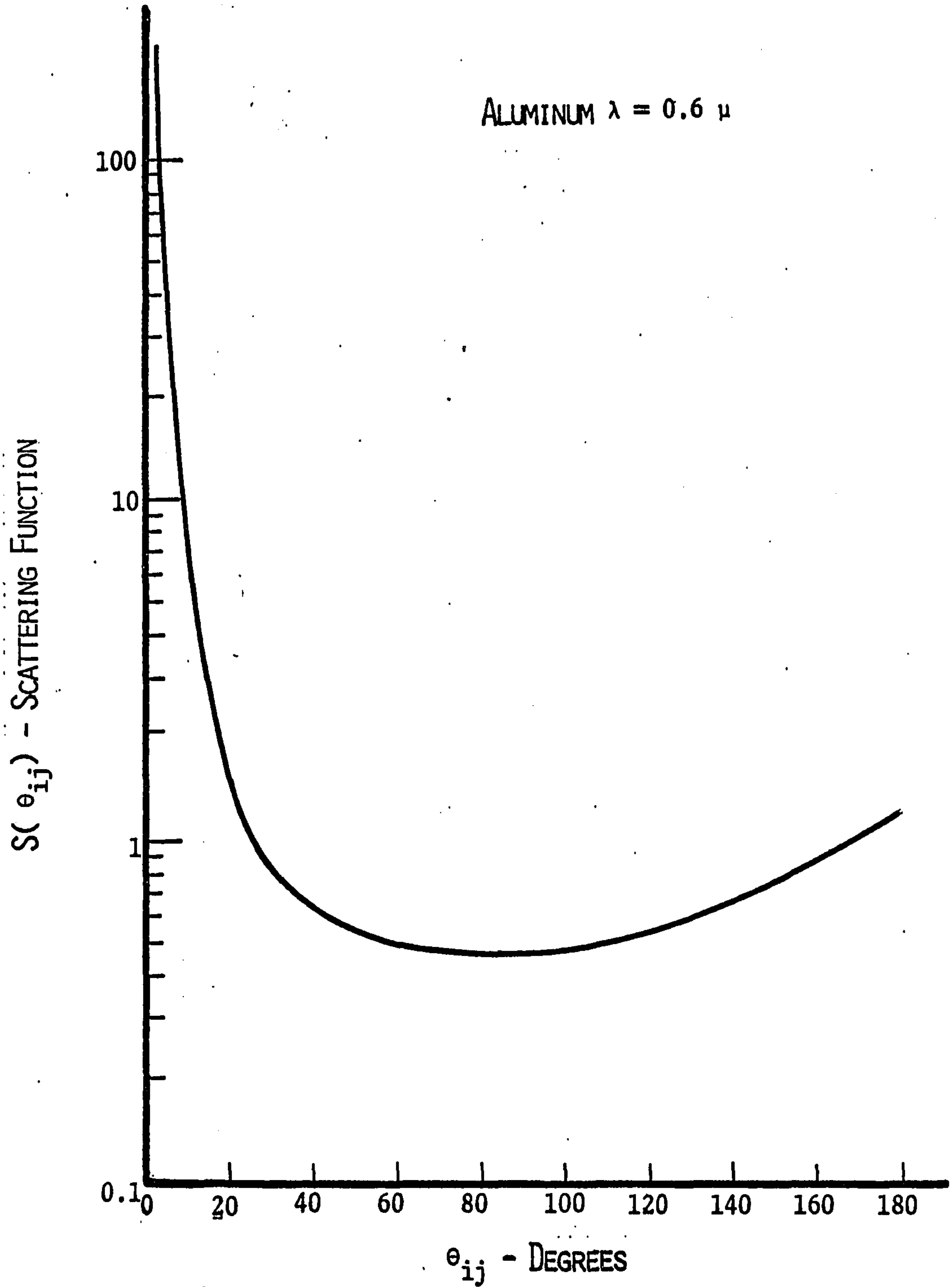

Figure 3 Angular Distribution of Scattering Function Experimental Data

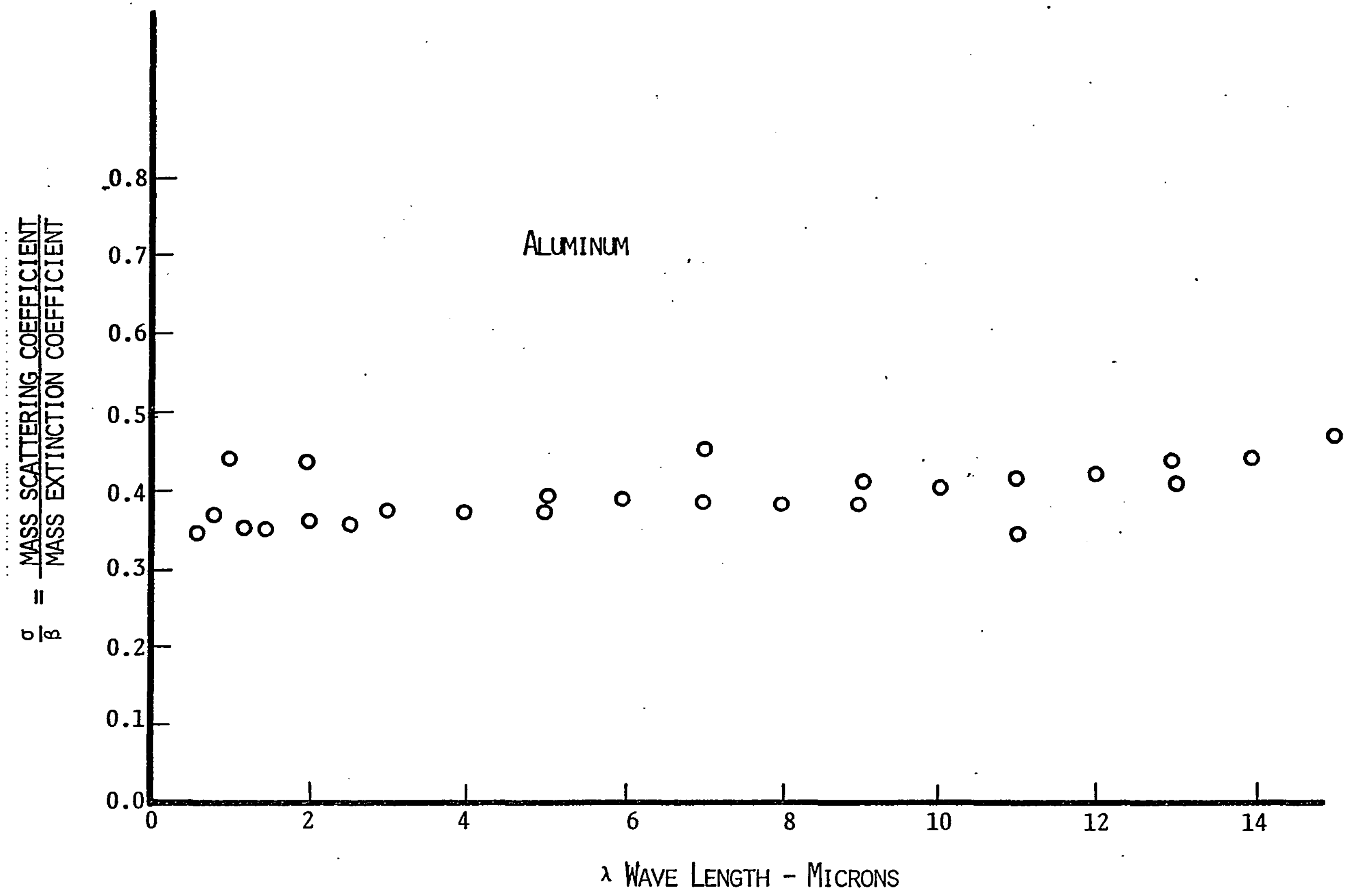

Figure 4 Variation σ/β with wave length

(5). The ratio of scattered radiation to the incident intensity as a function of wavelength was measured at discrete angles.

Wheasler (29) performed this experiment in 1964. Beattie (30) used a different particle generator and a different energy source for shorter wavelengths, and measured the scattering as a function of Θ_{ij}, the angle between the incident ray and the scattered rays. Love and Beattie (30) have presented the measurements of clouds of aluminum, carbonyl iron, glass, carbon and silica particles. Figure 3 presents a typical plot of such scattering functions. Also Figure 4 represents a typical plot of $\frac{\sigma}{\beta}$ verses wavelength, λ, for the tested materials.

In the final equation of transfer, $S(\mu_i, \mu_j)$ was used for the scattering function where μ_i and μ_j are the cosines of the polar angles of the incident ray and the scattered ray respectively. The relation between $S(\Theta_{ij})$ and $S(\mu_i, \mu_j)$ may be written as

$$S(\mu_i, \mu_j) = \frac{1}{2\pi} \int_0^{2\pi} S(\Theta_{ij}) d\phi \qquad (20)$$

where ϕ is azimuthal angle.

According to solid geometry

$$\cos(\Theta_{ij}) = \mu_i \mu_j + (1 - \mu_i^2)^{1/2} (1 - \mu_j^2)^{1/2} \cos \Delta\phi \quad (21)$$

Equation (21) has been evaluated in this work with an increment of 10 degrees for the azimuthal angle ($\phi - \phi' = 10^{\circ}$). Θ_{ij} was then calculated by using the third order Gaussian Quadrature. A Fortran language program (Appendix A) was used to perform the calculation. One may notice that the increment of the azimuthal angle ϕ is arbitrarily decided. It is obvious that a smaller increment will give more points of Θ_{ij} which in turn will provide more points of $S(\Theta_{ij})$ to be used for the integration in equation (20). Table 1 in Appendix A shows the value of Θ_{ij} corresponding to each μ_i, μ_j.

After the values of Θ_{ij} were calculated, the values of $S(\Theta_{ij})$ were sought. Data from Beattie's experimental results were used. Since the experimental data were taken only at twenty-six fixed Θ_{ij} angles and the calculated Θ_{ij} could be any angle value between 0° and 180°, the values of $S(\theta_{ij})$ have to be read from the $S(\Theta_{ij})$ - Θ_{ij} curves accordingly. For a third order Gaussian quadrature approximation, there are eighteen sets of $S(\mu_i, \mu_j)$ needed for each wavelength. But according to the rule of symmetry, that $S(\mu_i, \mu_j) = S(\mu_j, \mu_i)$, these eighteen sets of Θ_{ij} values will be reduced to twelve sets. This means for each wavelength the $S(\Theta_{ij})$ - Θ_{ij} curve was read twelve times. Each time nineteen points were taken. The following curves were read:

MATERIAL	WAVELENGTH (in micron)
Aluminum	0.6, 0.7, 0.8, 0.9, 1.0, 1.2, 1.4, 2.1, 2.5, 3.0, 4.0, 5.0, 6.0, 7.0, 8.0, 10.0 12.0, 13.0, 14,0, 15.0
Carbon	1.0, 3.0, 4.0, 10.0, 12.0
Glass	0.8, 1.0, 2.5, 4.0, 7.0, 8.0, 10.0, 11.0
Iron	0.6, 1.0, 3.0, 4.0, 5.0, 8.0, 10.0, 12.0 14.0
Silica	0.7, 1.0, 4.0, 6.0, 9.0, 10.0, 11.0, 13.0

It should be noted that only positive directions of μ_i need be considered since the Hemholtz reciprocity law is valid, i.e.

$$S(+\mu,+\mu') = S(-\mu,-\mu')$$

$$S(+\mu,-\mu') = S(-\mu,+\mu') \tag{22}$$

Then

$$S(\mu_i,\mu_j) = \frac{1}{\pi} \int_0^{\pi} S(\Theta_{ij})d\phi \tag{23}$$

To evaluate the $S(\mu_i,\mu_j)$ for a corresponding set of $S(\Theta_{ij})$ equation (23) was integrated by using the trapezoidal rule.

$$S(\mu_i,\mu_j) = \frac{10}{2\pi \times 57.3} [S(\Theta_{ij})_1 + 2 [S(\Theta_{ij})_2 + S(\Theta_{ij})_3 + \; . \; . \; . \; . \; . + S(\Theta_{ij})_{n-1}] + S(\Theta_{ij})_n] \qquad (24)$$

For a ten degree increment of azimuthal angle, ϕ, and third order approximation, nineteen Θ_{ij} for each $S(\mu_i,\mu_j)$ are needed, i.e. here n = 19.

One note should be made here, it was mentioned by Wheasler (29) and Beattie (30) that the experimental data of $S(\Theta_{ij})$ were not dependable when Θ_{ij} was close to either 0^o or 180^o. This is due to the difficulties of the physical limitation of the apparatus design and strong forward scattering ($\Theta_{ij} = 0^o$), that is the steep gradient in the region of $\Theta_{ij} = 0^o$ to 20^o. Figure 3 showed this condition. For this reason the data of $S(\Theta_{ij})$ at $\Theta_{ij} = 8^o$ were used for those at Θ_{ij} less than 8^o. A maximum value of $S(\Theta_{ij}) = 50$ was imposed on for these angles. This maximum value was chosen, since it was close to the theoretical value.

If absorption is absent, an integration of scattered flux must equal the incident flux, that is

$$1/2 \int_{-1}^{1} S(\mu,\mu')d\mu' = 1 \qquad (25)$$

or it may be written as

$$1/2 \; [\int_0^1 S(\mu,-\mu')d\mu' + \int_0^1 S(\mu,\mu')d\mu'] = 1 \qquad (26)$$

Utilizing the third order Gaussian Quadrature again for the integration, equation (26) may be rewritten as follows:

$$1/2 \, [\sum_{j=1}^{3} a_j S(\mu_i,\mu_j) + \sum_{j=1}^{3} a_j S(\mu_i,-\mu_j)] = 1 \qquad (27)$$

where a_j is the weight factor of Gaussian Quadrature.

This equation gives us a means to check the $S(\mu_i,\pm\mu'_j)$ produced from previous procedures. (Appendix B)

CHAPTER IV

THE DIMENSIONLESS PARAMETERS

M, N AND Q

In this section, the reduced experimental data for scattering functions, $S(\mu_i,\mu_j)$ were utilized to calculate the dimensionless parameters.

For the present problem, equation (11) in Chapter II is the final form of the equation of transfer. The matrix form of the same equation is shown in equation (12). M^* is the matrix of coefficients. To show how the scattering functions were used in M^*, Hsia (10) indicated in his work that

$$M^* = \begin{bmatrix} A^* & B^* \\ -B^* & -A^* \end{bmatrix} \qquad (28)$$

where

$$A^* = \begin{bmatrix} \left(-\frac{1}{\mu_1} + \frac{a_1S_{1,1}}{\mu_1}\right) & , \frac{a_2S_{1,2}}{\mu_1} & \ldots , & \frac{a_nS_{1,n}}{\mu_1} \\ \frac{a_1S_{2,1}}{\mu_2} & , \left(-\frac{1}{\mu_2} + \frac{a_2S_{1,2}}{\mu_2}\right) & . , & \frac{a_nS_{2,n}}{\mu_2} \\ \vdots & \vdots & \ddots & \vdots \\ \frac{a_1S_{n,1}}{\mu_n} & , \frac{a_2S_{n,2}}{\mu_n} & \ldots , & \left(-\frac{1}{\mu_n} + \frac{a_nS_{n,n}}{\mu_n}\right) \end{bmatrix}$$

$$B^* = \begin{bmatrix} \frac{a_1S_{1,-1}}{\mu_1}, & \frac{a_2S_{1,-2}}{\mu_1}, & \cdots, & \frac{a_nS_{1,-n}}{\mu_1} \\ \frac{a_1S_{2,-1}}{\mu_2}, & \frac{a_2S_{2,-2}}{\mu_2}, & \cdots, & \frac{a_nS_{2,-n}}{\mu_2} \\ \frac{a_1S_{n,-1}}{\mu_n}, & \frac{a_2S'_{n,-2}}{\mu_n} & \cdots, & \frac{a_nS_{n,-n}}{\mu_n} \end{bmatrix}$$

where $S_{i,j}$ corresponds to $\frac{\sigma}{2\beta} S(\mu_i,\mu_j)$

Once the $S(\mu_i,\mu_j)$ were known, M^* was formulated. Solutions of eigenvalues and eigenvectors were needed. Wilkinson (35) discussed various methods of solution for both symmetric and unsymmetric matrices. Hsia (10) developed a digital computer program for this purpose (The Program of the Scattering Functions and the Eigenvalues). Since the experimental values of $S(\mu_i,\mu_j)$ were known in this work, the computation of the theoretical scattering functions were no longer needed. A modified computer program was utilized for this study. Additional steps for eigenvector calculation were incorporated into this program. This program is designated as Program I in Appendix C.

Program II in Appendix C is for the calculation of the dimensionless parameters M, N and Q. Utilizing the eigenvalues and eigenvectors obtained from Program I and following the procedure developed by Love (2) (outlined in Chapter II), the values of M, N and Q may be computed. In order to have a comparison of the results with the theoretical data in reference (2), the same wall reflectance combinations were used. They are

	Wall 1	Wall 2
	0.1	0.1
	0.1	0.5
	0.1	0.9
	0.5	0.1
REFLECTANCE	0.5	0.5
	0.5	0.9
	0.9	0.1
	0.9	0.5
	0.9	0.9

The calculations were carried out for optical spacing values ranging from 0.1 to infinity.

As mentioned before $S(\mu_i, \mu_j)$ were obtained by integrating of $S(\Theta_{ij})$'s for different wavelengths. The corresponding values of σ/β -λ graph is shown in Figure 4. The dimensionless parameter calculation is limited to the existing experimental data listed in Chapter III (page 27). A few sets of data were discarded because they did not converge during the eigenvalue calculation.

The dimensionless parameters were obtained for the following materials and wavelengths:

Aluminum	Wavelength	2.0, 4.0, 6.0, 11.0, 12.0, 13.0, 14.0
	σ/β	.36, .37, .39, .41, .42, .43, .46
Carbon	Wavelength	1.0, 8.0, 10.0, 12.0
	σ/β	.43, .47, .48, .50
Glass	Wavelength	11.0, 8.0, 7.0, 4.0, 2.5, .80
	σ/β	.48, .58, .60, .64, .68, .71
Iron	Wavelength	.60, 1.0, 4.0, 5.0, 8.0, 10.0, 14.0
	σ/β	.25, .30, .38, .45, .54, .63, .75
Silica	Wavelength	4.0, 6.0, 8.0, 10.0, 11.0, 12.0, 13.0
	σ/β	.28, .38, .45, .50, .56, .62, .68

Since a large amount of data resulted from the above calculations, only one set of them is presented here as example for illustration.

The following points should be noted:

(1). The relationship among the dimensionless parameters is

$$M - N = Q \tag{29}$$

(2). Figure 5 shows M, N as functions of σ/β with the optical spacing, τ, as a parameter. Both wall reflectances are equal to 0.1($\rho_1=\rho_2=0.1$) for this particular graph. Figure 5 shows that the points of parameter M cluster along a line (drawn for clearness) regardless of optical spacing and material of the particle. The values of parameter N

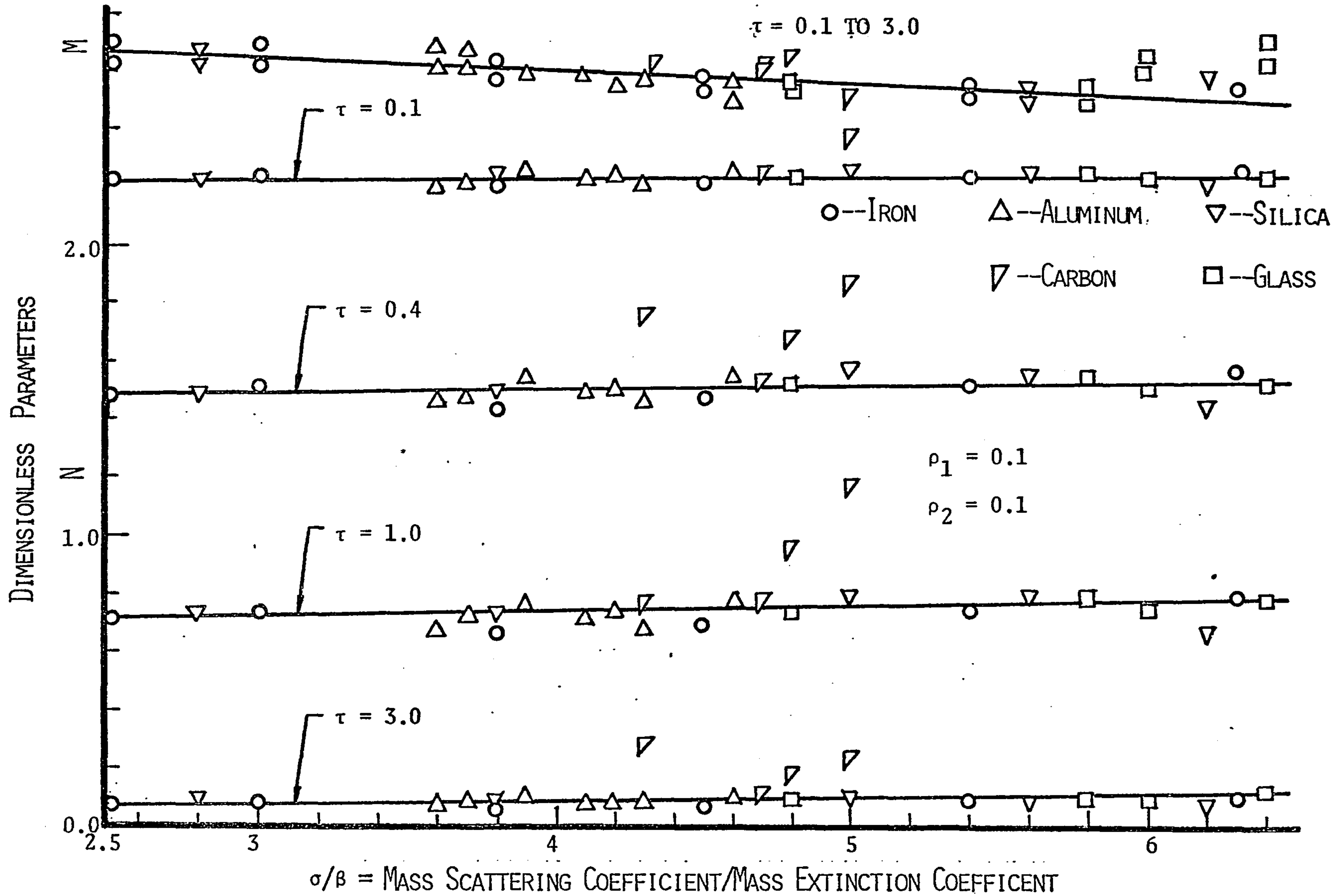

τ = 0.1 TO 3.0
M
τ = 0.1
○--IRON
△--ALUMINUM
▽--SILICA
--CARBON
□--GLASS
τ = 0.4
ρ_1 = 0.1
ρ_2 = 0.1
N
τ = 1.0
τ = 3.0
DIMENSIONLESS PARAMETERS
2.0
1.0
0.0
2.5
3
4
5
6
σ/β = MASS SCATTERING COEFFICIENT/MASS EXTINCTION COEFFICENT

Figure 5

stay on one line no matter what kind of material of the particle is, but they are distinct from one optical spacing to the other. This brings the interesting conclusion that the material of the particles is irrelevent to the radiative properties. Optical spacing, τ, is the important factor that influences the values of M and N, and hence the radiative heat transfer.

(3). Figure 6 shows the curves of M and N versus optical spacing, τ, with σ/β as parameter. The wall reflectances are equal to 0.5 for both surfaces. Also the curves of the parameters M and N for the zero-scattering case ($\sigma/\beta = 0$) were drawn. The data of the zero-scattering curve was taken from reference (2). All the experimental curves are similar to the $\sigma/\beta = 0$ curve in shape. The values of M increased and the values of N decreased while σ/β value increased. Although the M (or N) have different values at a given optical spacing, the differences are small. Thus these bundles of M and N curves could be treated as a band with the $\sigma/\beta = .25$ curve for iron as an upper bound and the $\sigma/\beta = .63$ curve for iron as a lower bound. All the other data for various materials fall inside these boundaries. It appears in these curves that if the optical spacing is greater than 3, the M and N values are almost constants and equal to those for infinite optical spacing. Hence it would be safe to say that when $\tau > 3$ the medium can be considered optically thick. On

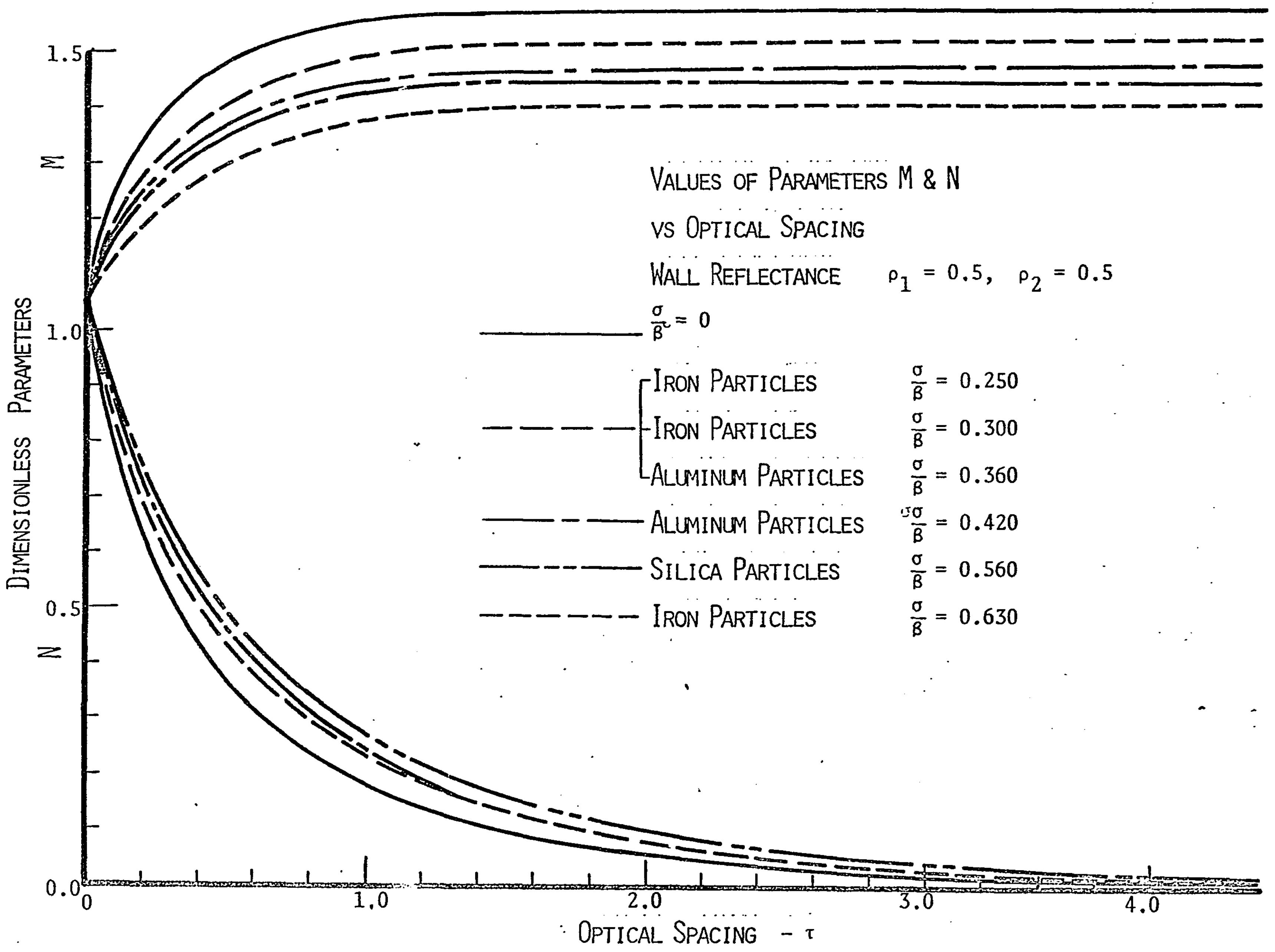

1.5
1.0
0.5
0.0
M
N
DIMENSIONLESS PARAMETERS
0
1.0
2.0
3.0
4.0
OPTICAL SPACING - τ
VALUES OF PARAMETERS M & N
VS OPTICAL SPACING
WALL REFLECTANCE ρ1 = 0.5, ρ2 = 0.5
σ/β = 0
IRON PARTICLES σ/β = 0.250
IRON PARTICLES σ/β = 0.300
ALUMINUM PARTICLES σ/β = 0.360
ALUMINUM PARTICLES σ/β = 0.420
SILICA PARTICLES σ/β = 0.560
IRON PARTICLES σ/β = 0.630

Figure 6

the other hand when $\tau \ll 1$ the medium can be considered optically thin.

The smallest value of τ used was 0.1 for each curve. It was found that by extropolating the curves, they would converge to the same point at $\tau = 0$. The value of this point agrees with results calculated from the following equation:

$$\text{at } \tau = 0; \qquad M = N = \frac{\pi(1 - \rho_1)(1 - \rho_2)}{(1 - \rho_1\rho_2)} \tag{29}$$

and $Q = 0$.

These equations are developed in reference (2). Hence this point at $\tau = 0$ may serve as a check point for the present results.

One set of Carbon data falls out of the general pattern. Some points of this set are located on the opposite side of the $\sigma/\beta = 0$ curve, which serves as a limiting case. Since this occurs only in one set of thirty-one sets of data, it was believed that this set was in error. Also, the $S(\theta_{ij})$ data of Carbon taken from reference (30) were about one tenth smaller than most of others and quite few sets of Carbon data did not converge during eigenvalue calculation.

(4). The experimental data of scattering functions should be considered anisotropic. Love (2) used the theoretical scattering functions for his calculations. A comparison between the isotropic and anisotropic theoretical results was made. One of the conclusions was that the isotropic scattering data may be used to represent anisotropic cases with good accuracy for the plane parallel cloud problems. It was desirable to make a similar comparison between the experimental data and theoretical isotropic data for the dimensionless parameters. Figure 7 and Figure 8 show these comparisons. The theoretical isotropic data of M and N was superimposed over the experimental data. It was clear that the shape of the curves are similar and the isotropic band would cover the experimental curves. In other words the isotropic band is wider than the experimental band. The width of the band is relatively small. Hence isotropic data may also be used to compute heat transfer for the theoretical anisotropic case and for a real EAS cloud.

(5). Also, a comparison was made between Q - σ/β curves for isotropic data and experimental data. Figure 9 shows that the experimental data agree well with the isotropic curve, especially at the low σ/β values.

In conclusion, the comparison of M, N and Q curves for the theoretical isotropic data with both the theoretical anisotropic data and the experimental data suggests that if the refractive indexes, shape, size, σ/β or even the material of the particle are unknown, the isotropic data for M, N and Q may be used to approximate the heat transfer from a surface with acceptable accuracy.

As far as which values of M, N and Q within the band would be used, a mean value at each optical spacing was chosen. These mean values of the parameters also constitute a curve.

Program I and Program II are in Fortran language. (Appendix C). The development of these programs and calculations were done on the Osage computer of the University of Oklahoma. Programs I and II could be combined into one larger program to save intermediate output and input processes.

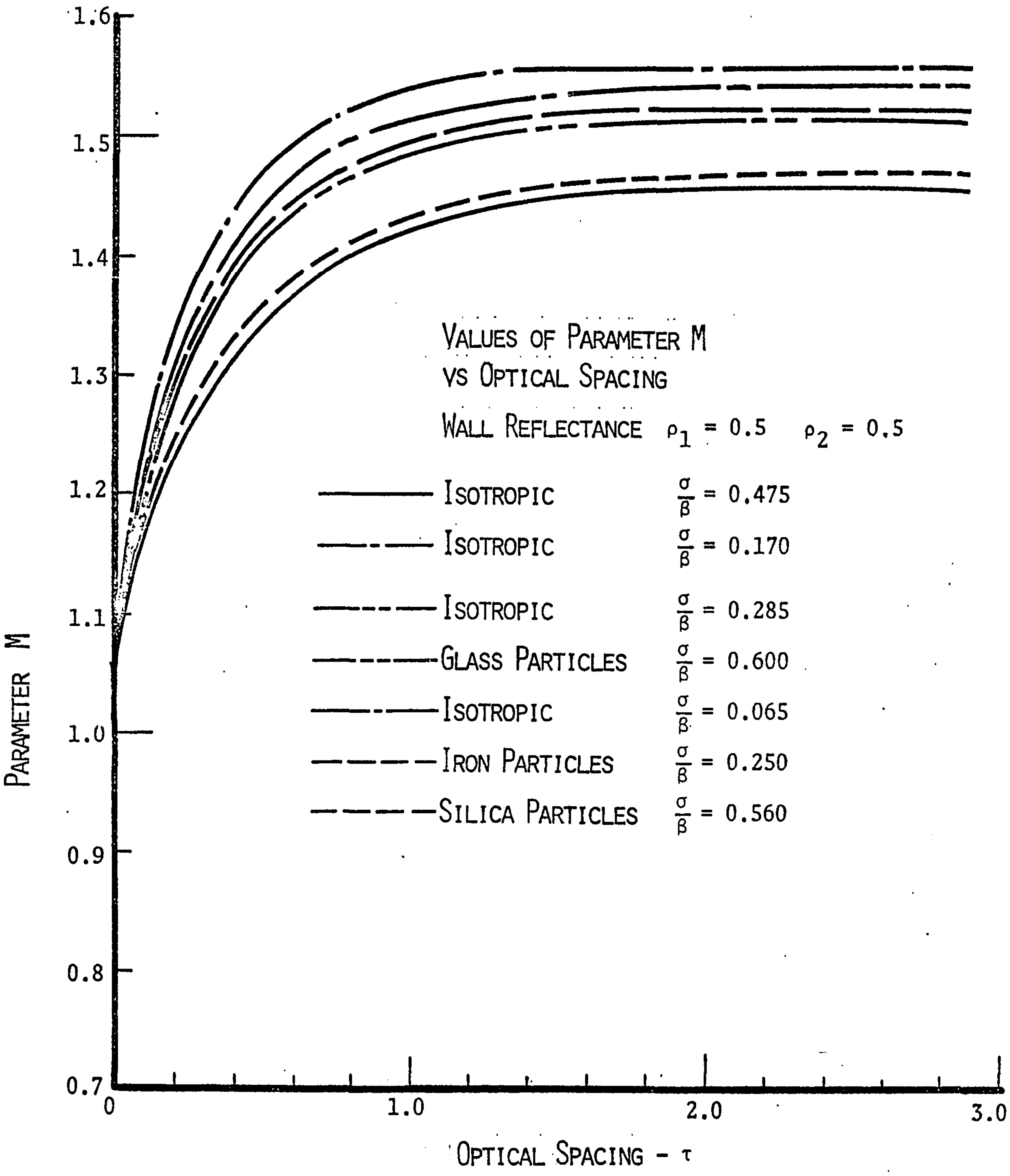
1.6
1.5
1.4
1.3
1.2
1.1
1.0
0.9
0.8
0.7
Parameter M
0
1.0
2.0
3.0
Optical Spacing - τ
Values of Parameter M
vs Optical Spacing
Wall Reflectance ρ1 = 0.5 ρ2 = 0.5
Isotropic σ/β = 0.475
Isotropic σ/β = 0.170
Isotropic σ/β = 0.285
Glass Particles σ/β = 0.600
Isotropic σ/β = 0.065
Iron Particles σ/β = 0.250
Silica Particles σ/β = 0.560

Figure 7

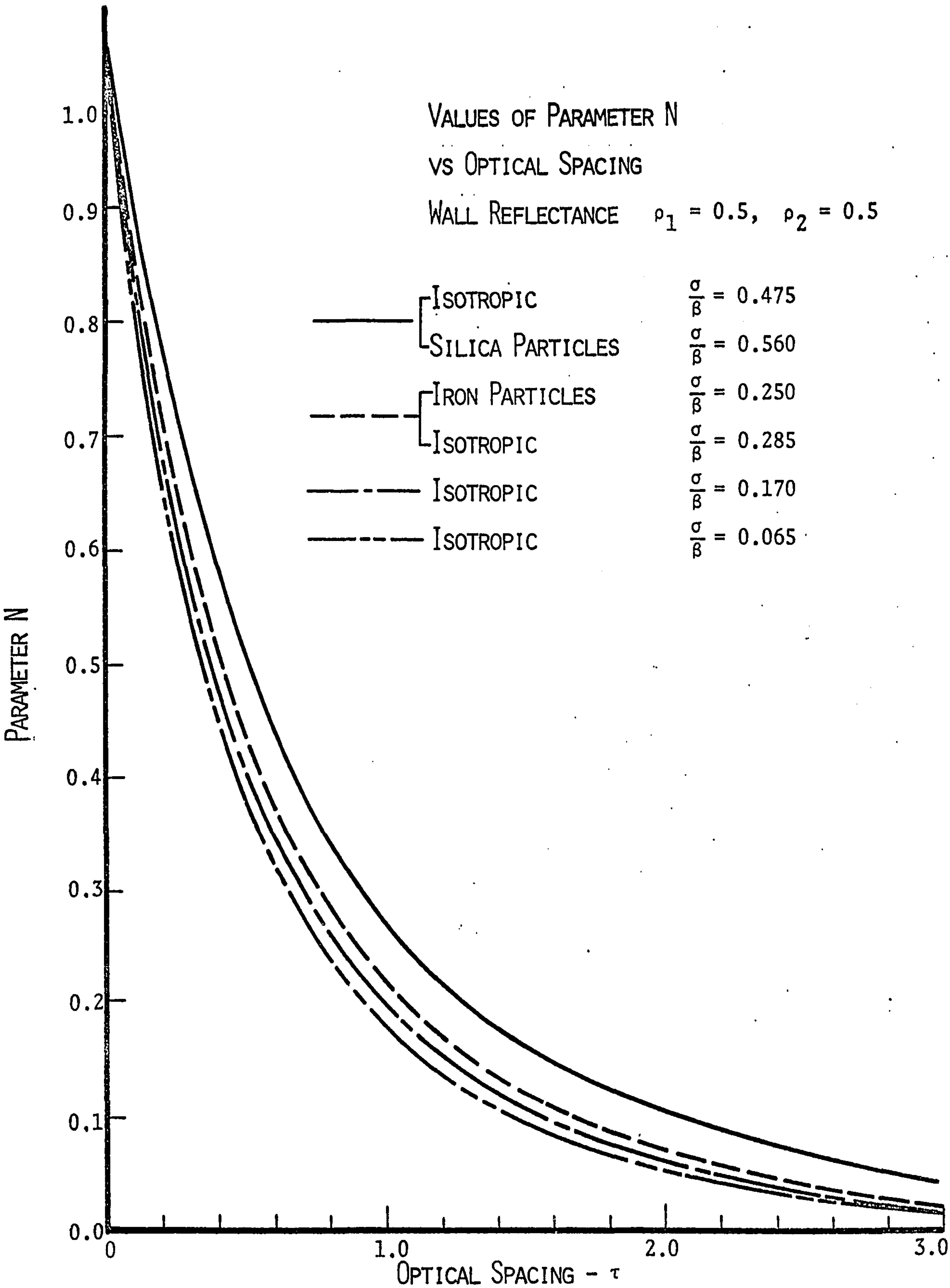
Values of Parameter N
vs Optical Spacing
Wall Reflectance ρ1 = 0.5, ρ2 = 0.5
Isotropic σ/β = 0.475
Silica Particles σ/β = 0.560
Iron Particles σ/β = 0.250
Isotropic σ/β = 0.285
Isotropic σ/β = 0.170
Isotropic σ/β = 0.065
Parameter N
0.0
0.1
0.2
0.3
0.4
0.5
0.6
0.7
0.8
0.9
1.0
0
1.0
2.0
3.0
Optical Spacing - τ

Figure 8

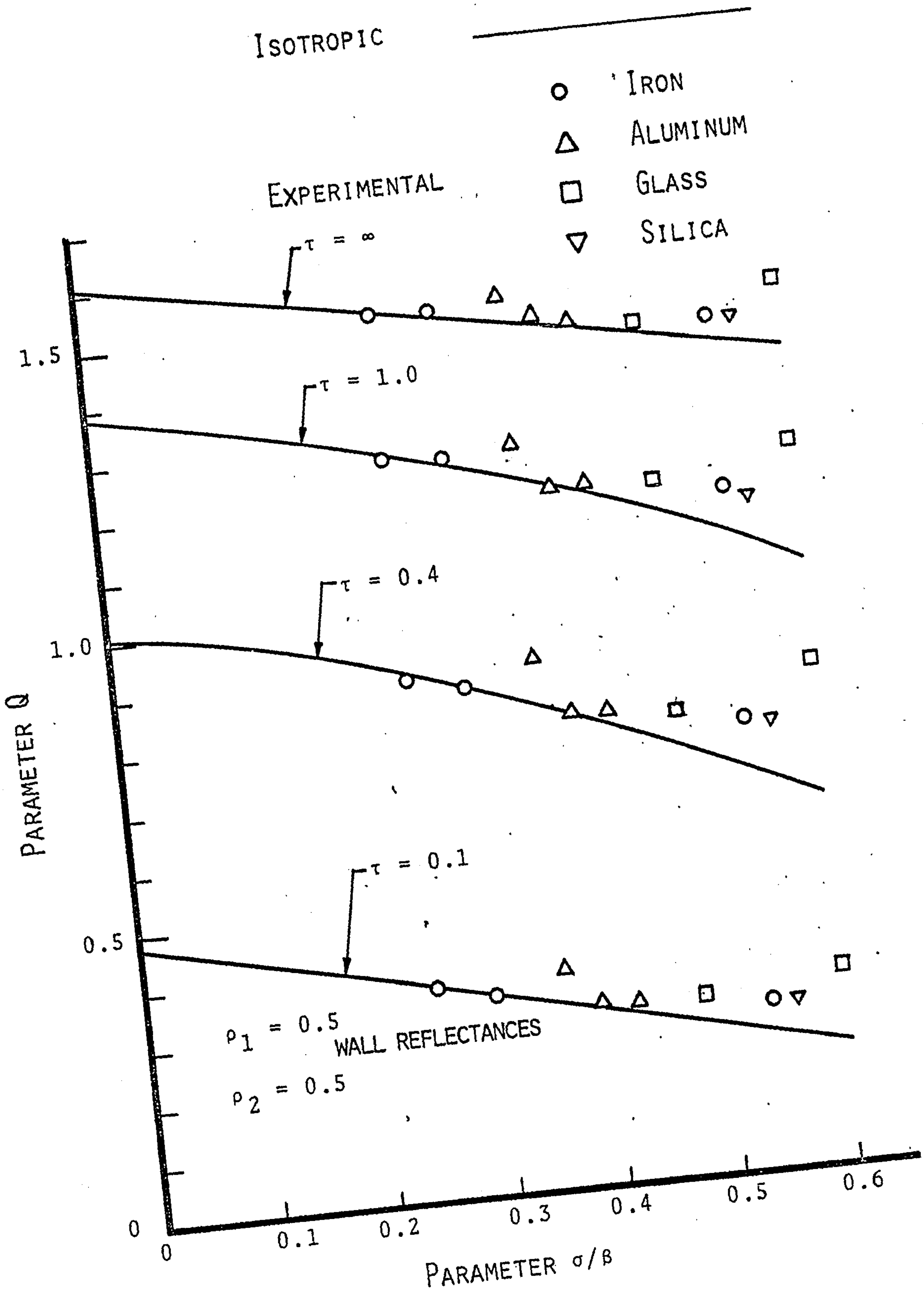
ISOTROPIC
EXPERIMENTAL
IRON
ALUMINUM
GLASS
SILICA
τ = ∞
τ = 1.0
τ = 0.4
τ = 0.1
ρ1 = 0.5
WALL REFLECTANCES
ρ2 = 0.5
PARAMETER Q
1.5
1.0
0.5
0
0
0.1
0.2
0.3
0.4
0.5
0.6
PARAMETER σ/β

Figure 9

CHAPTER V

RADIANT ENERGY TRANSFER IN AN EAS BOUNDARY LAYER

The problem of the combined radiative and convective heat transfer was studied for the case of fluid flow over a flat plate. The moving fluid was considered as an EAS medium. The solution of the heat transfer problem for a laminar fluid flow over a flat plate is well known, but, the solution of the same problem including radiant energy in an EAS medium is more complicated. The radiative contribution of heat transfer is important and should not be overlooked, particularly when high temperature conditions are present.

The Energy Equation

The basic principle governing the temperature field within an EAS medium is the same as that for a non-participating medium. The equation of conservation of energy is still the fundamental equation. The only difference is the additional mechanism of the radiative energy of the participating medium in the energy balance. The fluid was considered a continuum, incompressible and in local thermodynamic equilibrium. The fluid properties, such as density and specific heat are assumed constant. This is an ideal gas approach, especially for high temperature conditions. There was no change in the momentum equation. The equation of energy may be written as:

$$\rho C_p \frac{DT}{Dt} = \mathrm{div}(K\,\mathrm{grad}T) + \beta T \frac{DP}{Dt} + \mu\phi - \mathrm{div}\, q_r \qquad (30)$$

where ρ is the density of the fluid, C_p is the specific heat of the fluid, K is the thermal conductivity, the term KgradT is the quantity of thermal conduction in the medium, β is the coefficient of thermal expansion, $\beta T\frac{DP}{Dt}$ is the rate of change of pressure which is equal to zero for flow over flat plate, $\mu\phi$ is the viscous dissipation term, it is negligible if the speed of the fluid is small. q_r represents the radiative heat transfer terms.

The reduced equation would be

$$\rho C_p\left[\frac{\partial T}{\partial t} + u\frac{\partial T}{\partial x} + v\frac{\partial T}{\partial y}\right] = K\left[\frac{\partial^2 T}{\partial x^2} + \frac{\partial^2 T}{\partial y^2}\right] - \frac{\partial q_r}{\partial y} - \frac{\partial q_r}{\partial x} \qquad (31)$$

The fluid is considered in a steady state with constant properties. The radiation is assumed negligible in the X direction (Figure 10) for the low speed flow. Then the energy equation can be simplified further:

$$\rho C_p \int_0^\infty \left[u\frac{\partial T}{\partial x} + v\frac{\partial T}{\partial y} \right] dy = K\int_0^\infty \frac{\partial^2 T}{\partial y^2} dy - \int_0^\infty \frac{\partial q_r}{\partial y} dy \qquad (32)$$

Applying the continuity equation, equation (32) can be reduced to the following form:

$$\rho C_p \frac{d}{dx} \int_0^{\delta_t} [u(T-T_s)] dy = K\int_0^{\delta_t} \frac{d^2 T}{dy^2} dy - \int_0^{\delta_t} \frac{dq_r}{dy} dy \qquad (33)$$

After integration it becomes

$$\rho C_p \frac{d}{dx} \int_0^{\delta_t} [u(T-T_s)] dy = -K\left(\frac{dT}{dy}\right)_{y=0} - (q_r)_{y=\delta_t} + (q_r)_{y=0} \qquad (34)$$

There are two factors which need to be determined: first, the temperature and velocity distribution, and second, the quantities of radiant heat transfer q_r.

It is well known that exact solutions of the energy equation without radiation terms are not very simple even for the flow over a flat plate. These solutions are presented in most of the heat transfer books. Approximate methods using the von Karman and K. Pohlhausen's technique with acceptable accuracy are much simpler and are widely used. In this work, this technique was chosen to solve equation (34). Utilizing a fourth order polynomial for the velocity and the temperature profiles, and evaluating the coefficients by satisfying the following boundary conditions:

$$\text{at } y = 0: \quad T = T_w; \quad \frac{\partial^2 T}{\partial y^2} = 0 \text{ (steady low velocity)}$$

$$\text{at } y = \delta_t: \quad T = T_s \quad \frac{\partial T}{\partial y} = 0.$$

Eckert and Drake (31) obtained a temperature profile,

$$\frac{T - T_w}{T_s - T_w} = \frac{3}{2}\frac{y}{\delta_t} - \frac{1}{2}\left(\frac{y}{\delta_t}\right)^3 \tag{35}$$

where T_w and T_s are the temperatures at the wall and at the edge of the thermal boundary layer. A similar equation for velocity profile inside the velocity boundary layer is

$$\frac{u}{u_s} = \frac{3}{2}\frac{y}{\delta} - \frac{1}{2}\left(\frac{y}{\delta}\right)^3 \tag{36}$$

where u_s is the free stream velocity and δ is the velocity boundary layer thickness.

Substituting equations (35) and (36) into equation (34) gives

$$\rho C_p (T_w - T_s) u_s \frac{d}{dx} \int_0^{\delta_t} \left[1 - \frac{3}{2}\frac{y}{\delta_t} + \frac{1}{2}\left(\frac{y}{\delta_t}\right)^3\right] \left[\frac{3}{2}\frac{y}{\delta} - \frac{1}{2}\left(\frac{y}{\delta}\right)^3\right] dy =$$

$$\cdot \frac{3K(T_s - T_w)}{2\delta_t} + (q_r)_{y=0} - (q_r)_{y=\delta_t} \tag{37}$$

For a gaseous medium with the Prandtl number smaller than unity, δ_t should be greater than δ. Hence equation (37) may be rewritten as

$$\rho C_p u_s (T_w - T_s)\frac{d}{dx}\left[\int_0^{\delta}[1 - \frac{3}{2}(\frac{y}{\delta_t}) + \frac{1}{2}(\frac{y}{\delta_t})^3]\,[\frac{3}{2}(\frac{y}{\delta}) - \frac{1}{2}(\frac{y}{\delta})^3]dy + \int_{\delta}^{\delta_t}[1 - \frac{3}{2}\frac{y}{\delta_t} + \frac{1}{2}(\frac{y}{\delta_t})^3]dy\right] = \frac{3K(T_w - T_s)}{2\delta_t} + \Delta q_r \qquad (38)$$

where $\Delta q_r = (q_r)_{y=0} - (q_r)_{y=\delta_t}$.

Equation (38) is then integrated and evaluated with the limits.

$$\rho C_p u_s (T_w - T_s)\frac{d}{dx}[\frac{3}{8}(\delta_t - \delta) + \frac{3}{20}\frac{\delta^2}{\delta_t} - \frac{3}{280}\frac{\delta^4}{\delta_t^3}] - \frac{3K(T_w - T_s)}{2\delta_t} = \Delta q_r \qquad (39)$$

Recalling the step by step method of integration

$$\int_x^{x+\Delta x}\frac{dy}{dx}dx = y\Big|_x^{x+\Delta x} = y(x + \Delta x) - y(x) \qquad (40)$$

Equation (39) may be integrated with respect to x

$$\frac{\rho C_p u_s (T_w - T_s)}{\Delta x}\,[\frac{3}{8}(\delta_t(x+\Delta x) - \delta_t(x) - \delta(x+\Delta x) + \delta(x)\,)$$

$$+ \frac{3}{20}\left(\frac{\delta^2(x+\Delta x)}{\delta_t(x+\Delta x)} - \frac{\delta^2(x)}{\delta_t(x)}\right) - \frac{3}{280}\left(\frac{\delta^4(x+\Delta x)}{\delta_t^3(x+\Delta x)} - \frac{\delta^4(x)}{\delta_t^3(x)}\right)]$$

$$- \frac{3K(T_w - T_s)}{2\left[\frac{\delta_t(x+\Delta x)+\delta_t(x)}{2}\right]} = \Delta q_r \qquad (41)$$

For $\delta_t < \delta$ cases, equation (39) becomes

$$\rho C_p u_s (T_w - T_s)\frac{d}{dx}\left[\frac{3}{20}\frac{\delta_t^2}{\delta} - \frac{3}{280}\frac{\delta_t^4}{\delta^3}\right] - \frac{3K(T_w - T_s)}{2\delta_t} = \Delta q_r \qquad (42)$$

The temperature profile

$$\frac{T - T_s}{T_w - T_s} = 2\frac{y}{\delta_t} - 2\left(\frac{y}{\delta_t}\right)^3 + \left(\frac{y}{\delta_t}\right)^4 \qquad (43)$$

which is given in Schlichting (33), Page 321, is also used for this calculation.

The Treatment of the Radiation Terms

The radiation terms, $(q_r)_{y=0}$ and $(q_r)_{y=\delta_t}$ have to be determined. The fluid was considered as an EAS medium. $(q_r)_{y=0}$ represents the net radiative heat flux from the wall. $(q_r)_{y=\delta_t}$ represents the net radiative heat flux from the edge of the boundary layer. Figure 10 shows the physical model under study. The fluid was assumed to flow

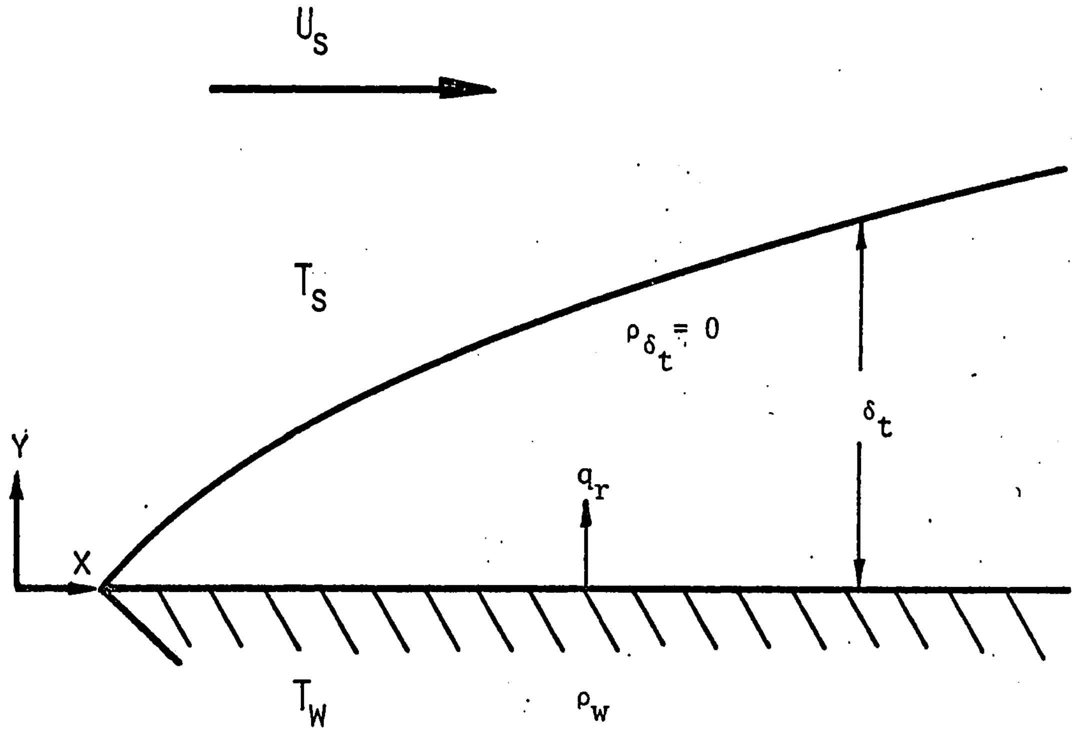

PHYSICAL MODEL AND COORDINATE SYSTEM

FOR BOUNDARY LAYER FLOW OVER FLAT PLATE

Figure 10

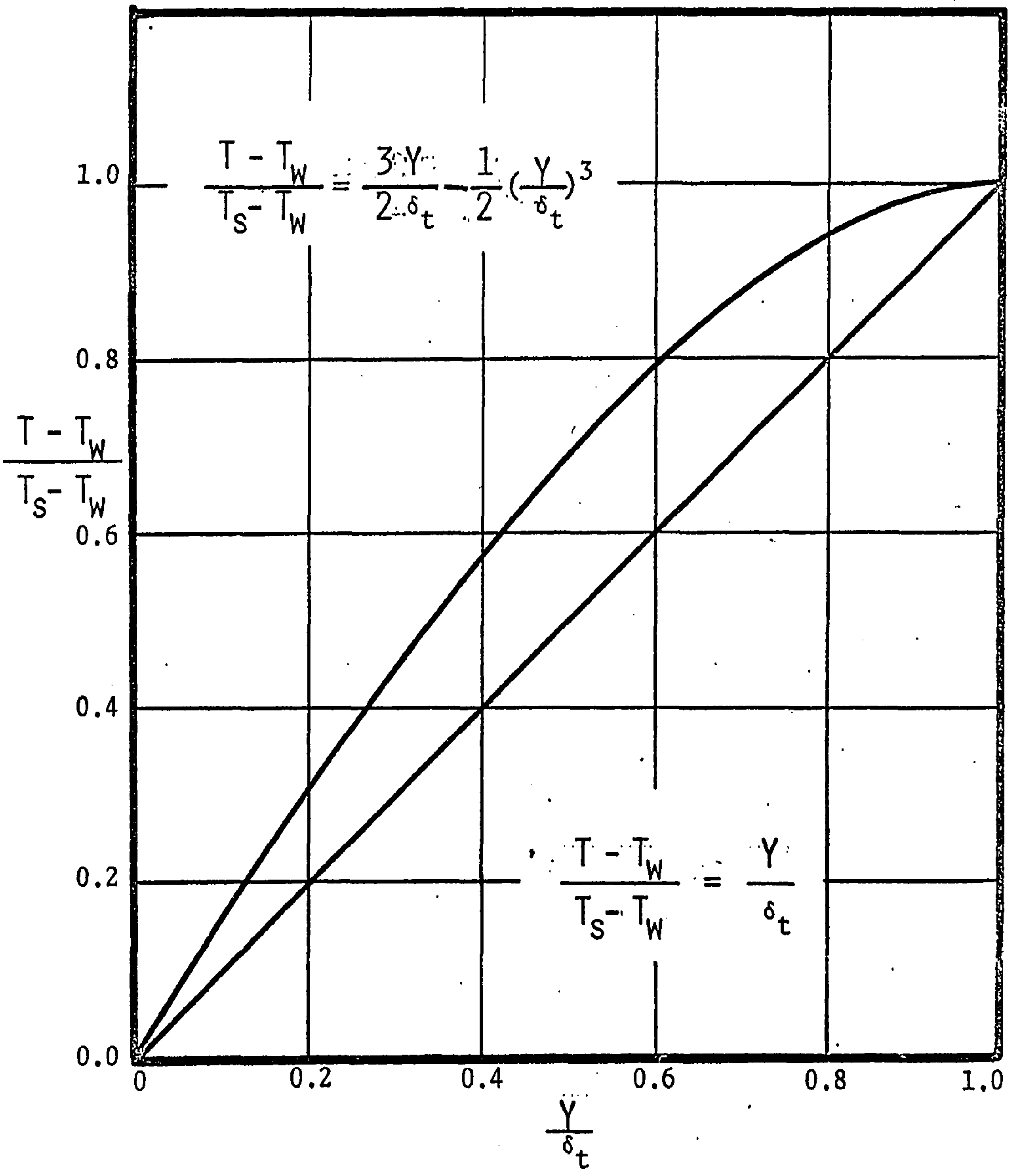

Figure 11 Temperature Profiles

parallel to the plates. This will be looked upon as if the medium were flowing between two isothermal, diffuse parallel walls with one wall having a temperature T_w and a reflectance ρ_w, and the other having the free stream temperature T_s and a reflectance equal to zero. Because the fluid beyond thermal boundary layer was assumed to be of infinite depth, the edge of the thermal boundary layer is considered as a black wall.

Hsia (10) in his study concluded that, if the temperature profile of the medium across the space between two plates is linear, then the medium may be treated as an isothermal medium with a temperature equal to the average of wall temperatures. Since the profile of equation (35) and the linear distribution shown in Figure 11 are very close the straight line linear distribution was used for the radiative heat transfer calculations. The use of the parabolic profile would complicate the computations with little gain in accuracy.

Recall (equation (19)) that radiant heat transfer in an isothermal medium from a wall may be calculated by

$$q_{net_1} = (10^{-11})[T_1^4 \sum_{j=1}^{n} A_j M_j - T_2^4 \sum_{j=1}^{n} A_j N_j - T_a^4 \sum_{j=1}^{n} A_j Q_j]$$

with the present conditions, two sets of dimensionless parameters were required. The reason for this is illustrated by Figure 12.

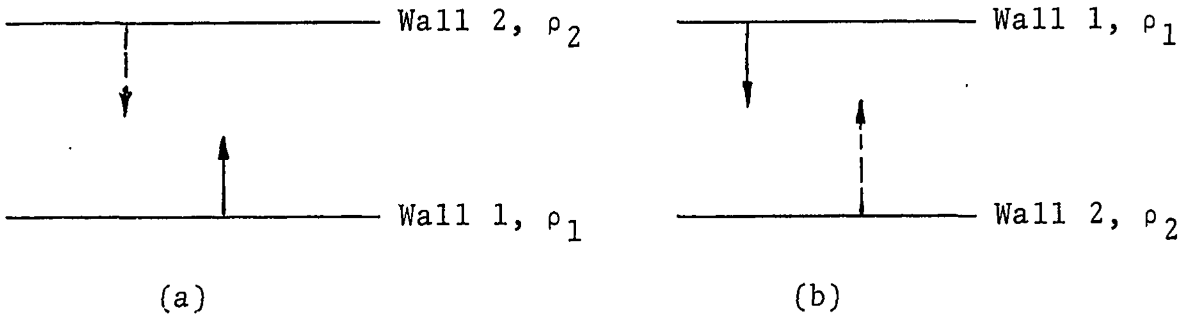

Figure 12. VIEWS OF WALL REFLECTANCE ARRANGEMENT.

Equation (19) was developed for radiation in the direction of the positive normal. Radiation in the negative normal direction (like that from the boundary layer) is equivalent to the condition shown in Figure 12b. The difference is the arrangement of wall reflectances. The net flux from wall 2 may be expressed as

$$q_{net_2} = (10)^{-11}[T_2^4 \sum_{j=1}^{n} A_j M_j' - T_1^4 \sum_{j=1}^{n} A_j N_j' - T_a^4 \sum_{j=1}^{n} A_j Q_j'] \qquad (44)$$

The prime superscripts indicate that these are different parameters.

In Chapter III, it has been illustrated that the dimensionless parameters are obtained at discrete points of the optical spacing. In general the variation is relatively large only between $\tau = 0$ and $\tau = 1.5$. They are almost a constant when $\tau > 3$. This has been shown in Figure 6.

To find the corresponding parameters, numerical polynomial curve fitting was used to establish equations for M and N curves as functions of τ. Then the equations were used to calculate M's and N's for any optical spacing value.

This raised a question of how to find optical spacing across the thermal boundary layer at each every point of x on the plate. By definition,

$$\tau = \int_0^L \rho\beta dy \tag{45}$$

If ρ and β are constants then

$$\tau = \rho\beta L \tag{46}$$

where ρ is the density of the medium and β is the extinction coefficient. β may be found by computing the following equation

$$\beta = \frac{3K^e}{2D\rho_m} \tag{47}$$

where D is the diameter of the particle, ρ_m is the density of the material of the particles and K^e is the extinction cross section. K^e is a function of particle size parameter $\alpha = \frac{\pi D}{\lambda}$. These terms, β, K^e, α and their relationship have been discussed by Love (2) and will not be repeated here. In reference (29) and (30) $K^e = 2$ was used for all particles. $K^e - \alpha$ curve of the particle with refractive index, m equal to 1.25 was used for this study and was represented by the equation of a polynomial between $\alpha = 0$ and $\alpha = 6$. When $\alpha > 6$, information of K^e is lacking. K^e is assumed equal to 2.44 for $\alpha > 6$.

The Numerical Iteration Solution for Equation (41)

It is very easy to see that equation (41) is not easily solved directly. Hence, a numerical iteration method was selected for use with the high speed digital computer. The numerical iteration method chosen for this calculation was the half interval method. The details of this method are discussed in most texts on numerical analysis. A simple example is given for purposes of illustration.

Consider the equation of $\sin \frac{\pi x}{2} - e^{-x} = 0$. The solution of x is desired. Let $y_1 = \sin \frac{\pi x}{2}$, $y_2 = e^{-x}$. Figure 13 shows these two curves. They intersect each other at point P. On the left side of point P, $y_2 > y_1$ on the other side $y_2 < y_1$. The value of the x coordinate at point P is the solution. By using the half interval method to adjust values of x and iterate the calculation until $y_1 - y_2 = \varepsilon$, a solution is found. ε is an acceptable error.

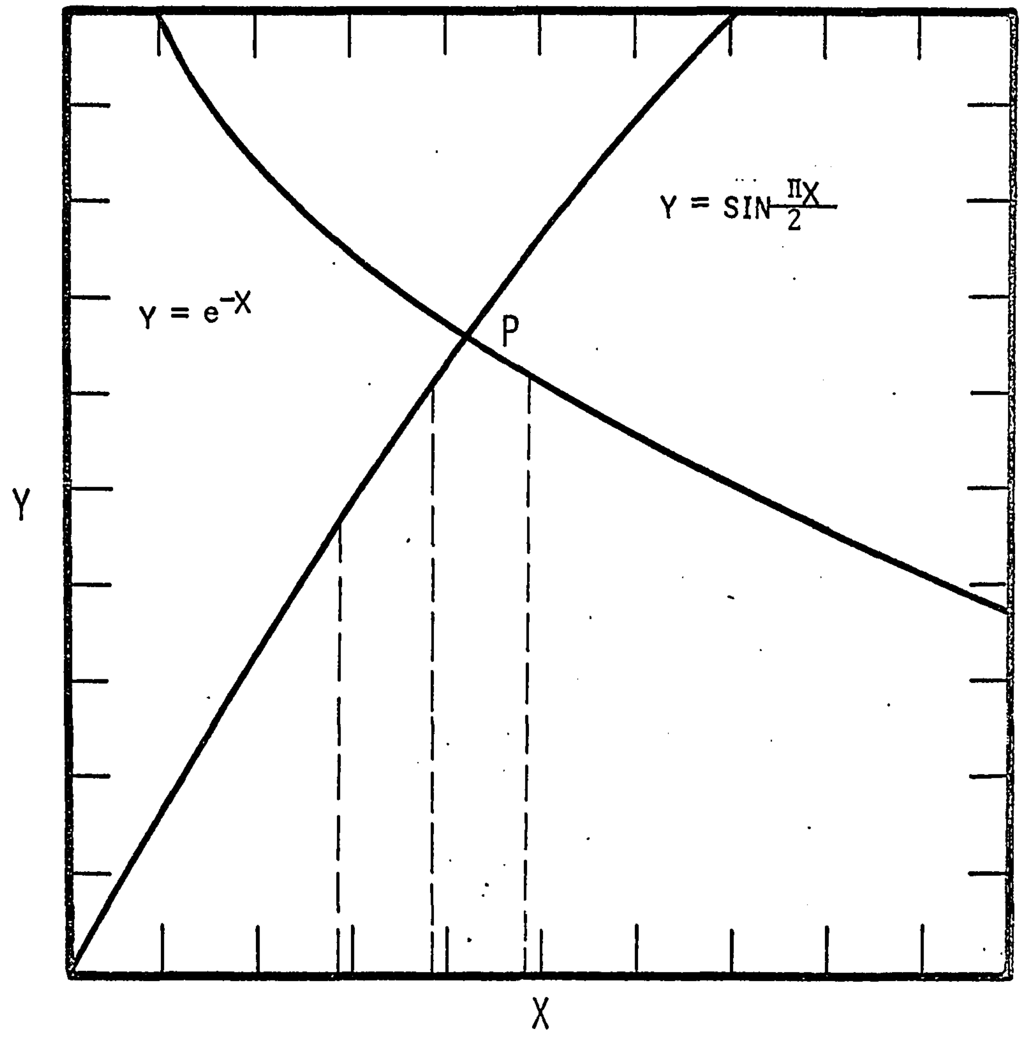

Figure 13 Half-Interval Search for the Root of

$\mathrm{SIN}\left[\frac{\pi x}{2}\right] = e^{-x}$

An Example Calculation and the Computer Program

It is desirable to have an example calculation carried out in order to have a qualitative knowledge of the effects on heat transfer in an EAS boundary layer.

A uniform fluid (air with iron particles) flows at a speed of 500 ft/sec over a flat plate. For hot wall cases, the free stream temperature is 500 ^{o}R. The flat plate is assumed to be isothermal and the temperatures of the wall are 1000 ^{o}R, 2000 ^{o}R, 3000 ^{o}R, 4000 ^{o}R, and 5000 ^{o}R which with free stream temperatures constitute five different temperature combinations. Cold wall cases are constructed by keeping the wall temperature 500 ^{o}R and changing the free stream temperature from 1000 ^{o}R to 5000 ^{o}R which makes another five cases. The reflectance at the edge of the thermal boundary layer is zero. The different reflectances and the different apparent densities of the particles in the fluid make the following four combinations, these are

Apparent density of particle = 0.1 lb/ft^3

Wall reflectance = 0.1, 0.5 and

Apparent density of the particle = 0.01 lb/ft^3[2]

Wall reflectance = 0.1, 0.5.

Also the fluid is assumed to be (i) an EAS medium, (ii) a non-scattering but emitting and absorbing medium. Totaling the different combinations, forty cases are formed. The energy equation without radiation terms, equation (48)

[2]Results for this density are not presented in this work.

is also iterated for the same wall and free stream temperature combinations.

$$\rho C_p u_s (T_w - T_s) \frac{d}{dx}\left[\frac{3}{8}(\delta_t - \delta) + \frac{3}{20}\frac{\delta^2}{\delta_t} - \frac{3}{280}\frac{\delta^4}{\delta_t^3}\right] = \frac{3K(T_w - T_s)}{2\delta_t} \tag{48}$$

Prior to the major iterative program, the following data had to be prepared in special form.

(i) The values of density, ρ, and specific heat, C_p, of the medium were determined.

$$\rho = \rho_a + \rho_{air}$$

ρ_{air} was taken at temperature T_a which is the average of the plate and free stream temperatures.

$$C_p = \frac{\rho_a}{\rho} \times C_{p\,iron} + \frac{\rho_{air}}{\rho} \times C_{p(air\ at\ T_a)}$$

(ii) K^e - α curve was numerically fitted.

(iii) Dimensionless parameters M, N and Q were computed for every combination of reflectance. In the present cases isotropic scattering functions were used. Figure 14 to Figure 17 show these results. As before, the results of dimensionless parameters were represented by a band of curves. Taking mean values of those M and N parameters at each optical spacing τ, a mean value curve was obtained. Then the numerical curve fitting method was used to form polynomials for M - τ and N - τ curves. The following

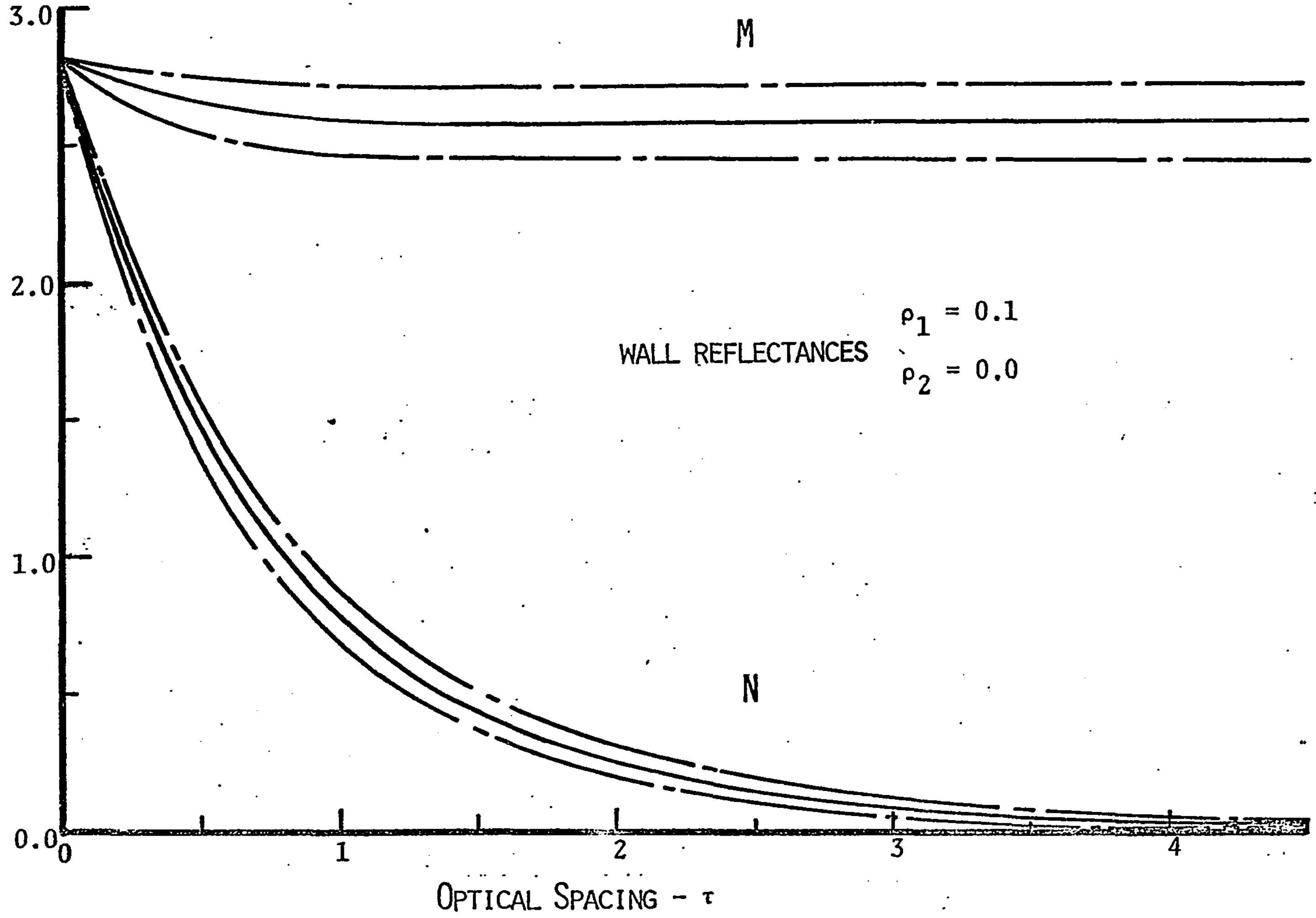
3.0
2.0
1.0
0.0
M
N
WALL REFLECTANCES
$\rho_1 = 0.1$
$\rho_2 = 0.0$
0
1
2
3
4
OPTICAL SPACING - τ

Figure 14

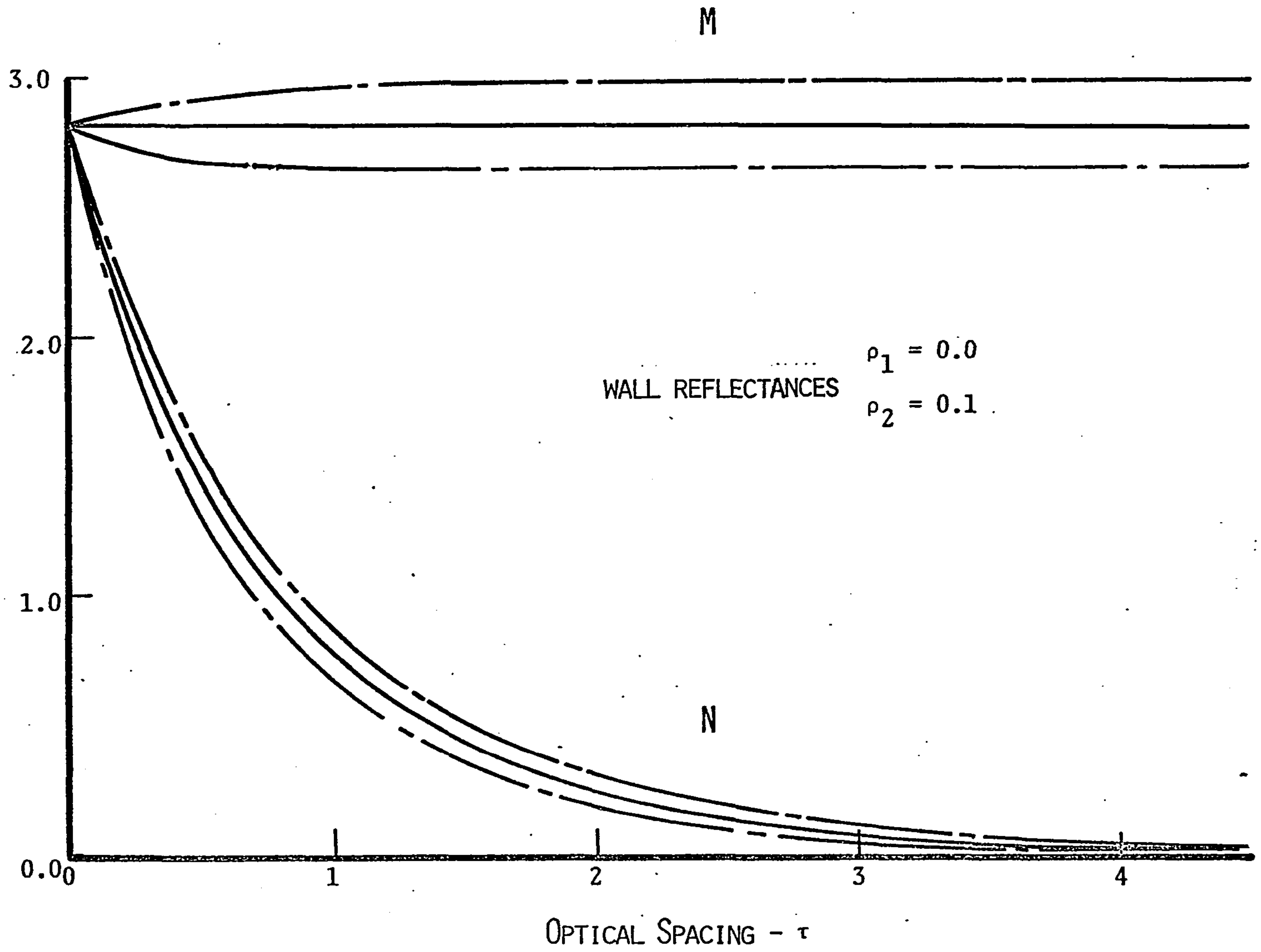
M
3.0
2.0
1.0
0.0
WALL REFLECTANCES
ρ1 = 0.0
ρ2 = 0.1
N
0
1
2
3
4
OPTICAL SPACING - τ

Figure 15

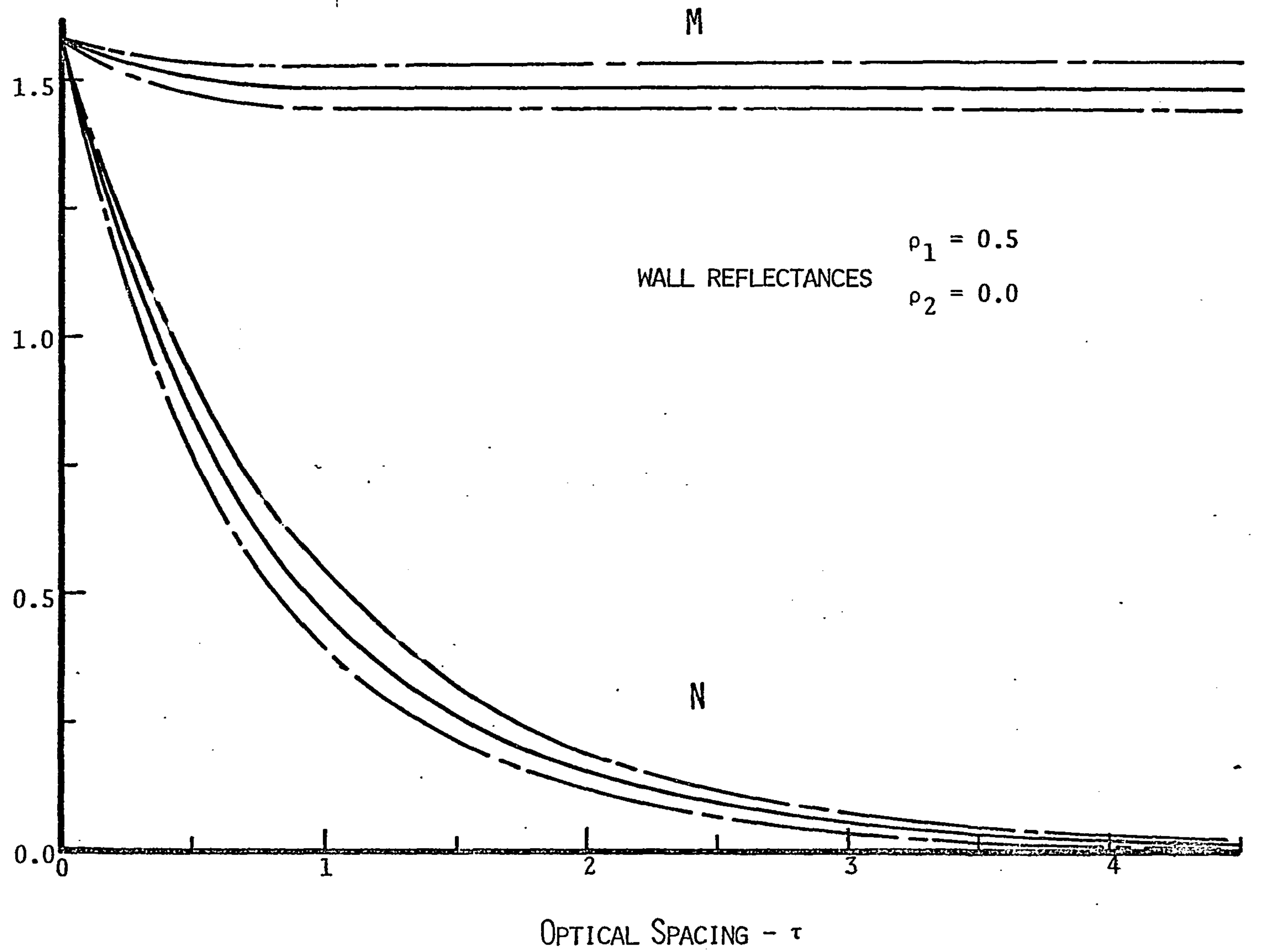
M
N
WALL REFLECTANCES
ρ1 = 0.5
ρ2 = 0.0
1.5
1.0
0.5
0.0
0
1
2
3
4
OPTICAL SPACING - τ

Figure 16

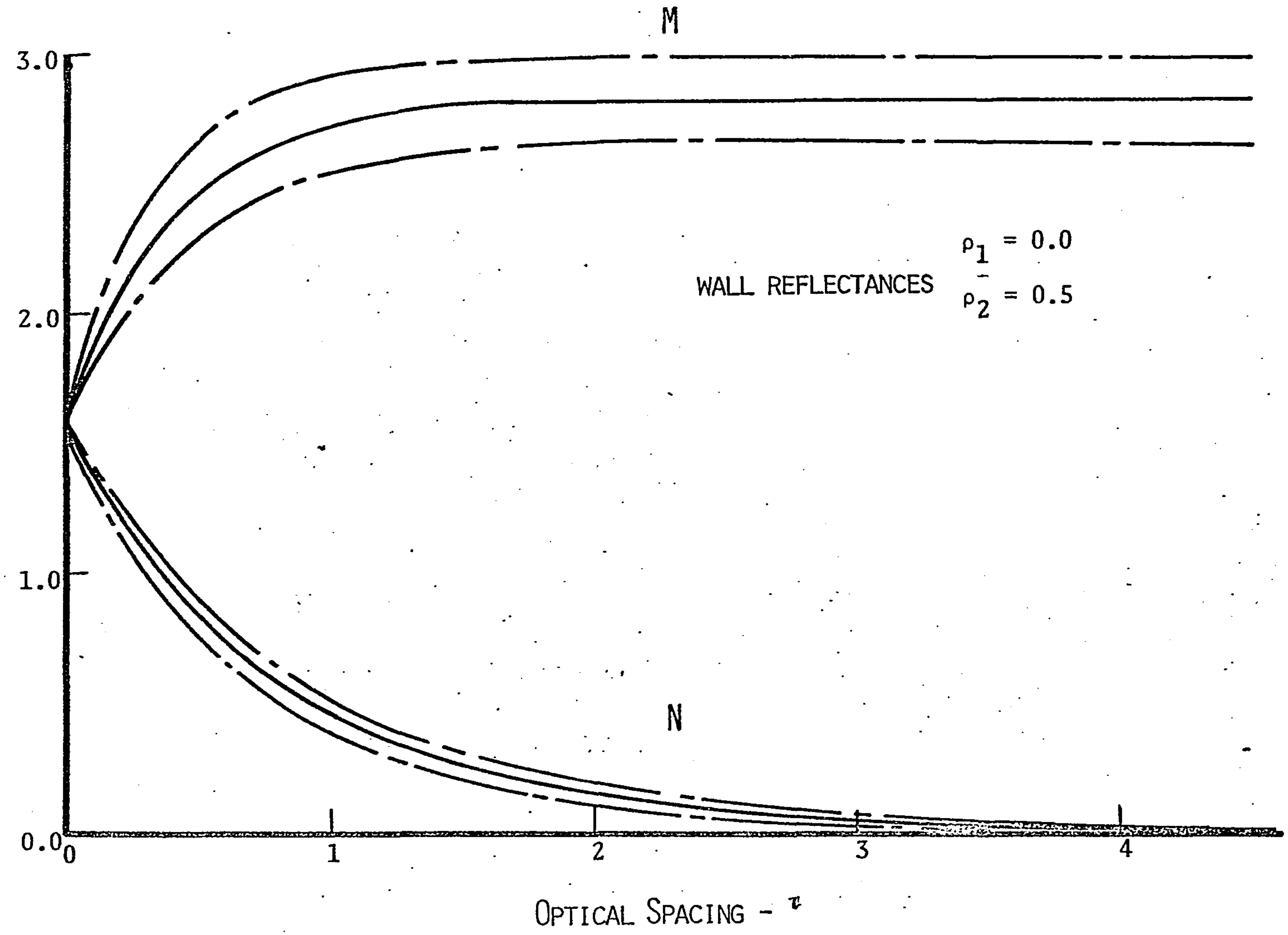
M
N
3.0
2.0
1.0
0.0
0
1
2
3
4
WALL REFLECTANCES
$\rho_1 = 0.0$
$\rho_2 = 0.5$
OPTICAL SPACING - τ

Figure 17

wall reflectance arrangements were treated: 0.1, 0.5, 0.9. The numerical curve fitting was done using the Osage computer. The curves were fitted by polynomials

$$M' = C_0 + C_1\tau + C_2\tau^2 + \ldots\ldots\ldots\ldots + C_9\tau^9 + \ldots$$

Both five terms and ten terms were examined. It was found that the use of five terms for fitting the data was sufficiently accurate. The "ORNOR" curve fitting subrouting program of the computer laboratory at the University of Oklahoma was utilized. This program was written in both the Fortran and the Algol languages.

With the above functional expressions, the entire calculation was written in Fortran language and the iteration was done by the computer. The calculation was made at every 0.1 foot interval of x up to 1.5 feet on the plate. The iteration was over the thermal boundary layer thickness δ_t of equation (41).

The main program has the following procedures:

(i). Compute δ, the velocity boundary layer thickness by

$$\delta = \frac{5x}{\sqrt{Re}} \tag{49}$$

(ii). Calculate the particle size parameters

$$\alpha_{ij} = C_i T_j D \tag{50}$$

where C_i are constants given in reference (2).

(iii). Compute K^e for each α_{ij} obtained above. (K^e - α curve was represented by fitted equation here)

(iv). Compute optical spacing, τ for three values of δ_t, by

$$\tau_{ij} = \rho\beta(\delta_t)_{ij} \tag{51}$$

The initial three values of δ_t were estimated.

(v). Compute M, N and Q and M', N' and Q' by their individual curve fitting equation.

(vi). Calculate the net radiative heat flux from both walls and compute their differences. These are equation (19) and equation (44) and

$$\Delta q_r = q_{net\ 1} + q_{net\ 2} \tag{52}$$

Substituting equations (19) and (44) into equation (53) we have

$$\Delta q_r = 10^{-11}[T_1^4 \left(\sum_{j=1}^{n} A_j M_j - \sum_{j=1}^{n} A_j N_j'\right) + T_2^4\left(\sum_{j=1}^{n} A_j M_j' - \sum_{j=1}^{n} A_j N_j\right)$$
$$- T_a^4\left(\sum_{j=1}^{n} A_j Q_j - \sum_{j=1}^{n} A_j Q_j'\right)] \tag{53}$$

q_r is always positive no matter whether a cold wall case or a hot wall case exists. This implies that in the energy balance of a control volume in the boundary layer, the net radiative heat always gives heat to the control volume. This is contrary to the conductive and convective transfer terms which may have different directions (in or out of the volume) depending on hot wall case or cold wall case.

(vii). Calculate the left hand side of equation (41)

(viii). Compare results of step (vi) and (vii). If the difference was within pre-determined accuracy, a solution was obtained. The calculation was then moved down stream to the next point. If the difference was greater than the pre-determined accuracy, the method of half interval was employed to obtain a narrower range of δ_t's. Then the same process was repeated until a satisfactory answer was obtained.

(ix). The outputs of the program were:

q_r, the heat transfer by radiation at the wall.

q_c, the heat transfer by conduction at the wall.

q_r/q_c, their ratio.

δ, the velocity boundary layer thickness.

δ_t, the thermal boundary layer thickness.

and $q_r + q_c$, the total heat flux.

The numerical results are presented in Figure 18 through Figure 29, for hot wall cases and in Figures 30 through

Figure 41 for cold wall cases. The programs and results are listed in Appendix (D), (E), (F) and (G).

Figures 26 to 29 show the thermal boundary layer thickness for the hot wall cases. Figures 38 to 41 show the thickness for the cold wall cases.

Results of equation (46) for the non-radiation case are shown in Figure 42.

From the study of the above results, it was concluded as follows:

The addition of radiant heat transfer terms in the energy equation has a strong influence on the thickness of boundary layer and the heat transfer. This addition is necessary especially when the temperature of the wall is relatively high. For hot wall cases, it is found that when the wall temperature is 2000 ^{o}R or under, the radiative heat transfer is rather small. It may only be a fraction of what is conducted and may be negligible. But when the wall temperature is above 2000 ^{o}R the radiative heat transfer begins to show its importance. When the wall temperature is higher than 3000 ^{o}R, the radiative heat transfer is dominant. Hence the radiative heat transfer should be taken into account. The above are also true for cold wall cases.

Quantitatively, under the same boundary conditions, the radiative heat transfer in the EAS medium is slightly less than that in the non-scattering medium. This may be explained by noting that the characteristics of the EAS medium are the factors attenuating the energy traversing the medium. A non-scattering medium means that one of the obstacles is removed, hence more heat may pass with less chance of changing direction or reducing intensity. Also, as would be expected, a wall with a small reflectance transfers more heat than a wall with a large reflectance.

The total heat transfer of the wall does not differ very much whether it is a hot wall case or a cold wall case. The direction of heat transfer at the wall is different for these two cases. Also, it should be mentioned here that the temperature profile of equation (43) was used for these calculations. The results show little difference from those computed by using the temperature profile of equation (35).

For hot wall cases, the thickness of the thermal boundary layer is increased, and as would be anticipated is greater than the thickness of the velocity boundary layer. For cold wall cases, when the free stream temperature is relatively small (under 2000 ^{o}R) the thermal boundary layer has about the same thickness as corresponding hot wall cases, but when the free stream has a higher temperature, the thermal boundary layer becomes smaller than the velocity boundary layer. This is due to the heat gain in the boundary layer by radiation. Since the thermal boundary is thin, the conductive heat transfer at the wall is also increased.

The thermal boundary layer thickness is greater for a radiating fluid than for non-radiation fluids except for cold wall cases of high free stream temperature. The thermal boundary layer is thicker in the non-scattering medium than in an EAS medium, although the difference is not very great. At wall temperatures of 2000 $^{\circ}$R or under the thickness is only increased slightly and the boundary layer maintains the usual familiar shape. When the wall temperature is higher than 2000 $^{\circ}$R, the thickness begins to increase rapidly, the usual shape of boundary layer also begins to change. The thickness of the boundary layer in both the EAS medium and the non-scattering medium certainly are much greater than that in the non-scattering medium but, the numerical value of the boundary layer thickness is still small comparing to the distance from the leading edge. At $x = 1.5$ feet, the largest thickness ever obtained was 0.024 feet. This shows that the plane parallel approximation for the radiative heat transfer should be valid.

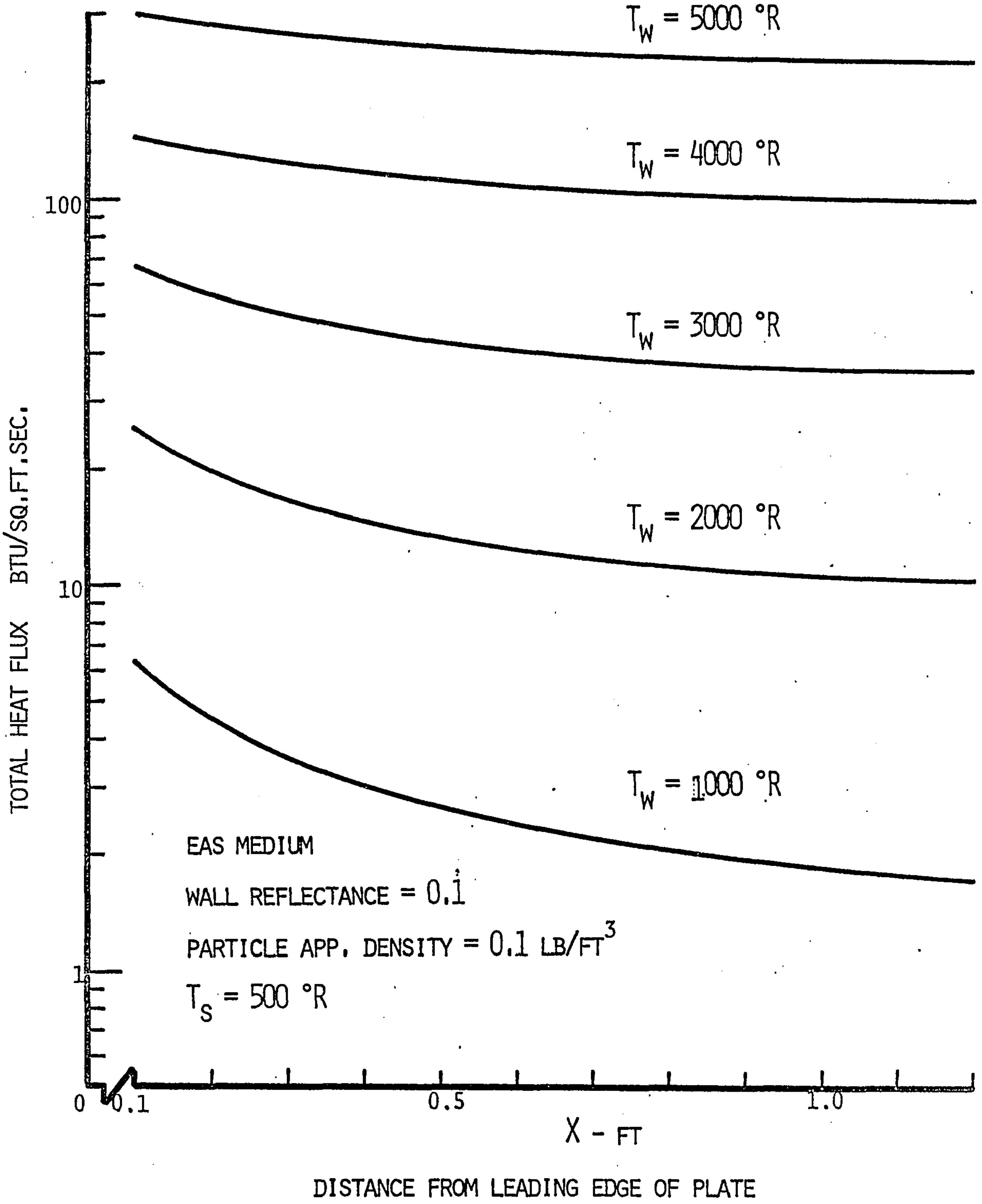

T_W = 5000 °R
T_W = 4000 °R
T_W = 3000 °R
T_W = 2000 °R
T_W = 1000 °R
100
10
1
TOTAL HEAT FLUX BTU/SQ.FT.SEC.
EAS MEDIUM
WALL REFLECTANCE = 0.1
PARTICLE APP. DENSITY = 0.1 LB/FT^3
T_S = 500 °R
0
0.1
0.5
1.0
X - FT
DISTANCE FROM LEADING EDGE OF PLATE

Figure 18

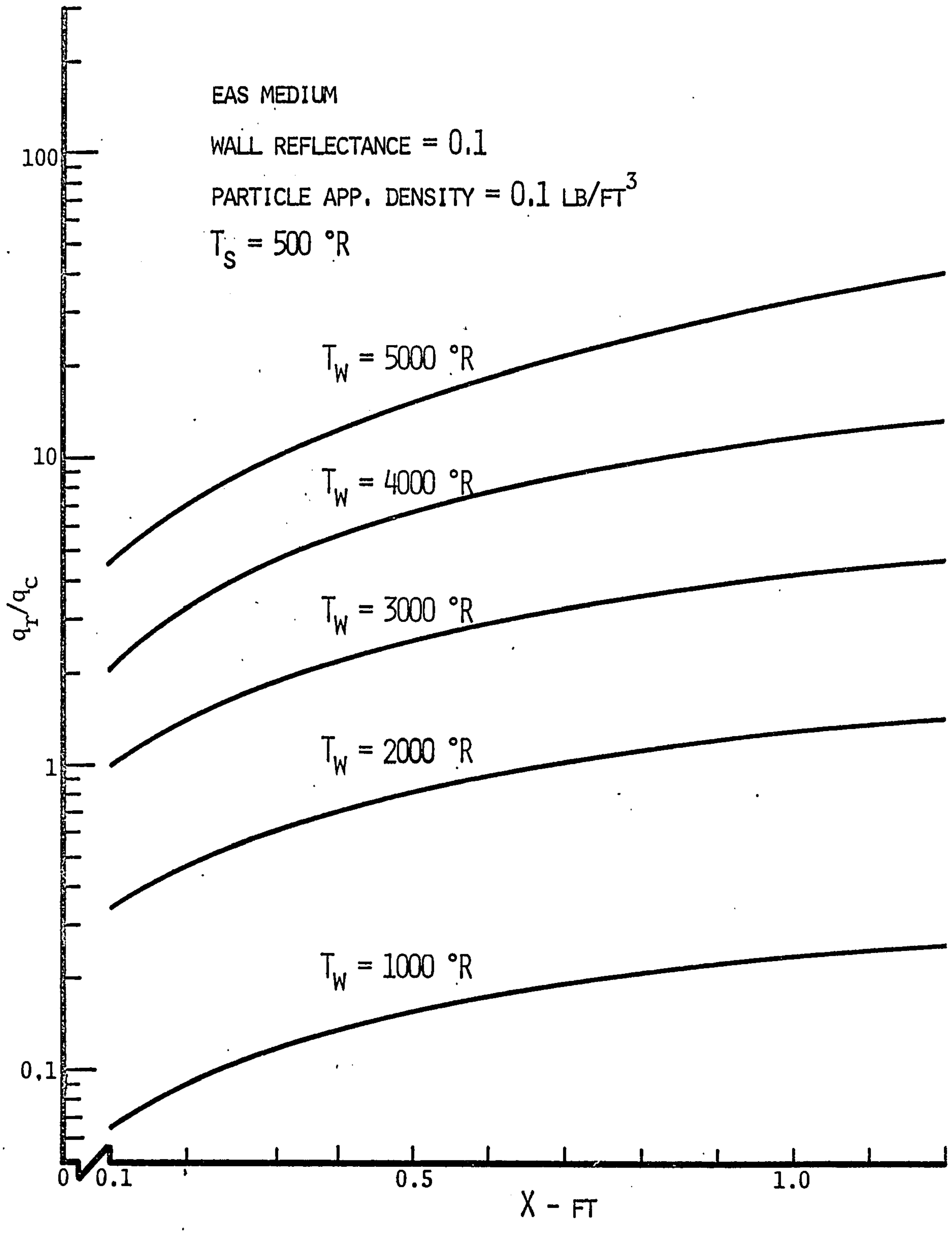

DISTANCE FROM LEADING EDGE OF PLATE

Figure 19

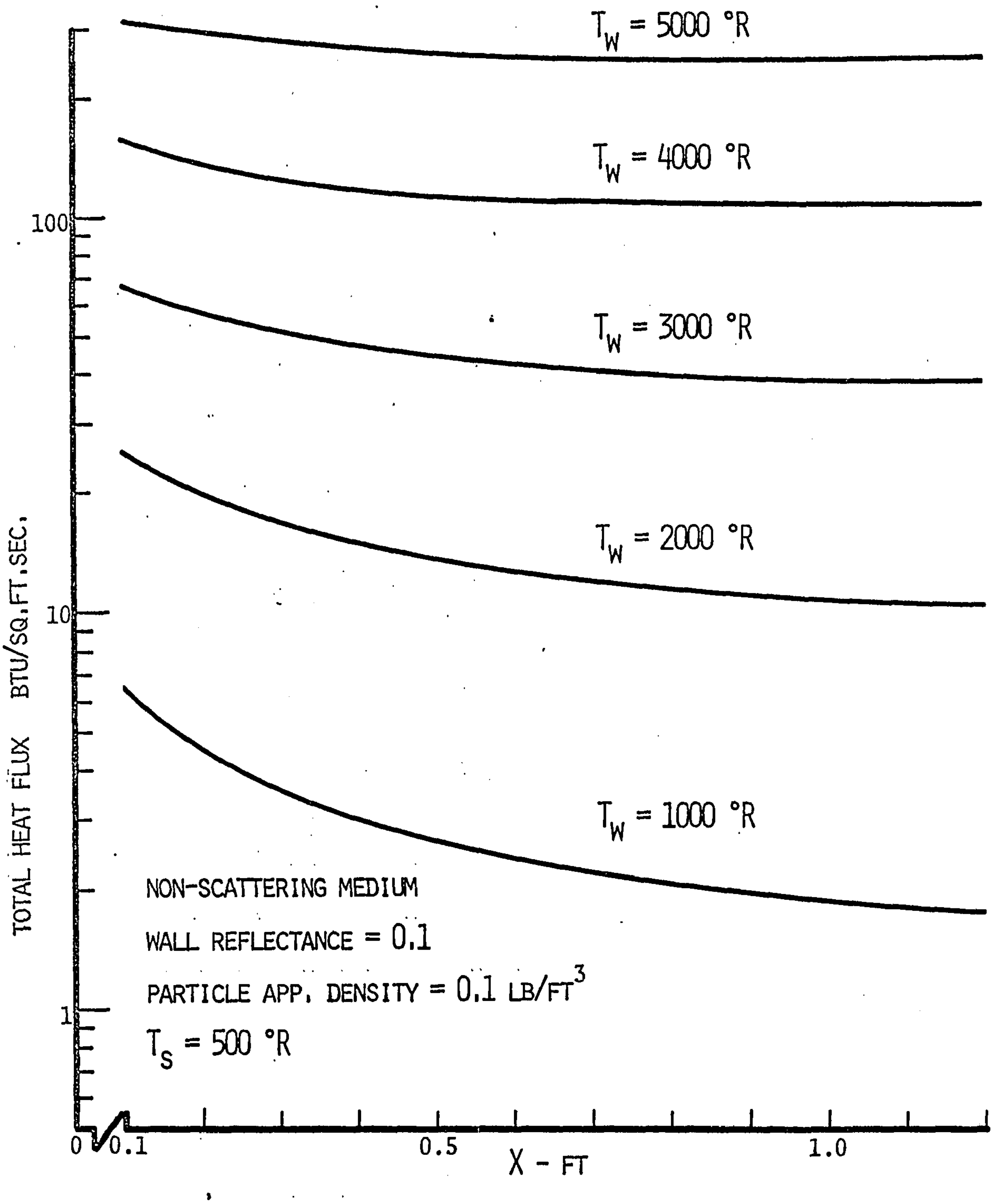

DISTANCE FROM LEADING EDGE OF PLATE

Figure 20

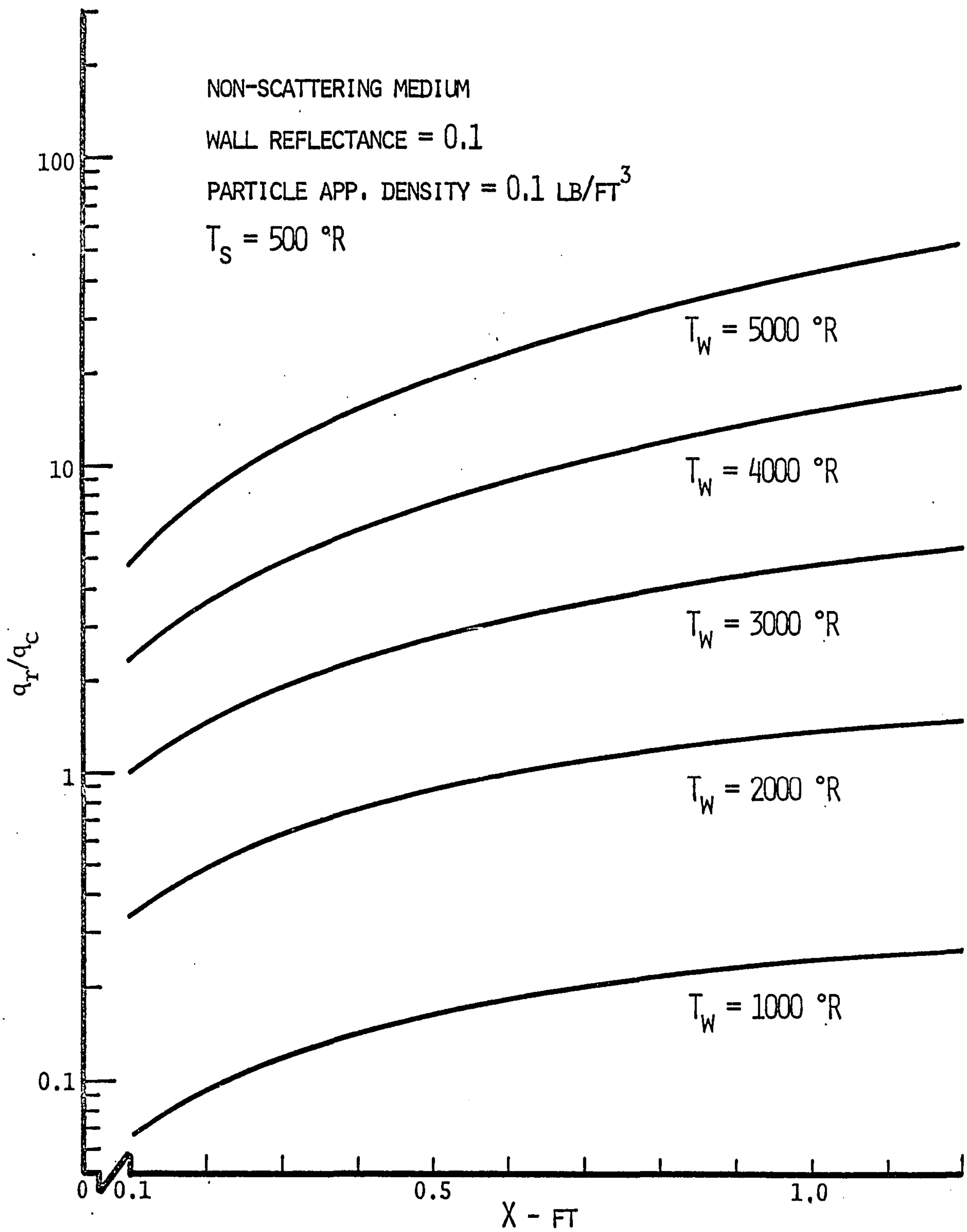

DISTANCE FROM LEADING EDGE OF PLATE

Figure 21

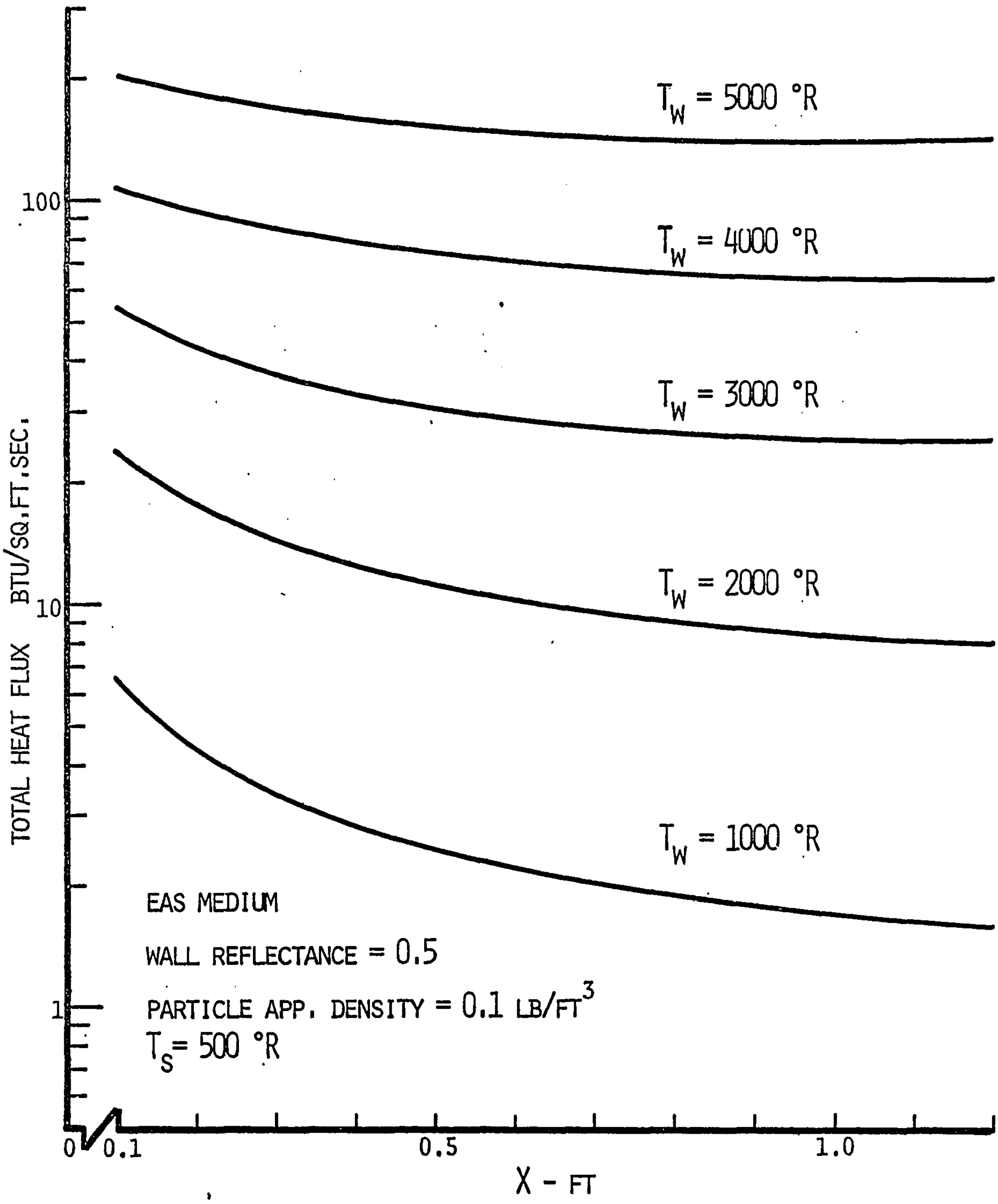

DISTANCE FROM LEADING EDGE OF PLATE

Figure 22

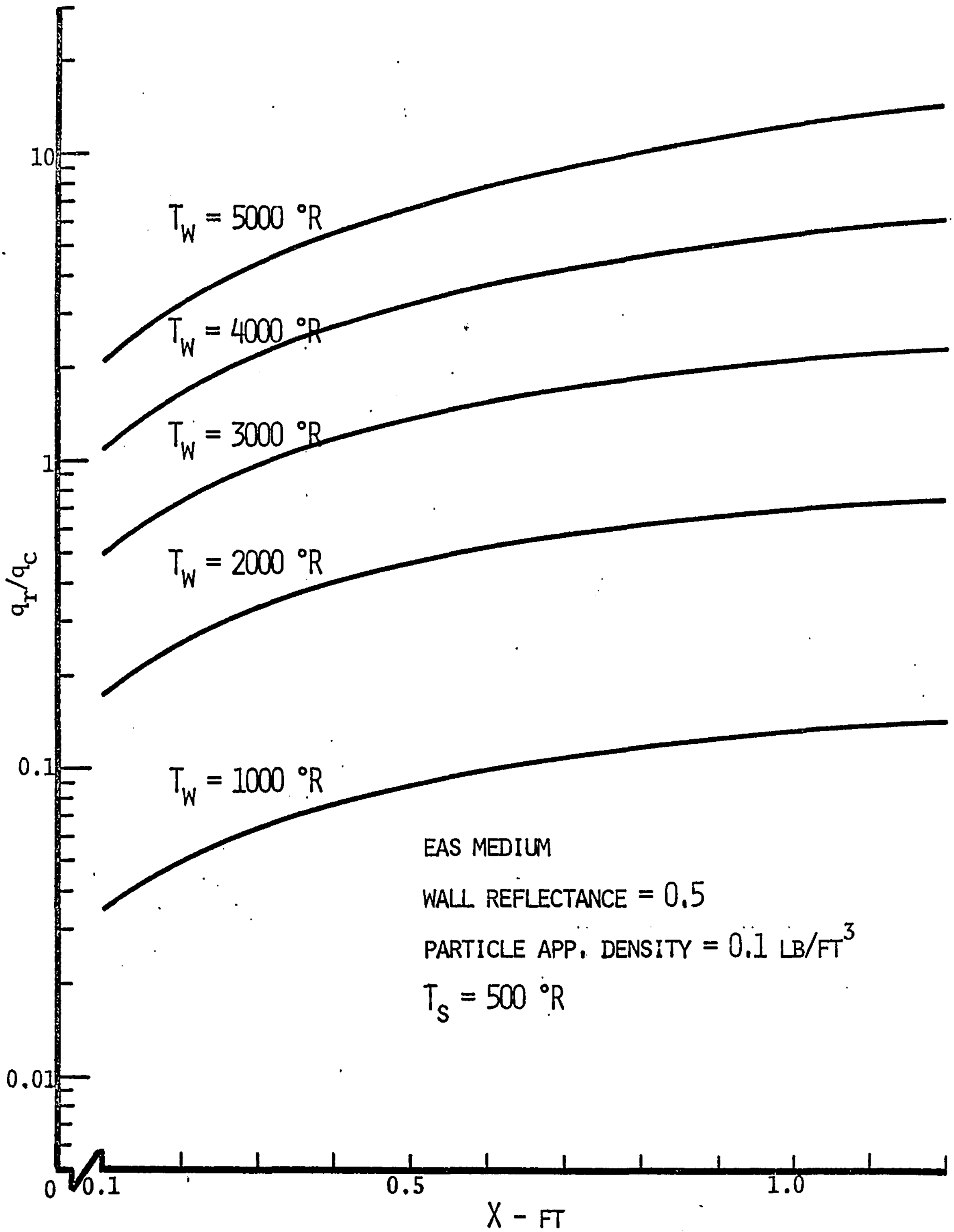

DISTANCE FROM LEADING EDGE OF PLATE

Figure 23

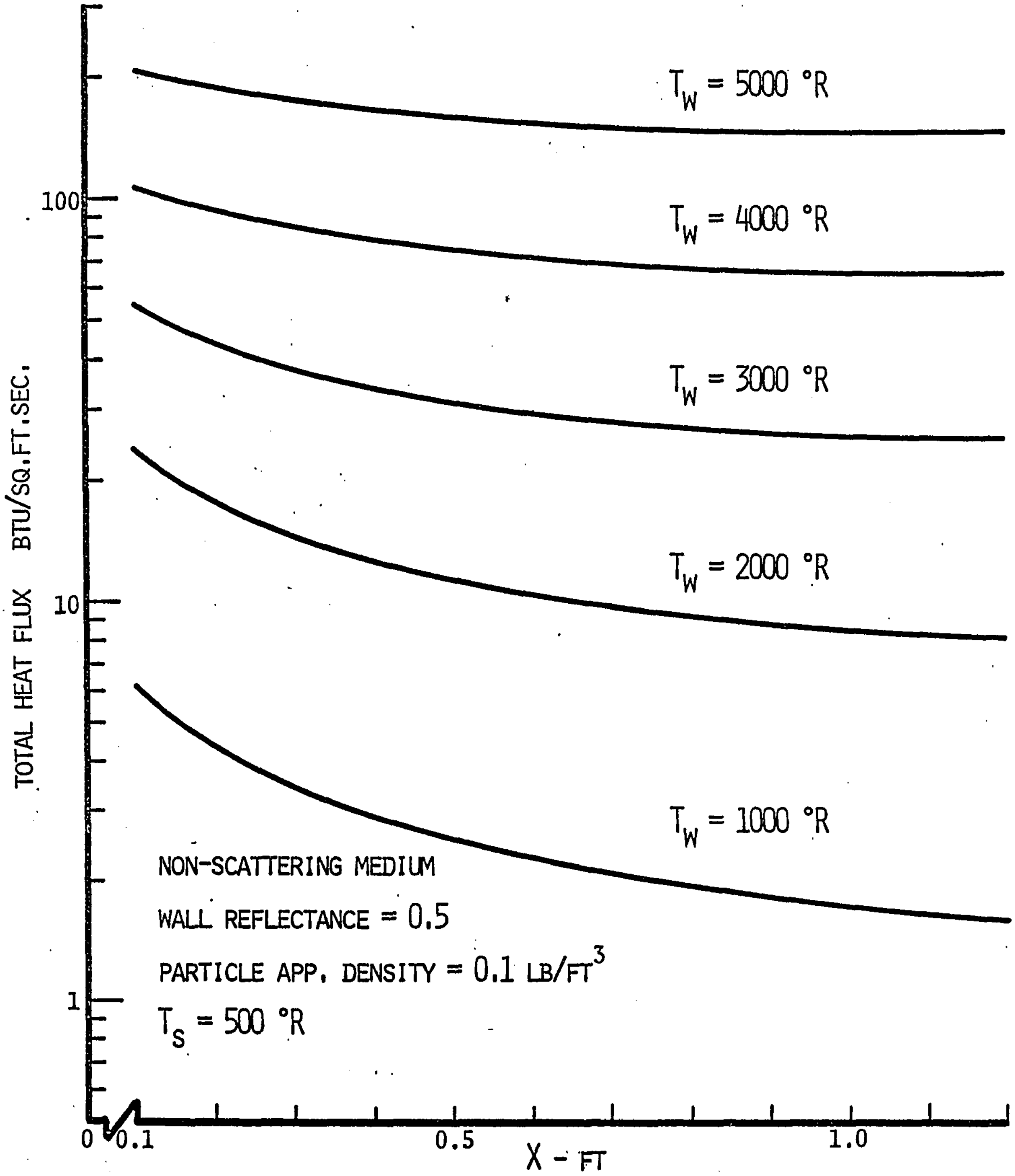

DISTANCE FROM LEADING EDGE OF PLATE

Figure 24

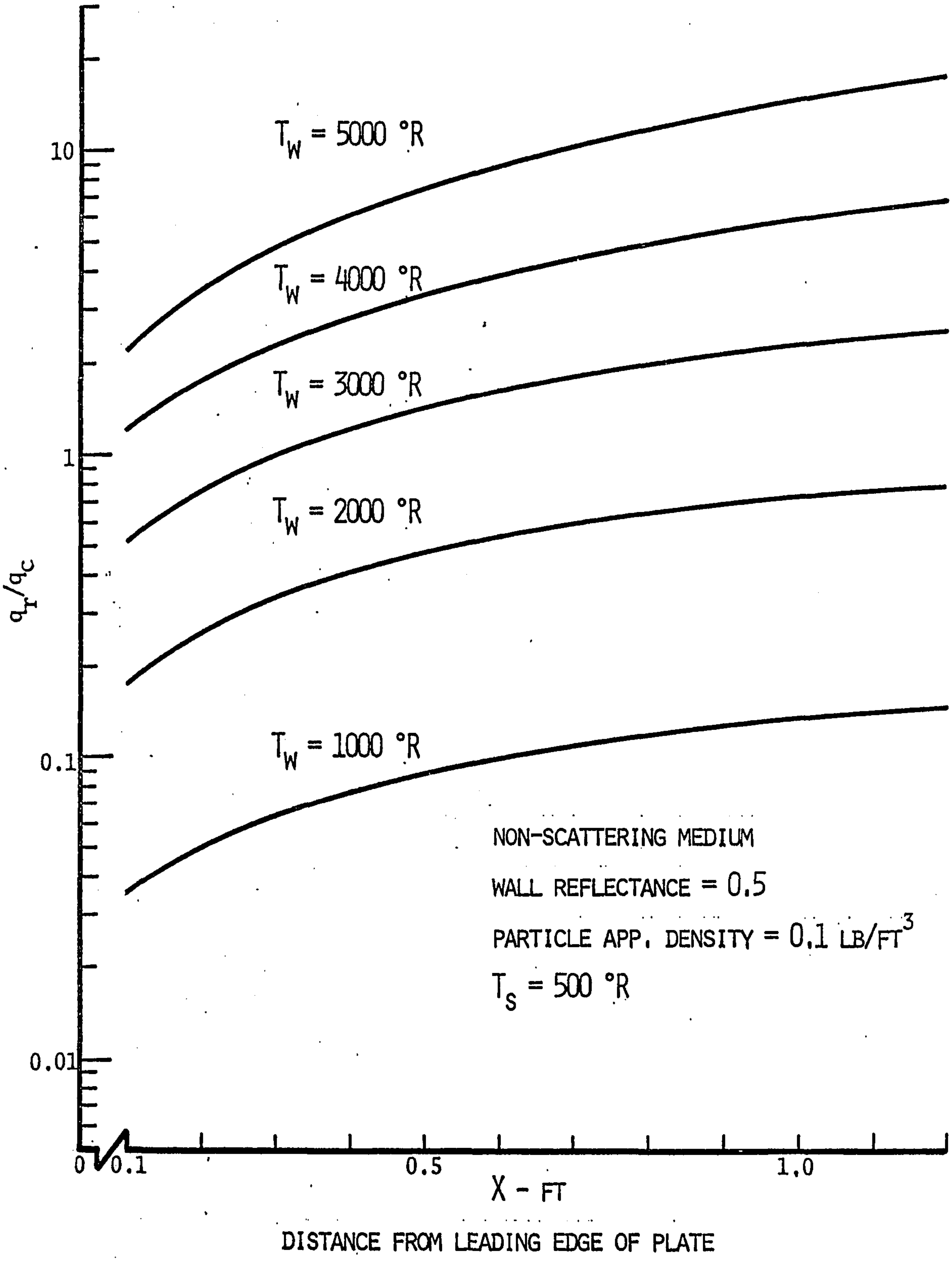

q_r/q_c
10
1
0.1
0.01
T_W = 5000 °R
T_W = 4000 °R
T_W = 3000 °R
T_W = 2000 °R
T_W = 1000 °R
NON-SCATTERING MEDIUM
WALL REFLECTANCE = 0.5
PARTICLE APP. DENSITY = 0.1 LB/FT^3
T_S = 500 °R
0
0.1
0.5
1.0
X - FT
DISTANCE FROM LEADING EDGE OF PLATE

Figure 25

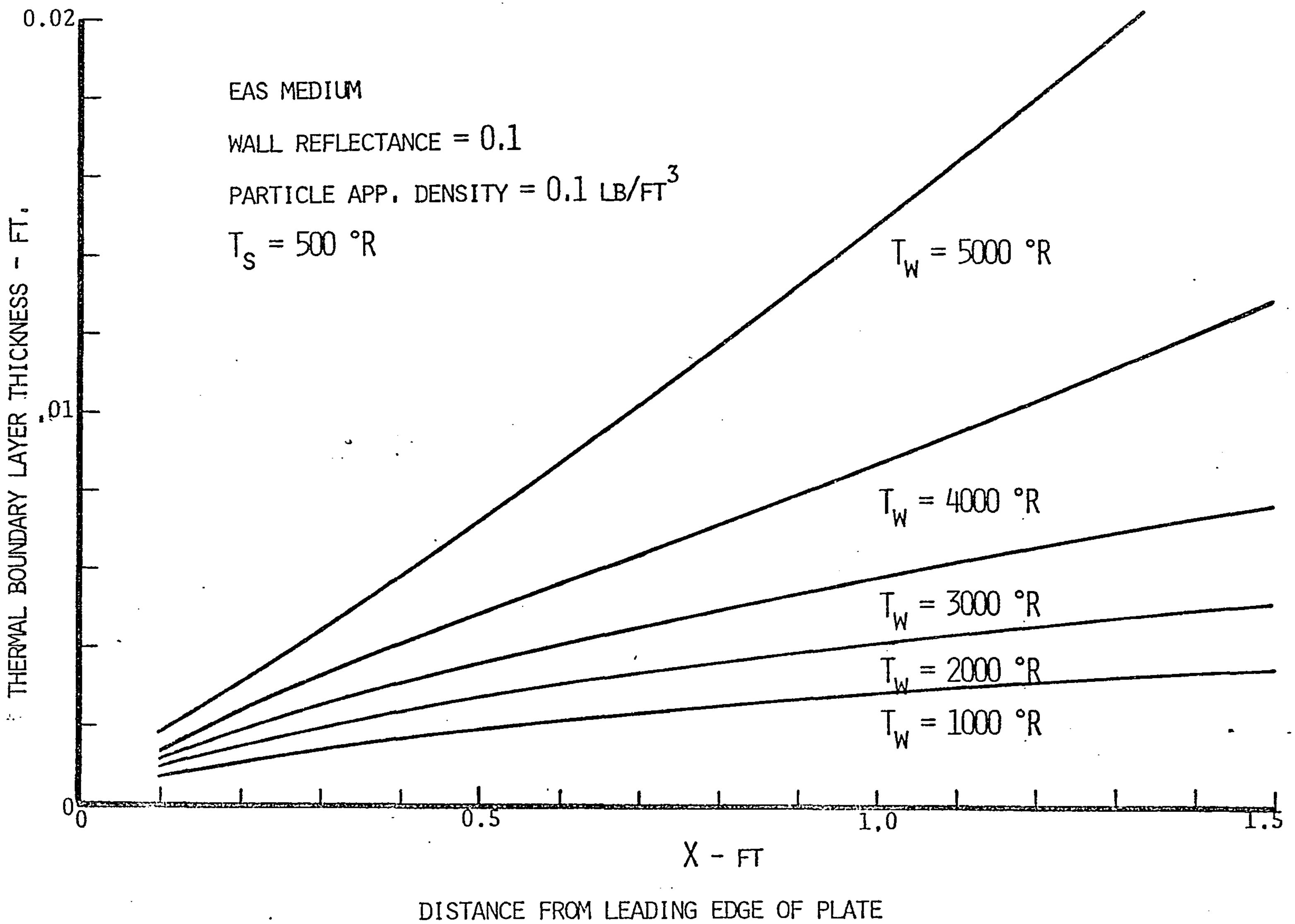

0.02
.01
0
0
0.5
1.0
1.5
THERMAL BOUNDARY LAYER THICKNESS - FT.
X - FT
DISTANCE FROM LEADING EDGE OF PLATE
EAS MEDIUM
WALL REFLECTANCE = 0.1
PARTICLE APP. DENSITY = 0.1 LB/FT^3
T_S = 500 °R
T_W = 5000 °R
T_W = 4000 °R
T_W = 3000 °R
T_W = 2000 °R
T_W = 1000 °R

Figure 26

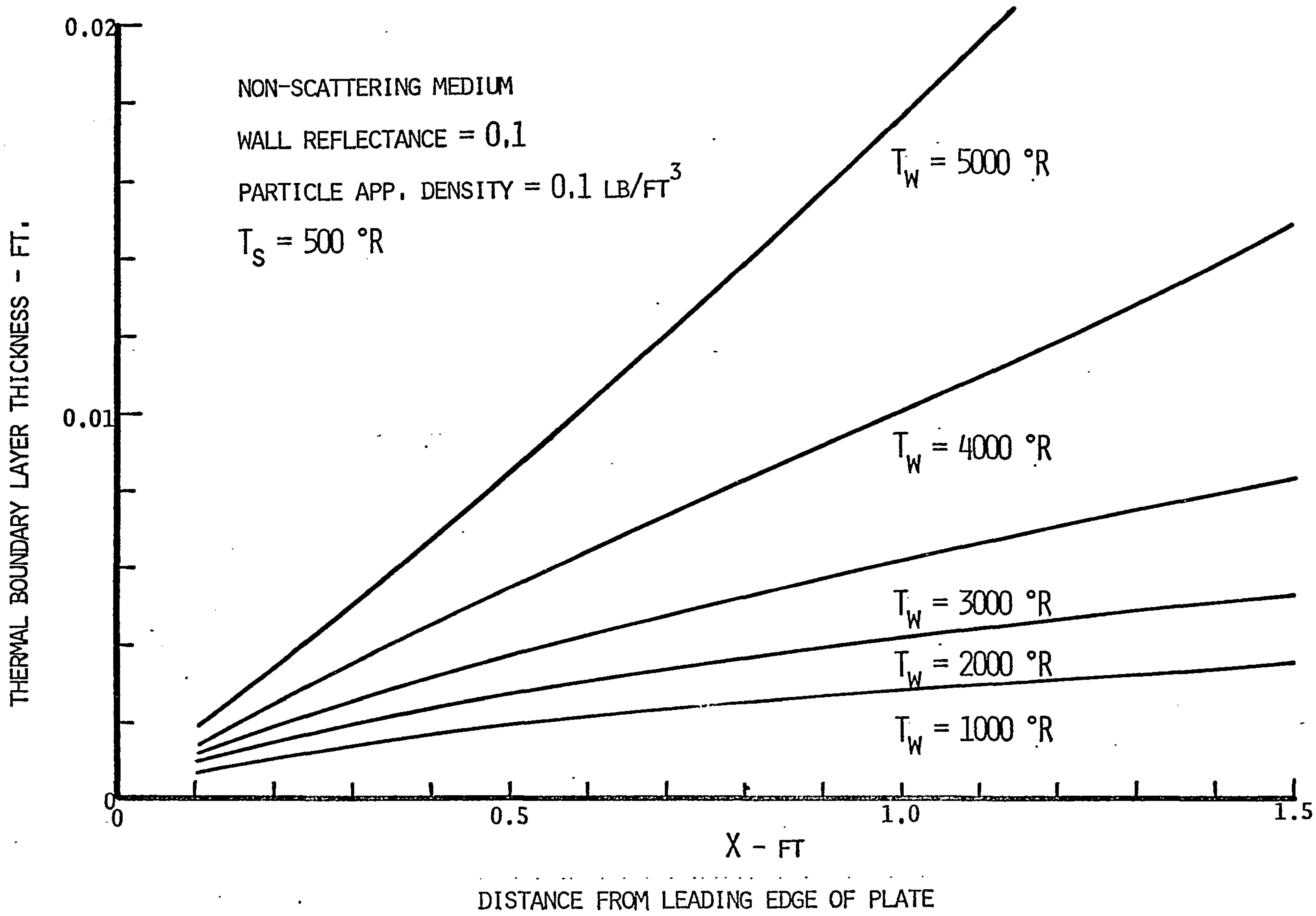
NON-SCATTERING MEDIUM
WALL REFLECTANCE = 0.1
PARTICLE APP. DENSITY = 0.1 LB/FT^3
T_S = 500 °R
T_W = 5000 °R
T_W = 4000 °R
T_W = 3000 °R
T_W = 2000 °R
T_W = 1000 °R
THERMAL BOUNDARY LAYER THICKNESS - FT.
0.02
0.01
0
0
0.5
1.0
1.5
X - FT
DISTANCE FROM LEADING EDGE OF PLATE

Figure 27

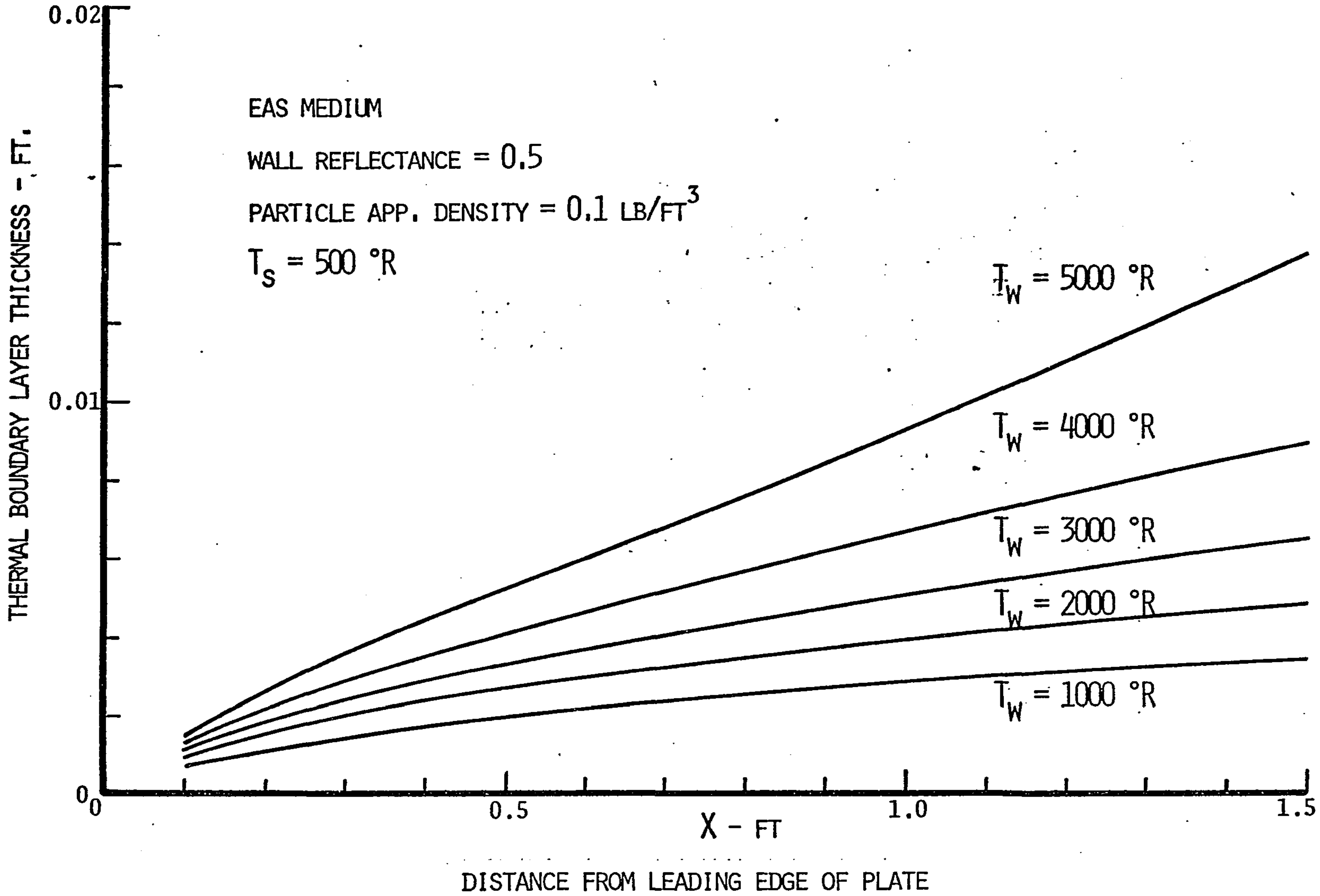
EAS MEDIUM
WALL REFLECTANCE = 0.5
PARTICLE APP. DENSITY = 0.1 LB/FT3
Ts = 500 °R
Tw = 5000 °R
Tw = 4000 °R
Tw = 3000 °R
Tw = 2000 °R
Tw = 1000 °R
THERMAL BOUNDARY LAYER THICKNESS - FT.
0.02
0.01
0
0
0.5
1.0
1.5
X - FT
DISTANCE FROM LEADING EDGE OF PLATE

Figure 28

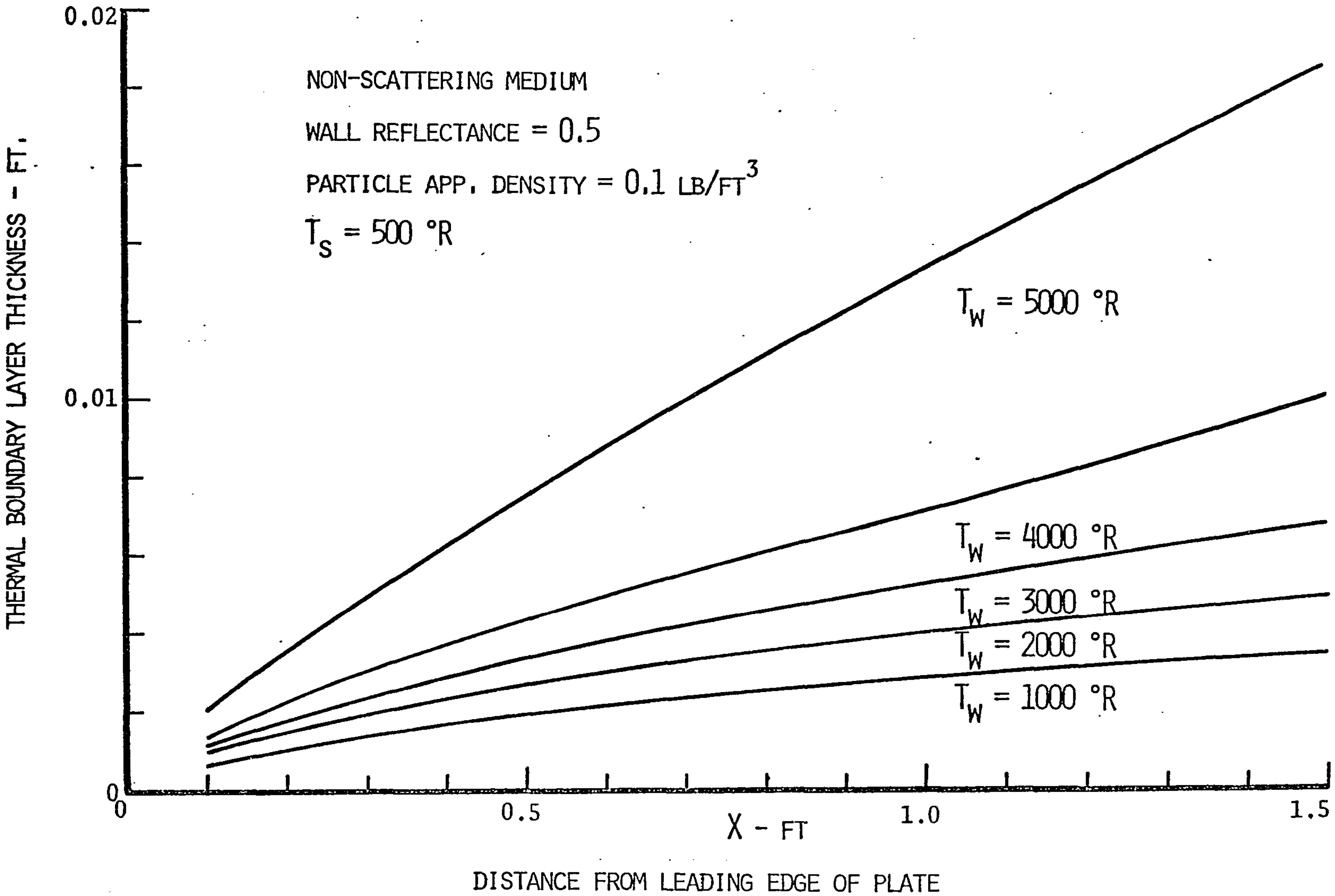
NON-SCATTERING MEDIUM
WALL REFLECTANCE = 0.5
PARTICLE APP. DENSITY = 0.1 LB/FT^3
T_S = 500 °R
T_W = 5000 °R
T_W = 4000 °R
T_W = 3000 °R
T_W = 2000 °R
T_W = 1000 °R
THERMAL BOUNDARY LAYER THICKNESS - FT.
0.02
0.01
0
0
0.5
1.0
1.5
X - FT
DISTANCE FROM LEADING EDGE OF PLATE

Figure 29

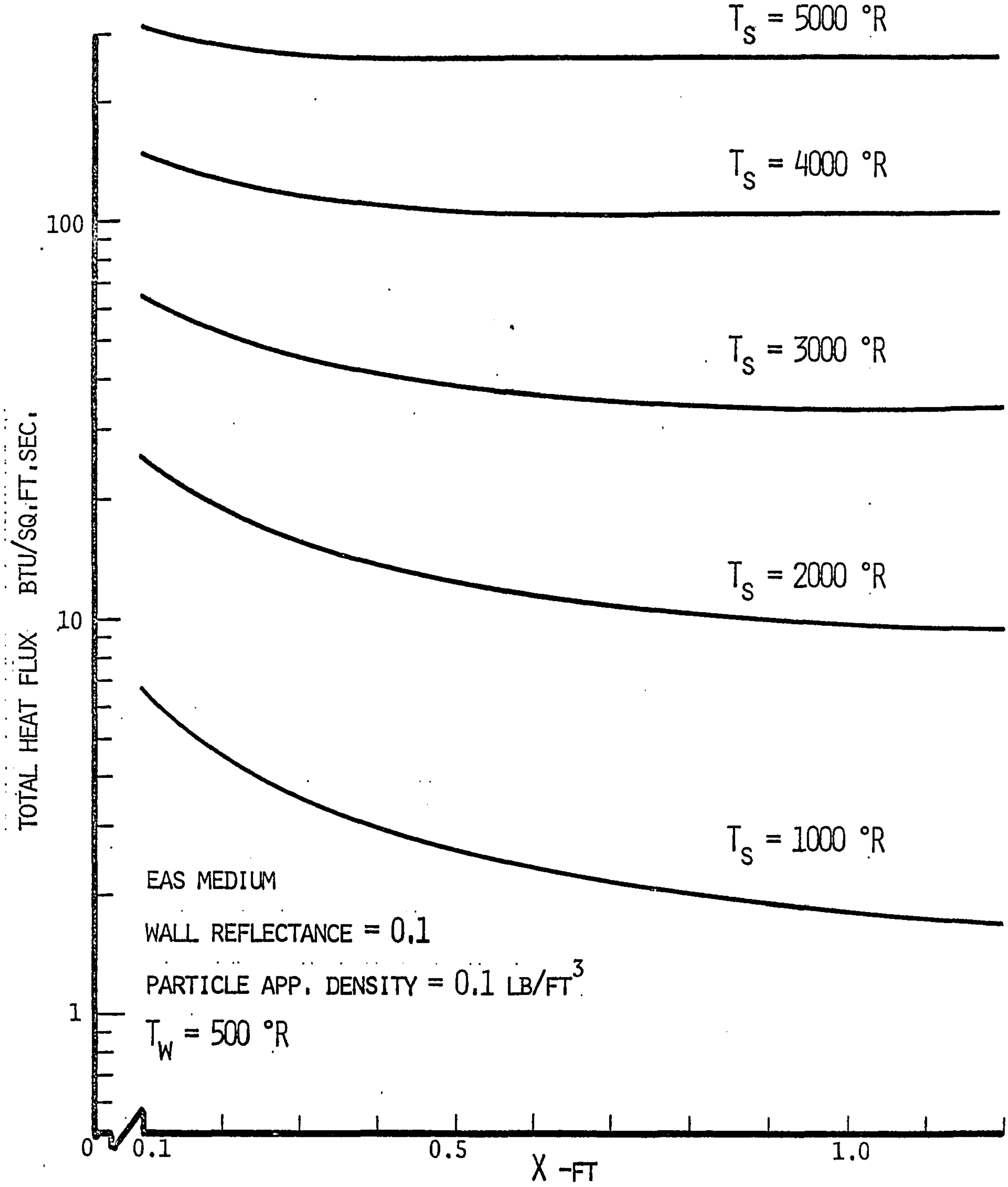

DISTANCE FROM LEADING EDGE OF PLATE

Figure 30

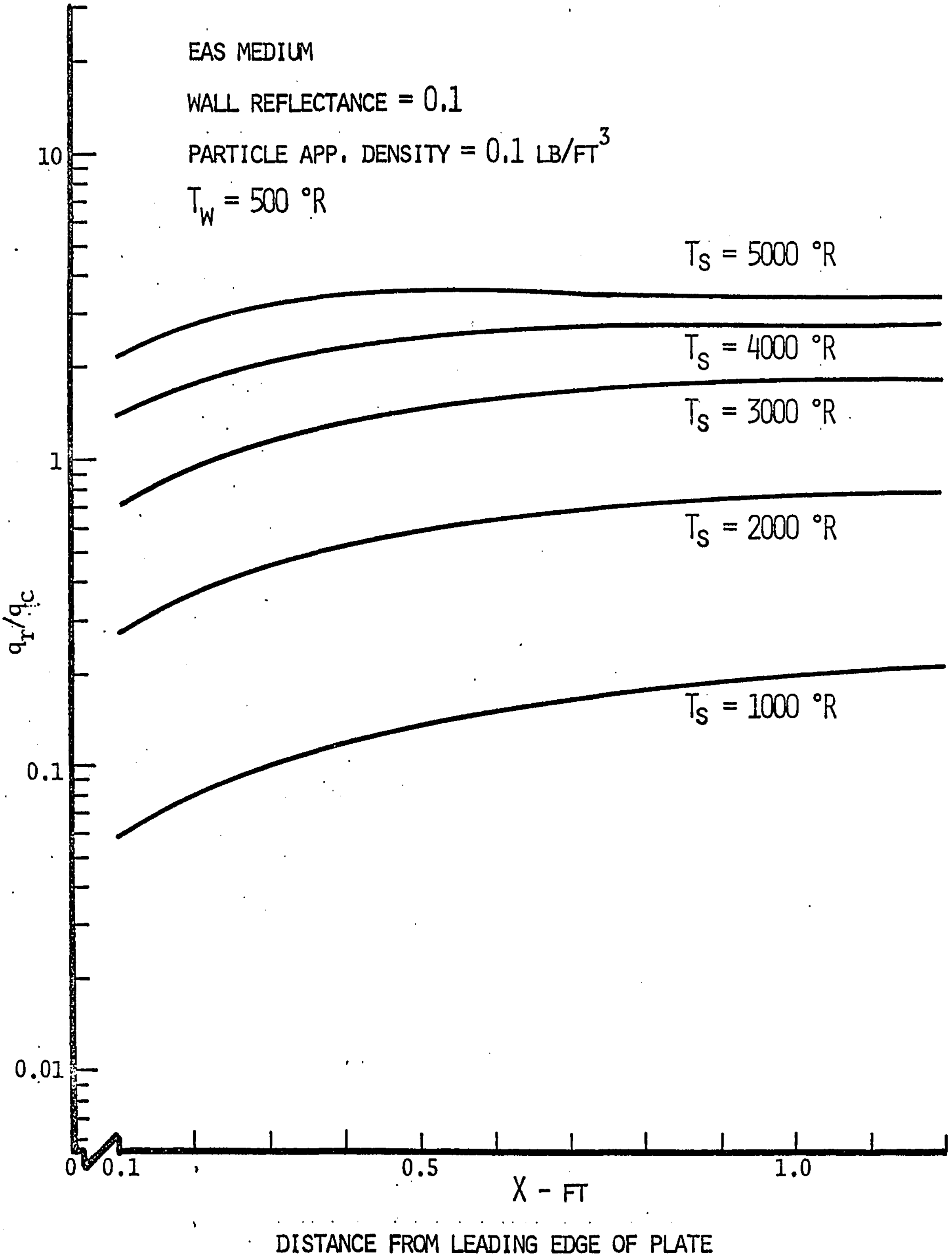
EAS MEDIUM
WALL REFLECTANCE = 0.1
PARTICLE APP. DENSITY = 0.1 LB/FT^3
T_W = 500 °R
T_S = 5000 °R
T_S = 4000 °R
T_S = 3000 °R
T_S = 2000 °R
T_S = 1000 °R
q_r/q_c
10
1
0.1
0.01
0
0.1
0.5
1.0
X - FT
DISTANCE FROM LEADING EDGE OF PLATE

Figure 31

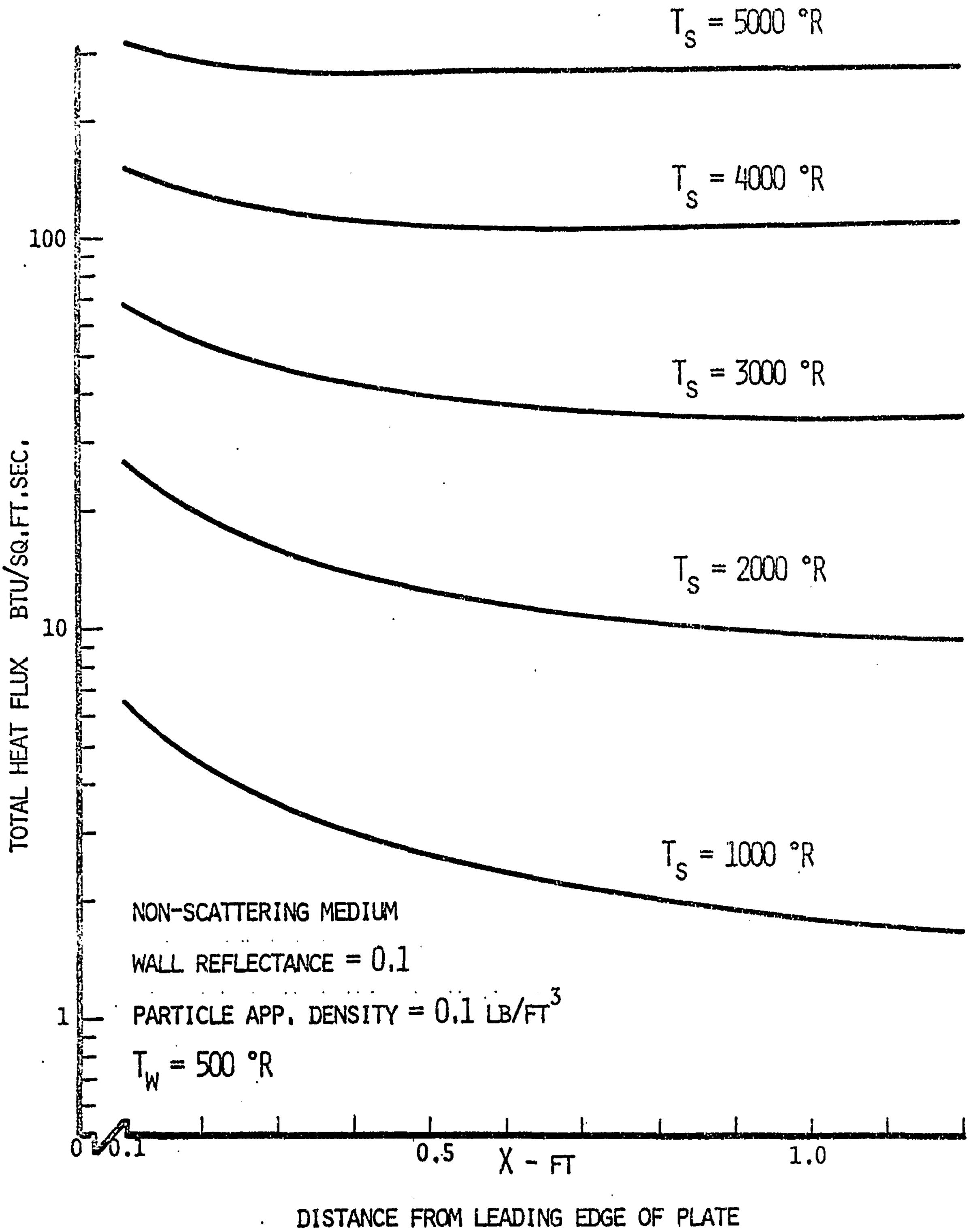
T_S = 5000 °R
T_S = 4000 °R
T_S = 3000 °R
T_S = 2000 °R
T_S = 1000 °R
100
10
1
TOTAL HEAT FLUX BTU/SQ.FT.SEC.
NON-SCATTERING MEDIUM
WALL REFLECTANCE = 0.1
PARTICLE APP. DENSITY = 0.1 LB/FT^3
T_W = 500 °R
0
0.1
0.5
X - FT
1.0
DISTANCE FROM LEADING EDGE OF PLATE

Figure 32

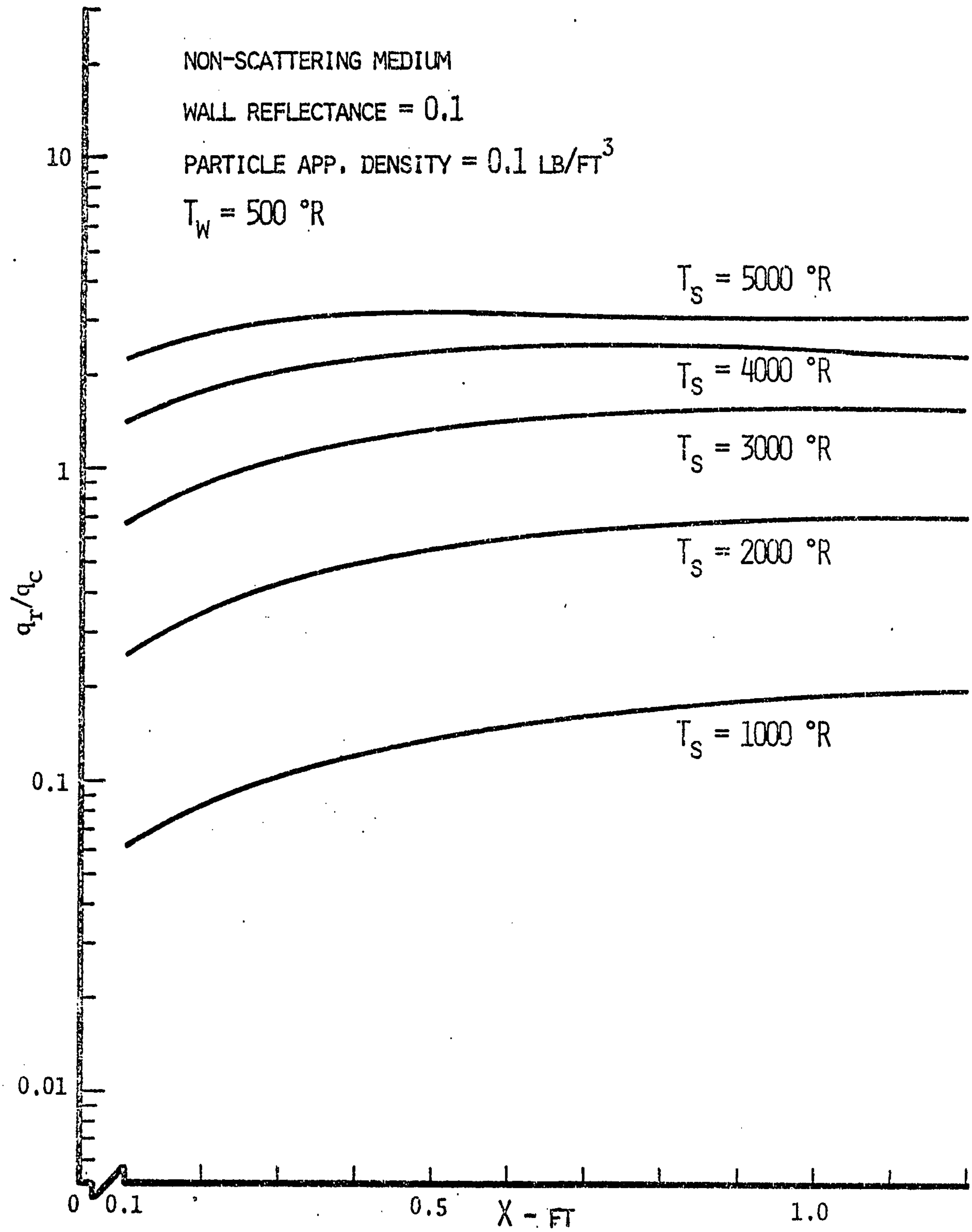

DISTANCE FROM LEADING EDGE OF PLATE

Figure 33

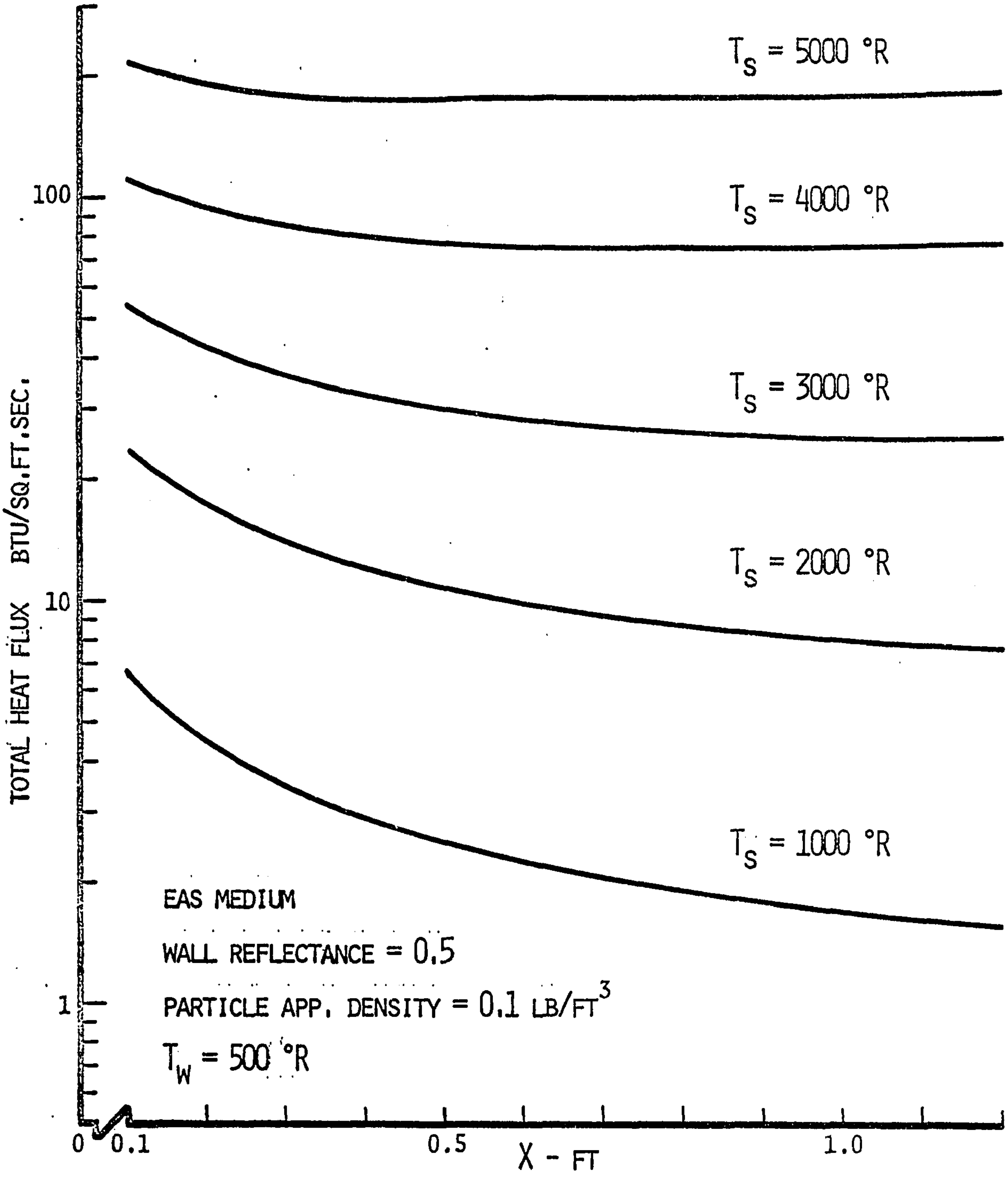

DISTANCE FORM LEADING EDGE OF PLATE

Figure 34

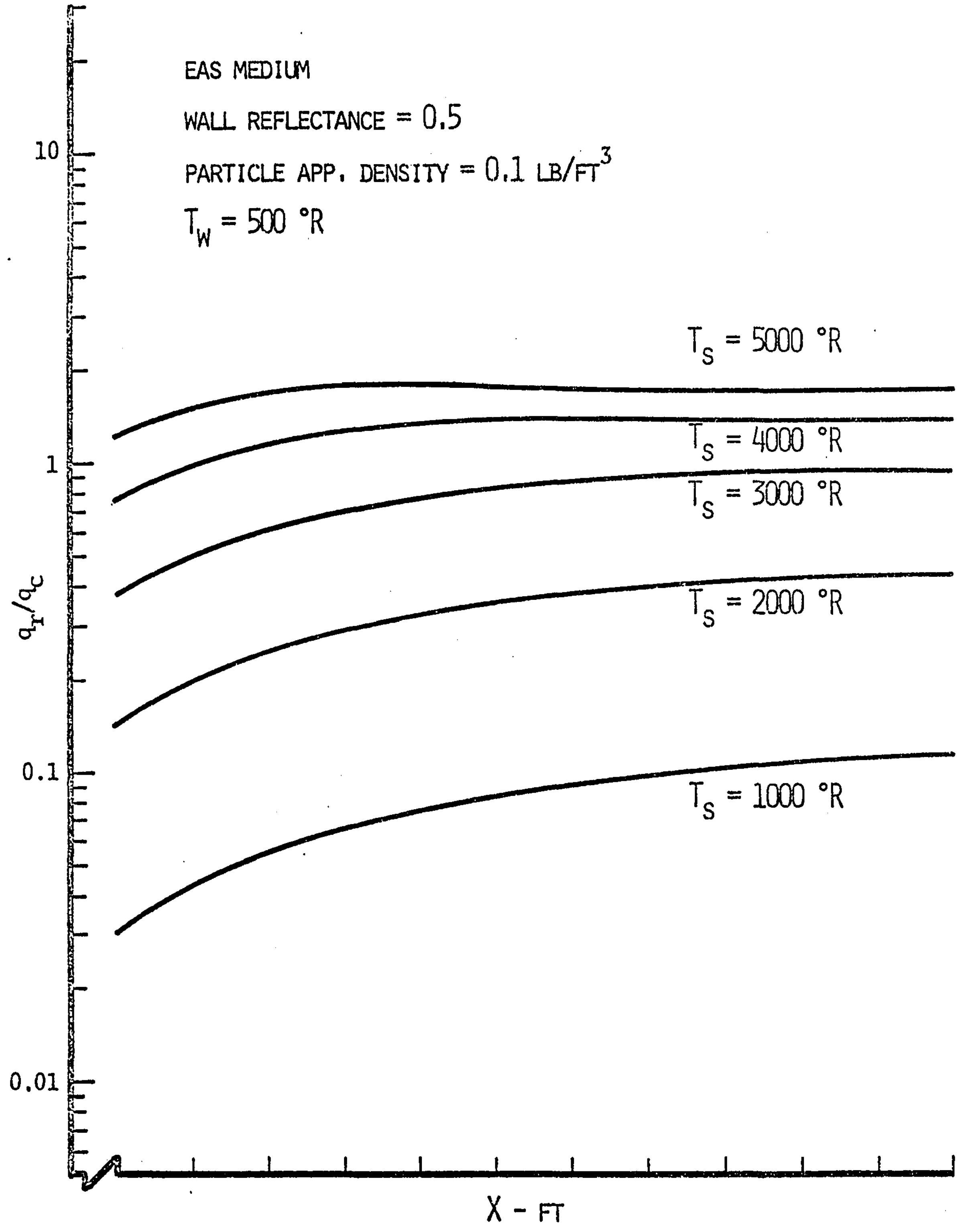

DISTANCE FROM LEADING EDGE OF PLATE

Figure 35

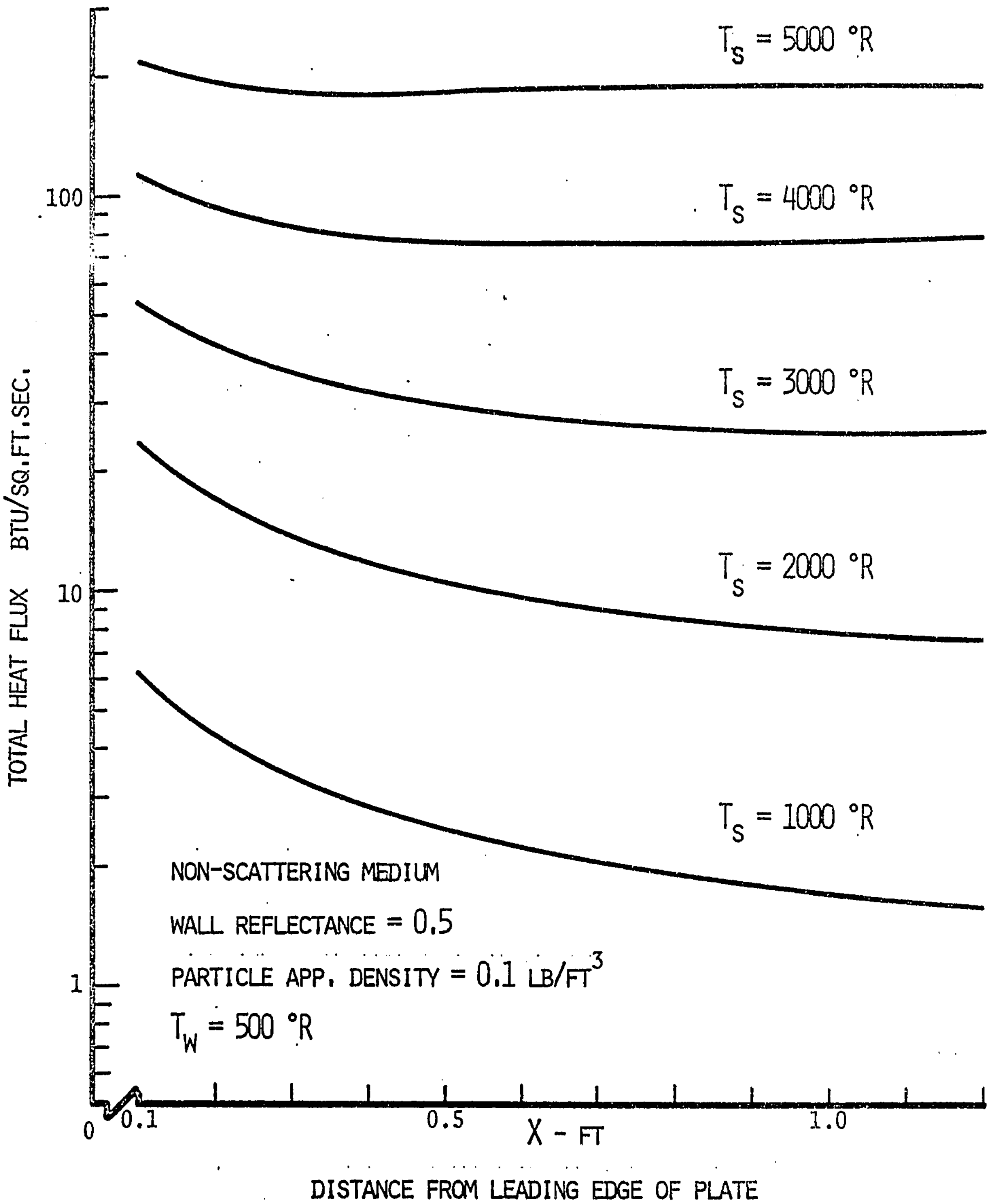

T_S = 5000 °R
T_S = 4000 °R
T_S = 3000 °R
T_S = 2000 °R
T_S = 1000 °R
NON-SCATTERING MEDIUM
WALL REFLECTANCE = 0.5
PARTICLE APP. DENSITY = 0.1 LB/FT^3
T_W = 500 °R
TOTAL HEAT FLUX BTU/SQ.FT.SEC.
100
10
1
0
0.1
0.5
1.0
X - FT
DISTANCE FROM LEADING EDGE OF PLATE

Figure 36

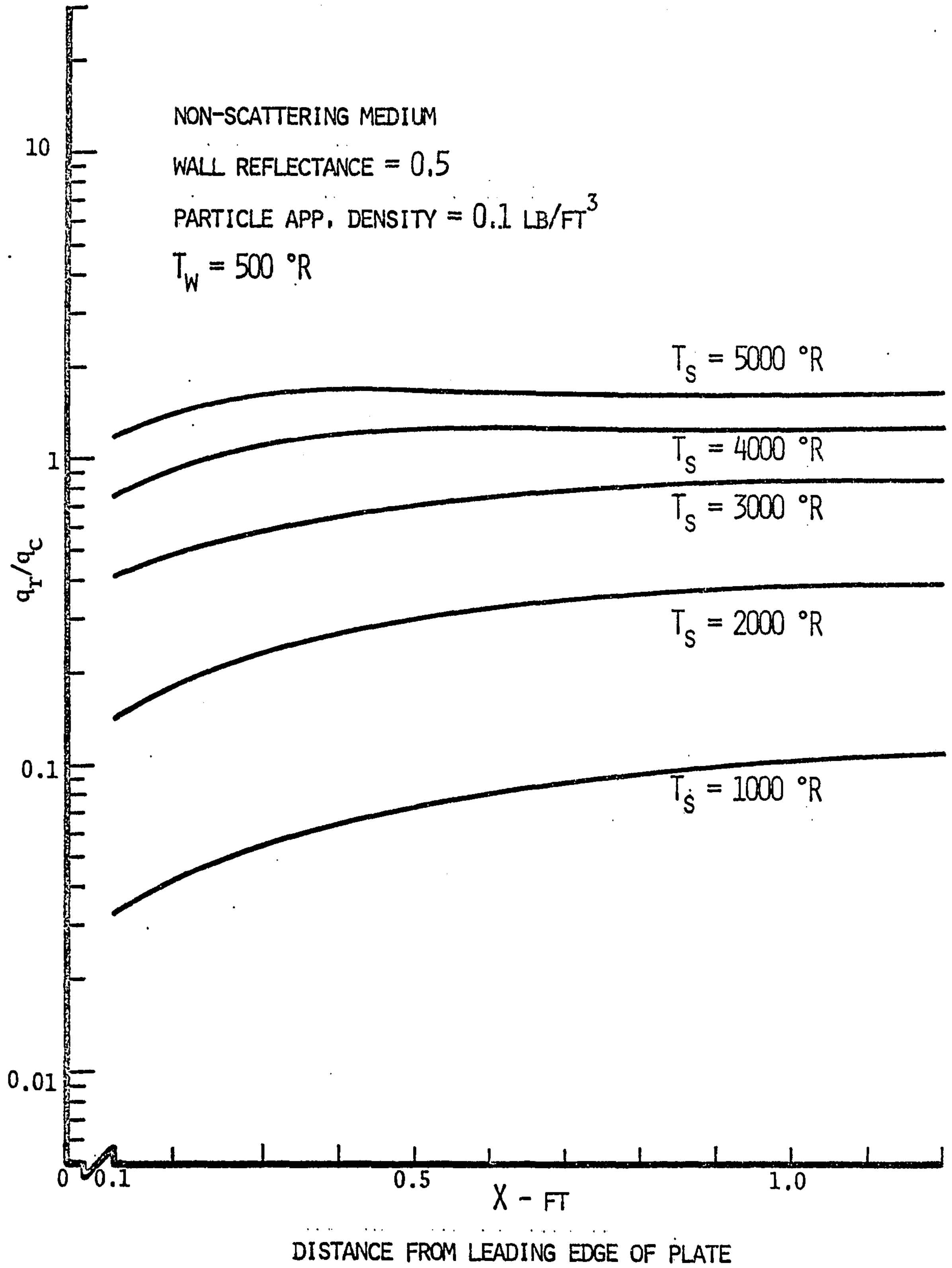
NON-SCATTERING MEDIUM
WALL REFLECTANCE = 0.5
PARTICLE APP. DENSITY = 0.1 LB/FT^3
T_W = 500 °R
T_S = 5000 °R
T_S = 4000 °R
T_S = 3000 °R
T_S = 2000 °R
T_S = 1000 °R
10
1
0.1
0.01
q_r/q_c
0
0.1
0.5
1.0
X - FT
DISTANCE FROM LEADING EDGE OF PLATE

Figure 37

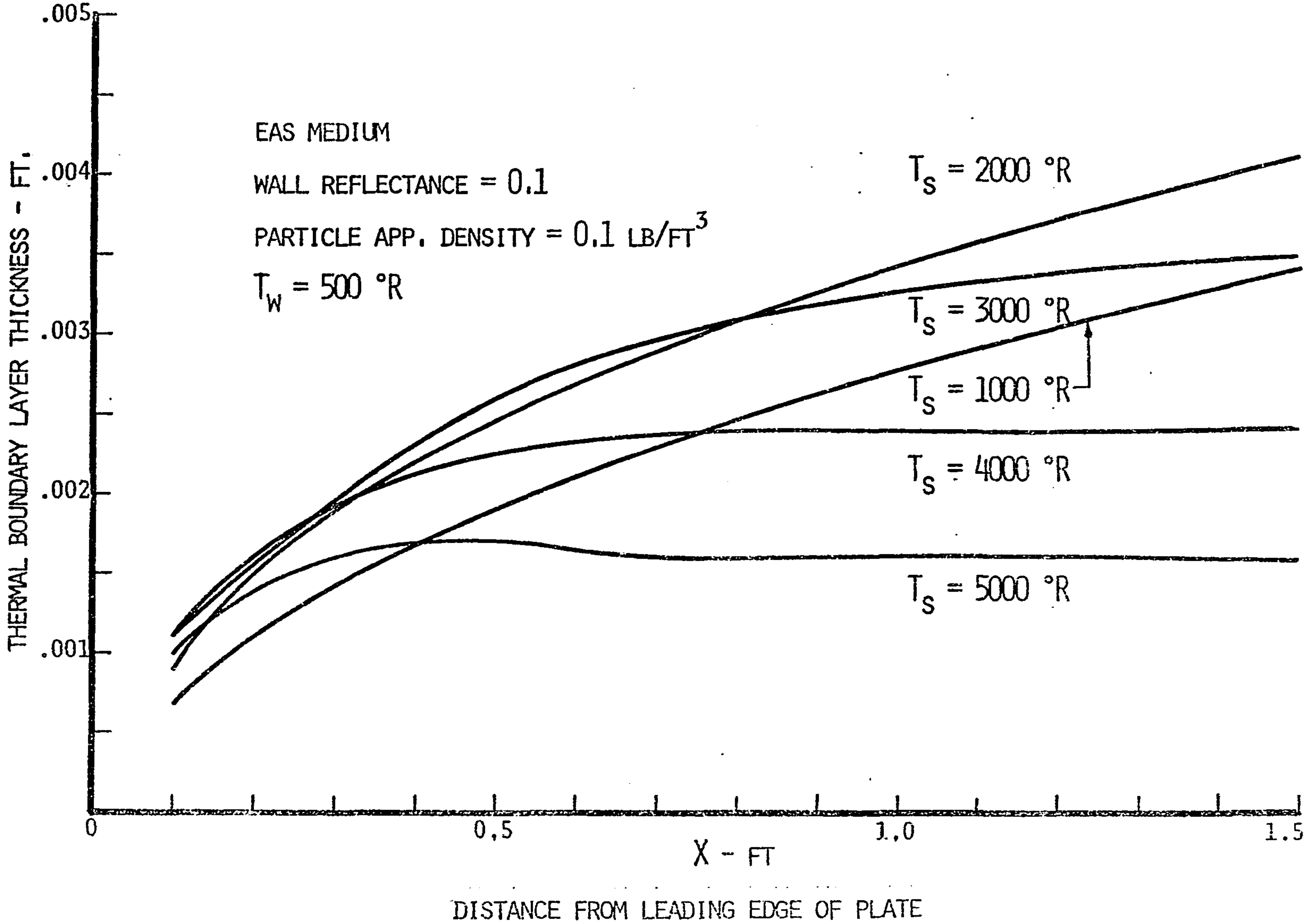
.005
.004
.003
.002
.001
THERMAL BOUNDARY LAYER THICKNESS - FT.
EAS MEDIUM
WALL REFLECTANCE = 0.1
PARTICLE APP. DENSITY = 0.1 LB/FT^3
T_W = 500 °R
T_S = 2000 °R
T_S = 3000 °R
T_S = 1000 °R
T_S = 4000 °R
T_S = 5000 °R
0
0.5
1.0
1.5
X - FT
DISTANCE FROM LEADING EDGE OF PLATE

Figure 38

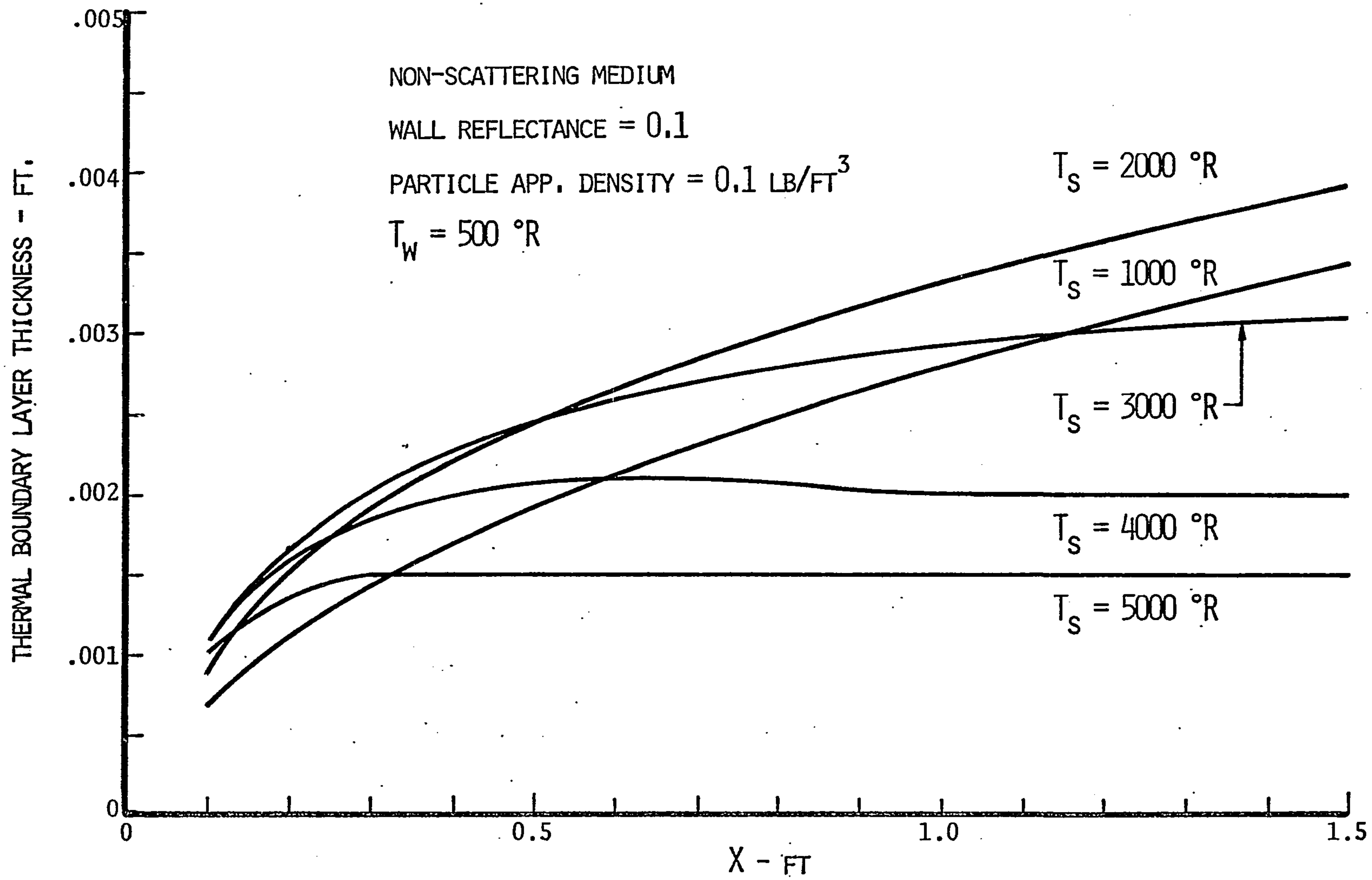

DISTANCE FROM LEADING EDGE OF PLATE

Figure 39

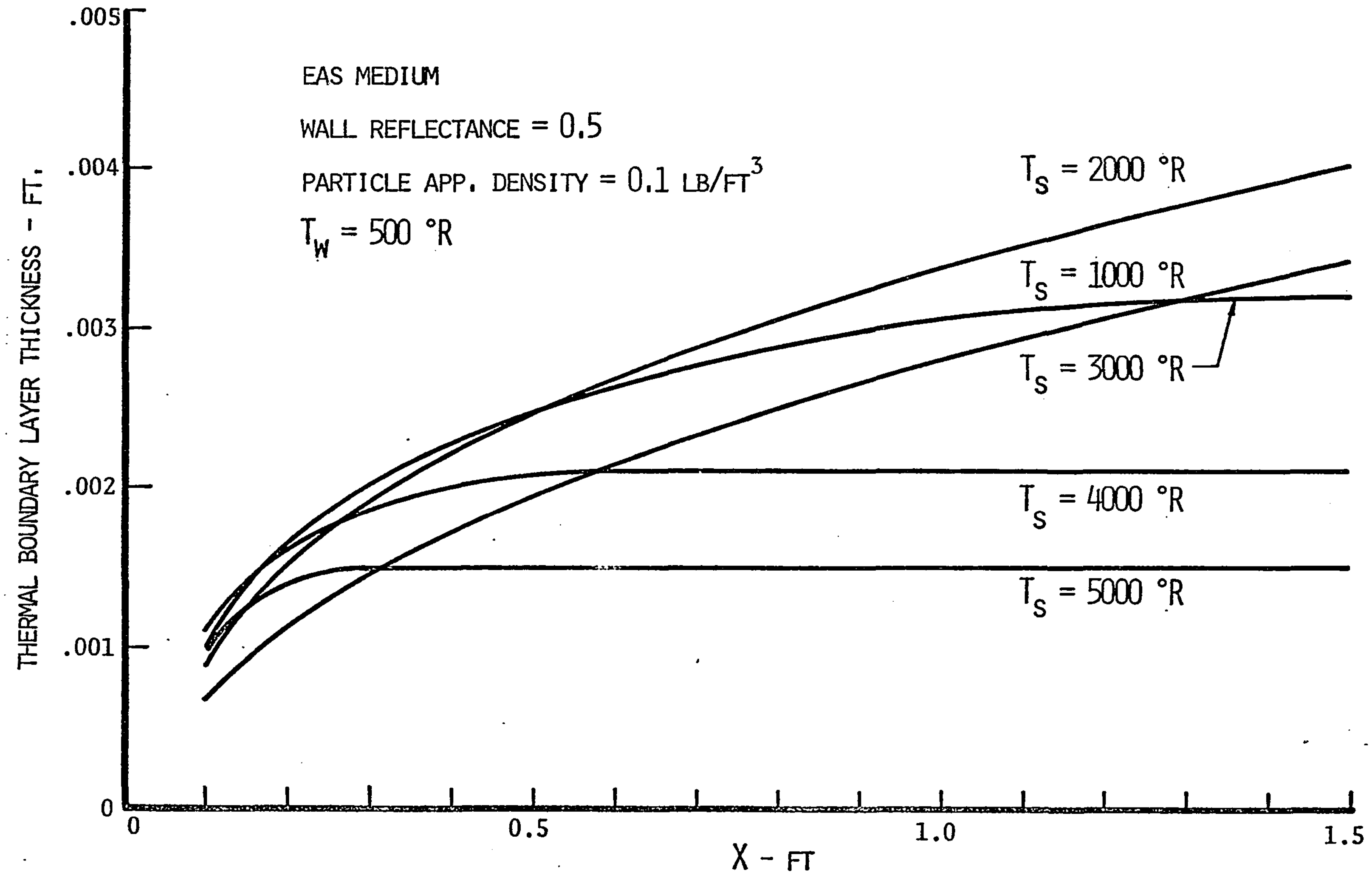

DISTANCE FROM LEADING EDGE OF PLATE

Figure 40

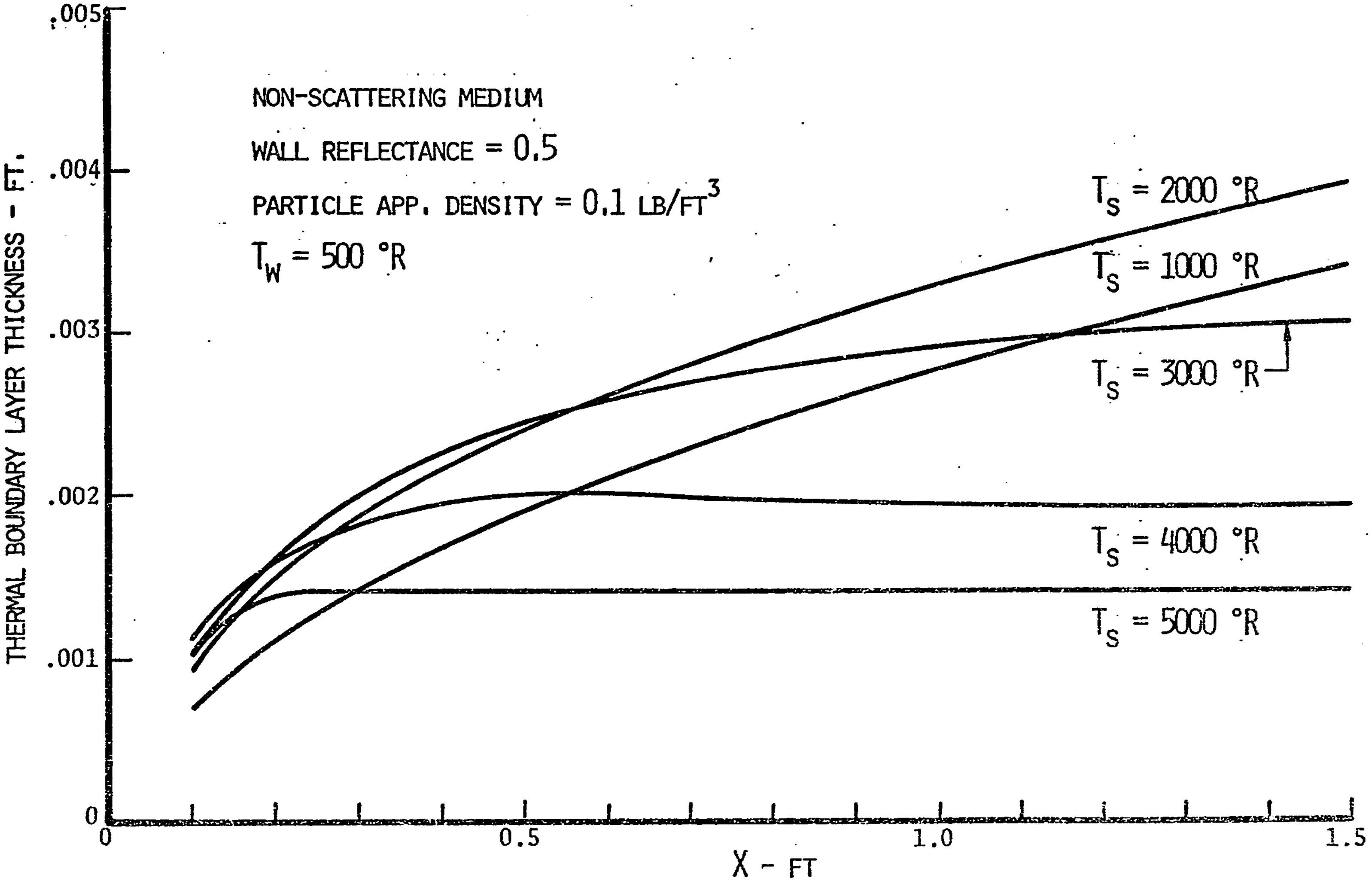

DISTANCE FROM LEADING EDGE OF PLATE

Figure 41

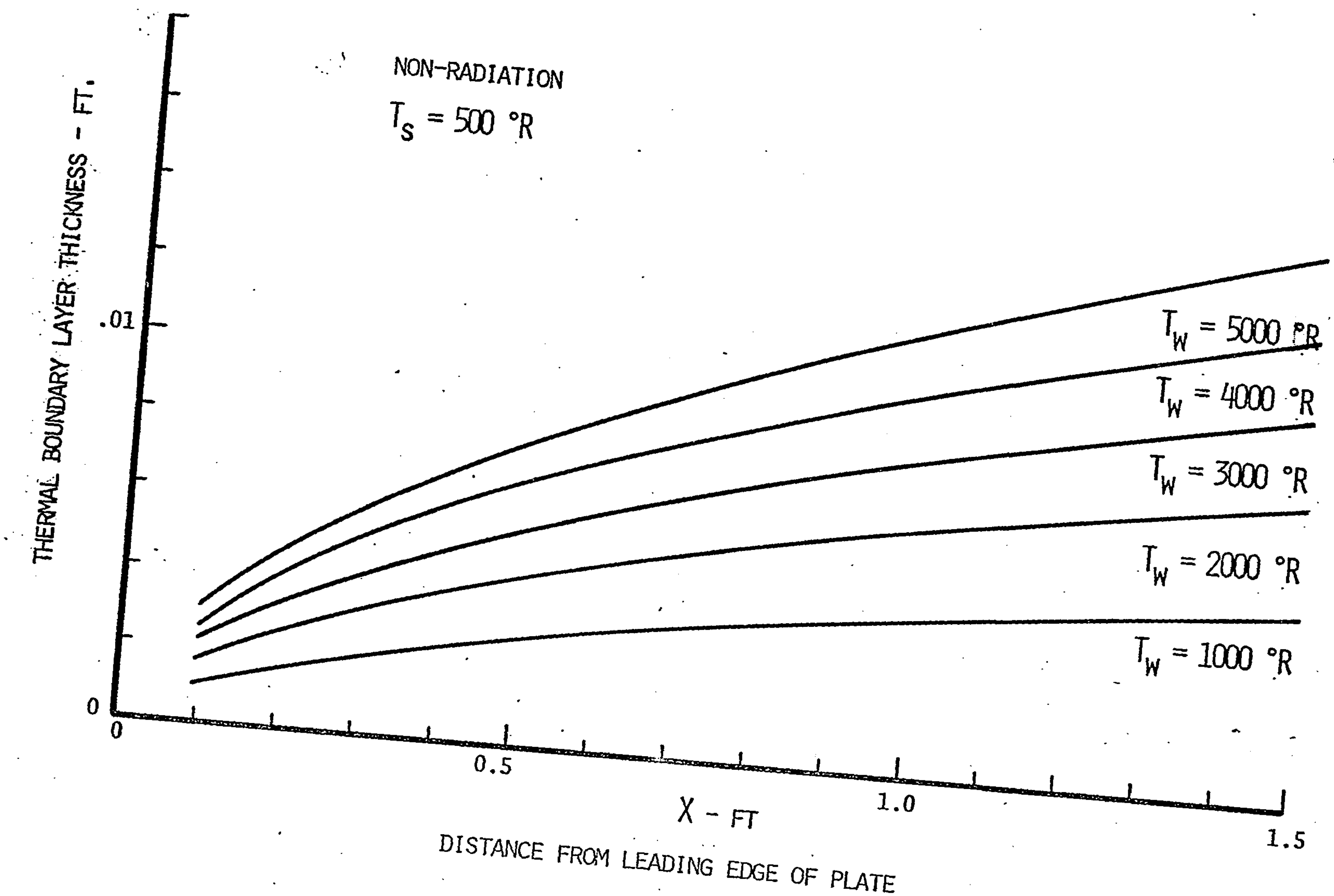
NON-RADIATION
T_S = 500 °R
THERMAL BOUNDARY LAYER THICKNESS - FT.
.01
0
0
0.5
1.0
1.5
X - FT
DISTANCE FROM LEADING EDGE OF PLATE
T_W = 5000 °R
T_W = 4000 °R
T_W = 3000 °R
T_W = 2000 °R
T_W = 1000 °R

Figure 42

CHAPTER VI

SUMMARY AND CONCLUSION

The experimental data of scattering functions $S(\Theta_{ij})$ for five different materials were reduced to the form of $s(\mu_i,\mu_j)$. These scattering functions were utilized to obtain the dimensionless parameters M, N and Q for the calculation of radiant heat transfer through plane parallel clouds of scattering particles. Examples of these parameters were given in graphic form. Comparison of the dimensionless parameters were made between theoretical isotropic data and the experimental data. Examples of this comparison are also presented in graphic form.

Radiant heat transfer in an emitting, absorbing and scattering boundary layer is studied by using a laminar flow over a flat plate. The edge of the boundary layer is considered black. Theoretical isotropic dimensionless parameters for a range of scattering to extinction ratios were calculated for the following combinations of reflectances.

(a) In an EAS medium;

Wall reflectance = 0.1, 0.5

(b). In a non-scattering but emitting and absorbing medium

Wall reflectance = 0.1, 0.5.

Mean values of these parameters were taken for heat transfer calculation. The Pohlhausen technique was used for temperature and velocity profiles. The energy equation was solved by an iteration method over the thickness of the thermal boundary layer. Digital computer programs have been written for all of the calculations of this study.

The conclusions which may be drawn from this study may be listed as follows:

(1). The effect of real particle scattering seems to be relatively independent of size, shape, and even of the material of the particles.

(2). The dimensionless parameters from theoretical isotropic data may be used to compute heat transfer in anisotropic real particle clouds for most engineering applications.

(3). Thermal radiation in an EAS boundary layer effects the thickness of the thermal boundary layer. It seems to thicken the boundary layer for all the hot wall cases. For cold wall cases, the thermal boundary layer becomes thin at high temperature.

(4). The heat transfer in an EAS boundary layer is smaller than that in a zero-scattering boundary layer.

(5). At higher temperature, radiation dominates the heat transfer from the wall.

(6). The reflectance of the wall would effect the heat transfer from the wall in such a way that the smaller the reflectance, the larger the heat transfer from the wall.

BIBLIOGRAPHY

(1) Van De Hulst, H. C., Light Scattering by Small Particles J. Wiley and Sons, 1957

(2) Love, Tom J., Jr. An Investigation of Radiant Heat Transfer in Absorbing, Emitting and Scattering Media, Norman, Oklahoma: University of Oklahoma Research Institute, 1963 (Contract AF 33(657)-8859) (ARL63-3)

(3) Love, Tom J., Jr. Radiative Heat Transfer (Text to be published in 1967 by Charles E. Merrill Books, Inc., Columbus, Ohio.)

(4) Love, Tom J., Jr. and Grosh, R. J. "Radiative Heat Transfer in Absorbing, Emitting and Scattering Media" ASME Journal of Heat Transfer, Vol. 87, Series C, May, 1964

(5) Usiskin, C. M., and Sparrow, E. M., "Thermal Radiation Between Parallel Plates Separated by an Absorbing-Emitting Nonisothermal Gas" International Journal of Heat and Mass Transfer, Vol. 1, No. 1, June, 1960

(6) Deissler, R. G., "Diffusion Approximation for Thermal Radiation in Gases with Jump Boundary Condition", ASME Journal of Heat Transfer, Vol. 86, Series C, May, 1964

(7) Howell, J. R. and Perlmutter, M., "Monte Carlo Solution of Thermal Transfer Through Radiant Media Between Grey Walls", ASME Journal of Heat Transfer, Vol. 86, February 1964.

(8) Perlmutter, M. and Howell, J. R., "Radiant Transfer Through a Grey Gas Between Concentric Cylinders Using Monte Carlo" ASME Journal of Heat Transfer Vol. 86 May, 1964

(9) Chandrasekhar, S. Radiative Transfer, Dover: 1961

(10) Hsia, H. M., "Radiative Heat Transfer Between Parallel Plates Separated by a Nonisothermal Medium with Anisotropic Scattering" ASME Journal of Heat Transfer Paper No. 66-WA/HT-28. Also PhD Thesis, University of Oklahoma 1965

(11) Cess, R. D. "The Interaction of Thermal Radiation with Conduction and Convection Heat Transfer" Advances in Heat Transfer, Vol 1, Academic Press, N. Y. 1964

(12) Goulard, R. and Goulard, M. "One Dimensional Energy Transfer in Radiant Media", International Journal of Heat and Mass Transfer, Vol. 1, 1960

(13) Viskanta, R. and Grosh, R. J., "Heat Transfer by Simultaneous Conduction and Radiation in an Absorbing Medium" ASME Journal of Heat Transfer February, 1962

(14) Viskanta, R., "Heat Transfer by Conduction and Radiation in Absorbing and Scattering Materials" ASME Journal of Heat Transfer Vol. 84, September, 1964

(15) Lick, W., "Energy Transfer by Radiation and Conduction" Proceedings of the 1963 Heat Transfer and Fluid Mechanics Institute, Stanford University Press, Palo Alto, Calif., 1963.

(16) Cess, R. D., "Radiation Effects upon Boundary Layer Flow of an Absorbing Gas" ASME Journal of Heat Transfer November, 1964.

(17) Sidorov, E. A., "Radiant-Convective Heat Exchange in an Absorbing Medium" U. S. Atomic Energy Commission Translation AEC-tr-4511

(18) Koh, J. C. Y. and De Silva, C. N., "Interaction Between Radiation and Convection in Hypersonic Boundary Layer on a Flat Plate" ARS Journal Vol. 32, 1962

(19) Oliver, C. C. and Mc Fadden, P. W. "The Interaction of Radiation and Convection in the Laminar Boundary Layer" ASME paper 65-HT-54, August, 1965

(20) Taitel, Y. and Hartnett, J. P. "Equilibrium Temperatures in a Boundary Layer Flow Over a Flat Plate of Absorbing-Emitting Gas" ASME Paper No. 66-WA/HT-48

(21) Smith, A. M. and Hassan, H. A., "Nongrey Radiation Effects on the Boundary Layer at Low Eckert Numbers" ASME Paper 66-WA/HT-35

(22) Kunz, K. S., Numerical Analysis, N. Y.: McGraw Hill Book Company, 1957

(23) Scarbrough, J. B., Numerical Mathematical Analysis, Baltimore: The Johns Hopkins Press, 5th edition, 1962

(24) Hildebrand, F. B., Advanced Calculus for Applications, Prentice Hall, 1962

(25) Pai, S. I., Radiation Gas Dynamics, New York: Springer-Verning New York, Inc., 1966

(26) Pennington, R. H., Introductory Computer Methods and Numerical Analysis, New York: The MacMillan Company, New York, 1965

(27) Kuo, S. S., Numerical Methods and Computers, Addison-Wesley Publishing Company, Inc. 1965

(28) Chu, C. M., Clark, C. C. and Churchill S. W. "Tables of Angular Distribution Coefficients for Light Scattering By Sphere" University Press, Engineering Research Institute, University of Michigan, 1957

(29) Wheasler, R. A. and Love, T. J. Jr. "An Experimental Study of Infra-red Scattering Clouds of Particles" ARL-64-109 Aerospace Research Laboratories Report, Office of Aerospace Research U.S.A.F., Also PhD Thesis, University of Oklahoma, June, 1964

(30) Beattie, J. F. and Love T. J. Jr., "Angular Distribution of Scattered Intensity From Various Aerosols" ARL-65-110 Aerospace Research Laboratories Report, Office of Aerospace Research, U.S.A.F. also PhD Thesis University of Oklahoma, June 1965

(31) Eckert, E. R. G. and Drake, R. M., Jr. Heat and Mass Transfer, McGraw-Hill Book Company, Inc., N.Y. 1959

(32) Sparrow, E. M. and Cess, R. D., Radiation Heat Transfer Brooks/Cole Publishing Company, Belmont, California: 1966

(33) Schlichting, H., Boundary Layer Theory, Translated by J. Kestin, McGraw-Hill Book Company 4th Edition, 1960

(34) Modern Computing Method, Philosophical Library, N.Y. 1958

(35) Wilkinson J. H., "The Calculation of the Latent Roots and Vectors of Matrices on The Pilot Model of A.C.E." Proceedings of the Cambridge Philosophical Society Vol. 50, London: 1964

(36) Faddeeva, V. N., Computational Methods of Linear Algebra, Translated by Benster, C. D. Dover: 1959

(37) Kourganoff, V., Basic Methods in Transfer Problem, Clarendon Press, Oxford, 1952.

(38) Jakob, M., Heat Transfer, Vol. I & II, New York: John Wiley and Sons Inc., 1957

(39) Chromy, F. C. "Evaluation of Mie Equations for Colored Spheres" Journal of the Optical Society of America, Vol. 50, No. 7, (1960)

(40) Sinclair A. R., "Radiation Heat Transfer in Boundary Layer Flow" M. S. Thesis, The University of Oklahoma

(41) Goulard, R. and Goulard, M., "Energy Transfer in the Couette Flow of a Radiant and Chemically Reacting Gas", Proceedings of the 1959 Heat Transfer and Fluid Mechanics Institute, Stanford University Press, Stanford, California, 1959.

(42) Chen, J. C. "Simultaneous Radiative and Convective Heat Transfer in an Absorbing Medium in Slug Flow Between Parallel Plates" A.I.CH.E. Journal 10, 253. (1964).

NOMENCLATURE

A_j	Adjusted quadrature weight factor	$(Btu)(hr)^{-1}(ft)^{-2}(R)^{-4}$
a_j	Quadrature weight factor	none
A, B	Matrices	none
C_p	Specific heat	$(Btu)(lb)^{-1}(F)^{-1}$
c	Velocity of light	$(ft)(hr)^{-1}$
C	Integration constants	none
D	Diameter of spherical particle	ft
F	Monochromatic heat flux from a surface	$(Btu)(ft)^{-2}$
h	Planck's constant	$(Btu)(hr)^{-1}$
I	Monochromatic intensity of radiation	$(Btu)(ft)^{-2}(stearad)^{-1}$
J	Monochromatic intensity of scattered or emitted radiant energy	
k	Boltzman constant	$(Btu)(^{o}R)^{-1}$
K	Thermal conductivity	$(Btu)(ft)^{-1}(hr)^{-1}(^{o}F)^{-1}$
K^e	Extinction cross section	none
M	Dimensionless parameter	none
N	Dimensionless parameter	none
Q	Dimensionless parameter	
q_{net}	Net heat flux for walls	$(Btu)(hr)^{-1}(ft)^{-2}$
s	Distance along a ray (See Fig. 1)	ft
S	Scattering function	

S^*	Scattering function	
t	Time	hr. sec.
T	Temperature	^oR
T_a	Temperature of medium	^oR
x	Distance from leading edge of plate	ft
X	Eigenvectors	none
Y	A polynomial	none
y	Normal coordinate	ft
α	Particle size parameter	none
β	Monochromatic mass extinction coefficient	$(ft)^2(lb_m)^{-1}$
γ	Eigenvalue of a matrix	none
δ	Boundary layer thickness	ft
δ_t	Thermal boundary layer thickness	ft
ε	Surface emittance	none
Θ	Angle between incident and leaving ray	radiant
θ	Polar angle (Fig. 1)	radians
κ	Monochromatic mass absorption coefficient	$(ft)^2(lb_m)^{-1}$
λ	Radiation wave length	ft
μ	Cosine 0	none
ν	Frequency of radiation	$(hr)^{-1}$
ρ	Mass density	$(lb_m)(ft)^{-3}$
ρ_m	Mass density of the particles	$(lb_m)(ft)^{-3}$
ρ_a	Apparent mass density	$(lb_m)(ft)^{-3}$
ρ	Surface reflectance	none
π	3.1416	none

σ	Monochromatic mass scattering coefficient	$(lb_m)(ft)^{-3}$
τ	Optical depth	none
ϕ	Azimuthal angle	radian

SUBSCRIPTS

ν	Monochromatic
bb	Black body
i,j	Iteration indices
1	Refer to wall 1
2	Refer to wall 2, or refer to the edge of boundary layer
r	Radiation
c	Conduction
s	Free stream
w	Wall

SUPERSCRIPTS

'	A distinction of M, N, Q
'	A indication of incident ray
*	A matrix
+,-	Sometime refers to a positive (or negative) direction of a ray defined in Fig. 1

APPENDIX A

1. COMPUTER PROGRAM FOR Θ_{ij} (THIRD ORDER APPROXIMATION).

2. TABLE 1

   Θ_{ij} (BASED ON $\phi = 10^{o}$) FOR DISCRETE POSITION OF INCIDENT RAY AND WAVE LENGTH

```
C      PROGRAM FOR THETA IJ.
C      U1 IS THE GAUSSIAN QUADRATURE COORDINATES.
C      THETA IS THE ANGLE THETA(I,J)
C      PROGRAM FOR THETA IJ.
       DIMENSION U1(3),U2(6),A(19),C1(3,6,19),S1(3,6,19),
      1TN(3,6,19),THETA(3,6,19)
       READ 1, (U1(I), I=1,3)
     1 FORMAT(3E16.8)
       DO 3 I=1,3
     3 U2(I)=U1(I)
       DO 4 I=1,3
     4 U2(I+3)=-U1(I)
       A(1)=0.0
       DO 7 I=2,19
       SUM=I
     7 A(I)=3.1416*10./180.*(SUM-1.)
       DO 8 I=1,3
       DO 8 J=1,6
       DO 8 K=1,19
       C1(I,J,K)=U1(I)*U2(J)+SQRTF(1.-U1(I)**2)*
      1SQRTF(1.-U2(J)**2)*COSF(A(K))
       S1(I,J,K)=SQRTF(1.-C1(I,J,K)*C1(I,J,K))
       TN(I,J,K)=S1(I,J,K)/C1(I,J,K)
       IF(TN(I,J,K))11,11,12
    11 THETA(I,J,K)=180.*(1.+ATANF(TN(I,J,K))/3.1416)
       GO TO 8
    12 THETA(I,J,K)=ATANF(TN(I,J,K))*180./3.1416
     8 CONTINUE
       DO 9 I=1,3
       PUNCH 10,((THETA(I,J,K),J=1,6),K=1,19)
     9 PRINT 10,((THETA(I,J,K),J=1,6),K=1,19)
    10 FORMAT(1H1/////(6F10.2))
       STOP
       END
```

TABLE I

Θ_{ij} - Degree

$\Theta_{1,1}$	$\Theta_{1,2}$	$\Theta_{1,3}$	$\Theta_{1,-1}$	$\Theta_{1,-2}$	$\Theta_{1,-3}$
.10	23.52	56.06	12.94	36.47	69.00
9.93	25.33	56.54	16.34	37.71	69.43
19.87	30.12	57.95	23.78	41.21	70.69
29.80	36.71	60.20	32.61	46.45	72.73
39.73	44.31	63.18	41.96	52.92	75.46
49.65	52.44	66.76	51.54	60.21	78.78
59.57	60.88	70.78	61.25	68.04	82.58
69.48	69.47	75.12	71.03	76.23	86.74
79.38	78.12	79.65	80.86	84.65	91.17
89.27	86.76	84.26	90.72	93.23	95.73
99.13	95.34	88.82	100.61	101.87	100.34
108.96	103.76	93.25	110.51	110.52	104.87
118.74	111.95	97.41	120.42	119.11	109.21
128.45	119.78	101.21	130.34	127.55	113.23
138.04	127.07	104.53	140.26	135.68	116.81
147.38	133.54	107.26	150.19	143.28	119.79
156.21	138.78	109.30	160.12	149.87	122.04
163.65	142.28	110.56	170.06	154.66	123.45
167.05	143.52	110.99	179.89	156.47	123.93

TABLE I - continued

Θ_{ij} - Degree

$\Theta_{2,1}$	$\Theta_{2,2}$	$\Theta_{2,3}$	$\Theta_{2,-1}$	$\Theta_{2,-2}$	$\Theta_{2,-3}$
23.52	.06	32.53	36.47	59.99	92.53
25.33	8.65	33.17	37.71	60.75	92.88
30.12	17.29	35.01	41.21	62.94	93.91
36.71	25.90	37.85	46.45	66.45	95.61
44.31	34.45	41.44	52.92	71.06	97.91
52.44	42.93	45.54	60.21	76.57	100.77
60.88	51.31	49.95	68.04	82.81	104.11
69.47	59.56	54.53	76.23	89.62	107.88
78.12	67.65	59.13	84.65	96.87	111.98
86.76	75.52	63.66	93.23	104.47	116.33
95.34	83.12	68.01	101.87	112.34	120.86
103.76	90.37	72.11	110.52	120.43	125.46
111.95	97.18	75.88	119.11	128.68	130.04
119.78	103.42	79.22	127.55	137.06	134.45
127.07	108.93	82.08	135.68	145.54	138.55
133.54	113.54	84.39	143.28	154.09	142.14
138.78	117.05	86.08	149.87	162.70	144.98
142.28	119.24	87.11	154.66	171.34	146.82
143.52	120.00	87.46	156.47	179.93	147.46

TABLE I - continued

Θ_{ij} - Degree

$\Theta_{3,1}$	$\Theta_{3,2}$	$\Theta_{3,3}$	$\Theta_{3,-1}$	$\Theta_{3,-2}$	$\Theta_{3,-3}$
56.06	32.53	.07	69.00	92.53	125.07
56.54	33.17	4.60	69.43	92.88	125.29
57.95	35.01	9.18	70.69	93.91	125.97
60.20	37.85	13.71	72.73	95.61	127.09
63.18	41.44	18.15	75.46	97.91	128.63
66.76	45.54	22.47	78.78	100.77	130.58
70.78	49.95	26.66	82.58	104.11	132.91
75.12	54.53	30.67	86.74	107.88	135.60
79.65	59.13	34.48	91.17	111.98	138.62
84.26	63.66	38.06	95.73	116.33	141.93
88.82	68.01	41.37	100.34	120.86	145.51
93.25	72.11	44.39	104.87	125.46	149.32
97.41	75.88	47.08	109.21	130.04	153.33
101.21	79.22	49.41	113.23	134.45	157.52
104.53	82.08	51.36	116.81	138.55	161.84
107.26	84.39	52.90	119.79	142.14	166.28
109.30	86.08	54.02	122.04	144.98	170.81
110.56	87.11	54.70	123.45	146.82	175.39
110.99	87.46	54.92	123.93	147.46	179.92

APPENDIX B

1. TABLE II

   INTEGRATED AXIALLY-SYMMETRIC SCATTERING FUNCTIONS FOR DISCRETE POSITIONS AND WAVE LENGTHS (λ) BASED ON EXPERIMENTAL DATA

2. TABLE III

   $1/2\ [\sum_{n=1}^{3} a_j S(\mu_i, \cdot \mu_j)]$ FOR DISCRETE POSITIONS OF INCIDENT RAY AND WAVE LENGTHS (λ) ---BASED ON EXPERIMENTAL DATA

TABLE II

ALUMINUM

INTEGRATED AXIALLY-SYMMETRIC SCATTERING FUNCTIONS FOR DISCRETE POSITIONS AND WAVE LENGTHS (λ) BASED ON EXPERIMENTAL DATA

Wave Length	Integrated Functions					
λ	$S(\mu_1,\mu_1')$	$S(\mu_1,\mu_2')$	$S(\mu_1,\mu_3')$	$S(\mu_1,-\mu_1')$	$S(\mu_1,-\mu_2')$	$S(\mu_1,-\mu_3')$
0.6	1.4436	0.5892	0.4706	0.8400	0.5647	0.4811
0.7	1.0897	0.5758	0.4606	0.8333	0.5367	0.3169
0.8	3.1078	0.5017	0.3447	1.0517	0.4478	0.3572
0.9	2.9675	0.3706	0.2072	0.7750	0.2986	0.2122
1.0	3.1489	0.3481	0.2222	0.8842	0.2969	0.2271
1.2	2.3548	0.3236	0.1768	0.5596	0.2569	0.1791
1.4	1.3303	0.2025	0.0948	0.4842	0.1550	0.0976
2.0	1.2356	0.4786	0.2922	0.7728	0.4675	0.3161
2.5	1.5484	0.6411	0.3886	0.9764	0.5550	0.4142
3.0	1.9675	0.4508	0.2147	0.9933	0.3372	0.2197
4.0	1.3567	0.5847	0.3750	0.9842	0.5128	0.3922
5.0	2.0981	0.6672	0.2666	1.2139	0.4598	0.2587
6.0	1.3745	0.9900	0.7267	1.1564	0.8647	0.7272
7.0	1.1847	0.7975	0.5817	1.0145	0.7228	0.5489
8.0	0.8200	0.6061	0.4451	0.7258	0.5464	0.4244
9.0	1.0181	0.8382	0.6581	0.9989	0.8214	0.6556
10.0	1.0578	0.9439	0.7911	1.0317	0.8858	0.6889
11.0	1.0295	0.9295	0.8156	1.0133	0.9000	0.7717
12.0	0.9667	0.8820	0.7780	0.9650	0.8883	0.8028
13.0	0.9697	0.8445	0.6928	1.8756	0.8583	0.7225
14.0	0.7872	0.6783	0.5472	0.8025	0.6917	0.5622
15.0	1.1358	0.9808	0.8158	1.1589	1.0058	0.8125

TABLE II - Continued

ALUMINUM

Wave Length λ	Integrated Functions $S(\mu_2,\mu_1')$	$S(\mu_2,\mu_2')$	$S(\mu_2,\mu_3')$	$S(\mu_2,-\mu_1')$	$S(\mu_2,-\mu_2')$	$S(\mu_2,-\mu_3')$
0.6	0.5892	1.4478	0.5236	0.5647	0.5883	0.5397
0.7	0.5758	1.8234	0.5261	0.5367	0.5497	0.9978
0.8	0.5017	2.2989	0.4017	0.4478	0.4778	0.4264
0.9	0.3706	3.6181	0.2958	0.2986	0.3000	0.2647
1.0	0.3481	3.2146	0.2700	0.2969	0.3129	0.2739
1.2	0.3236	2.6959	0.2400	0.2570	0.2831	0.2263
1.4	0.2024	1.6229	0.1483	0.1550	0.1459	0.1308
2.0	0.4786	1.2514	0.3433	0.4675	0.5247	0.4573
2.5	0.6411	1.6978	0.4783	0.5550	0.5633	0.5397
3.0	0.4508	2.2761	0.3456	0.3372	0.3067	0.2806
4.0	0.5847	1.3881	0.4522	0.5128	0.5092	0.4878
5.0	0.6672	2.2771	0.4973	0.4598	0.3867	0.3403
6.0	0.9900	1.4142	0.8461	0.8647	0.8625	0.8075
7.0	0.7975	1.4997	0.7750	0.7228	0.6933	0.5817
8.0	0.6061	0.8172	0.5797	0.5464	0.5150	0.4547
9.0	0.8392	0.9233	0.7747	0.8214	0.8506	0.7431
10.0	0.9439	1.0456	1.0056	0.8858	0.8111	0.6733
11.0	0.9295	1.0086	0.9561	0.9000	0.8767	0.7770
12.0	0.7781	0.9030	0.8033	0.8028	1.2933	0.8942
13.0	0.8445	0.8481	0.7350	0.8583	0.9181	0.8536
14.0	0.6783	0.6800	0.5975	0.6917	0.7445	0.6656
15.0	0.9808	1.0090	0.9155	1.0058	1.0644	0.9200

TABLE II - Continued

ALUMINUM

Wave Length	Integrated Functions					
λ	$S(\mu_3,\mu_1')$	$S(\mu_3,\mu_2')$	$(S\mu_3\mu_3')$	$S(\mu_3,-\mu_1')$	$S(\mu_3,-\mu_2')$	$S(\mu_3,-\mu_3')$
0.6	0.4706	0.5236	2.4220	0.4811	0.5397	0.7292
0.8	0.4606	0.5261	3.1184	0.3169	0.9978	0.6561
0.8	0.3447	0.4017	5.9912	0.3573	0.4264	0.6336
0.9	0.2072	0.2958	5.2209	0.2122	0.2642	0.4019
1.0	0.2222	0.2700	5.9605	0.2271	0.2739	0.4180
1.2	0.1768	0.2400	5.0075	0.1791	0.2263	0.4029
1.4	0.0948	0.1483	2.9040	0.0976	0.1308	0.2090
2.0	0.2922	0.3433	2.0778	0.3161	0.4572	0.8050
2.5	0.3886	0.4783	3.0756	0.4142	0.5397	0.8008
3.0	0.2147	0.3456	4.1278	0.2197	0.2806	0.4247
4.0	0.3750	0.4522	2.3014	0.3922	0.4878	0.6778
5.0	0.2667	0.4973	4.2264	0.2587	0.3403	0.5480
6.0	0.7267	0.8461	2.0481	0.7272	0.8075	1.0295
7.0	0.5817	0.7750	1.7628	0.5489	0.5817	0.8136
8.0	0.4451	0.5797	1.2400	0.4245	0.4547	0.5925
9.0	0.6581	0.7747	1.2242	0.6556	0.7431	1.0645
10.0	0.7311	1.0056	1.5075	0.6889	0.6733	0.8461
11.0	0.8156	0.9561	1.2920	0.7717	0.7770	0.9389
12.0	0.7781	0.8033	1.0050	0.8028	0.8942	1.0933
13.0	0.6938	0.7350	0.9714	0.7225	0.8536	1.1822
14.0	0.5472	0.5975	0.8058	0.5622	0.6656	0.9708
15.0	0.8158	0.9155	1.2553	0.8124	0.9200	1.3278

TABLE II - Continued

CARBON

INTEGRATED AXIALLY-SYMMETRIC SCATTERING FUNCTIONS FOR DISCRETE POSITIONS AND WAVE LENGTHS (λ) BASED ON EXPERIMENTAL DATA

Wave Length	Integrated Functions					
λ	$S(\mu_1,\mu_1')$	$S(\mu_1,\mu_2')$	$S(\mu_1,\mu_3')$	$S(\mu_1,-\mu_1')$	$S(\mu_1,-\mu_2')$	$S(\mu_1,-\mu_3')$
1.0	3.3482	0.1491	0.0768	0.8868	0.1229	0.0670
4.0	1.1809	0.2093	0.0280	0.5092	0.0642	0.0153
10.0	1.6086	0.6639	0.3764	0.9275	0.4692	0.3063
12.0	1.1490	0.2181	0.1029	0.5074	0.1967	0.4432
λ	$S(\mu_2,\mu_1')$	$S(\mu_2,\mu_2')$	$S(\mu_2,\mu_3')$	$S(\mu_2,-\mu_1')$	$S(\mu_2,-\mu_2')$	$S(\mu_2,-\mu_3')$
1.0	0.1491	3.7305	0.1793	0.1229	0.0873	0.0719
4.0	0.2093	1.3807	0.1473	0.6422	0.0217	0.0109
10.0	0.6639	1.8620	0.6888	0.4629	0.3031	0.2397
12.0	0.8686	2.3345	0.8664	0.6131	0.4428	0.3735
λ	$S(\mu_3,\mu_1')$	$S(\mu_3,\mu_2')$	$S(\mu_3,\mu_3')$	$S(\mu_3,-\mu_1')$	$S(\mu_3,-\mu_2')$	$S(\mu_3,-\mu_3')$
1.0	0.0768	0.1793	7.3232	0.0670	0.0719	0.0991
4.0	0.0280	0.1473	2.6032	0.0153	0.0109	0.0433
10.0	0.3764	0.6888	3.5989	0.3063	0.2397	0.2051
12.0	0.5221	0.8664	4.1483	0.4432	0.3735	0.3326

TABLE II - Continued

GLASS BEADS

INTEGRATED AXIALLY-SYMMETRIC SCATTERING FUNCTIONS FOR DISCRETE POSITIONS AND WAVE LENGTHS (λ) BASED ON EXPERIMENTAL DATA

Wave Length	Integrated Functions					
λ	$S(\mu_1,\mu_1')$	$S(\mu_1,\mu_2')$	$S(\mu_1,\mu_3')$	$S(\mu_1,-\mu_1')$	$S(\mu_1,-\mu_2')$	$S(\mu_1,-\mu_3')$
0.8	1.1381	0.9114	0.7200	1.1000	0.9222	0.7264
1.0	1.5383	0.9725	0.6042	1.3161	0.9158	0.6572
4.0	1.1490	0.2181	0.1029	0.5074	0.1967	0.1040

λ	$S(\mu_2,\mu_1')$	$S(\mu_2,\mu_2')$	$S(\mu_2,\mu_3')$	$S(\mu_2,-\mu_1')$	$S(\mu_2,-\mu_2')$	$S(\mu_2,-\mu_3')$
0.8	0.9114	1.0206	0.8150	0.9222	0.9733	0.8650
1.0	0.9725	1.4200	0.7364	0.9158	0.9561	0.8872
4.0	0.2181	1.3047	0.1659	0.1967	0.2216	0.1558

λ	$S(\mu_3,\mu_1')$	$S(\mu_3,\mu_2')$	$S(\mu_3,\mu_3')$	$S(\mu_3,-\mu_1')$	$S(\mu_3,-\mu_2')$	$S(\mu_3,-\mu_3')$
0.8	0.7200	0.8150	1.3183	0.7264	0.8650	1.2806
1.0	0.6042	0.7364	2.1370	0.6572	0.8872	1.3992
4.0	0.1029	0.1660	2.4150	0.1040	0.1558	0.4168

TABLE II - Continued

IRON

INTEGRATED AXIALLY-SYMMETRIC SCATTERING FUNCTIONS
FOR DISCRETE POSITIONS AND WAVE LENGTHS (λ)
BASED ON EXPERIMENTAL DATA

Wave Length	Integrated Functions					
λ	$S(\mu_1,\mu_1')$	$S(\mu_1,\mu_2')$	$S(\mu_1,\mu_3')$	$S(\mu_1,-\mu_1')$	$S(\mu_1,-\mu_2')$	$S(\mu_1,-\mu_3')$
0.6	1.9202	0.7536	0.4950	1.2877	0.6711	0.5233
1.0	3.2074	0.7928	0.3344	1.6305	0.4867	0.2747
4.0	0.7578	0.6195	0.4150	0.7506	0.6353	0.4552
10.0	1.1370	0.9342	0.6167	1.1378	0.9762	0.6600
14.0	1.1406	0.9561	0.7331	1.1550	0.9622	0.7392

λ	$S(\mu_2,\mu_1')$	$S(\mu_2,\mu_2')$	$S(\mu_2,\mu_3')$	$S(\mu_2,-\mu_1')$	$S(\mu_2,-\mu_2')$	$S(\mu_2,-\mu_3')$
0.6	0.7536	2.0049	0.5689	0.6711	0.7105	0.6605
1.0	0.7928	3.6230	0.6333	0.4867	0.3533	0.2961
4.0	0.6195	0.4615	0.7492	0.6353	0.6347	1.0147
10.0	0.9342	0.8686	0.7311	0.9792	1.0378	0.9353
14.0	0.9561	0.9853	0.8542	0.9622	1.0331	0.8881

λ	$S(\mu_3,\mu_1')$	$S(\mu_3,\mu_2')$	$S(\mu_3,\mu_3')$	$S(\mu_3,-\mu_1')$	$S(\mu_3,-\mu_2')$	$S(\mu_3,-\mu_3')$
0.6	0.4950	0.5689	3.3719	0.5233	0.6605	0.9972
1.0	0.3344	0.6333	6.7923	0.2747	0.2961	0.4019
4.0	0.4150	0.6075	0.4615	0.4552	0.6664	0.6347
10.0	0.6167	0.7311	1.1145	0.6600	0.9353	1.5684
14.0	0.7331	0.8542	1.2539	0.7392	0.8881	1.3522

TABLE II - Continued

SILICA

INTEGRATED AXIALLY-SYMMETRIC SCATTERING FUNCTIONS FOR DISCRETE POSITIONS AND WAVE LENGTHS (λ) BASED ON EXPERIMENTAL DATA

Wave Length	Integrated Functions					
λ	$S(\mu_1,\mu_1')$	$S(\mu_1.\mu_2')$	$S(\mu_1,\mu_3')$	$S(\mu_1,-\mu_1')$	$S(\mu_1,-\mu_2')$	$S(\mu_1,-\mu_3')$
0.7	2.3755	0.7597	0.2958	1.3533	0.4786	0.2505
1.0	2.2857	0.6848	0.1785	1.3225	0.3507	0.1361
4.0	1.6645	0.9347	0.4574	1.2395	0.6881	0.3483
10.0	1.0620	0.8981	0.5653	1.1242	0.8401	0.5683
13.0	1.1364	0.9567	0.7306	1.0700	0.8314	0.6411
λ	$S(\mu_2,\mu_1)$	$S(\mu_2,\mu_2')$	$S(\mu_2,\mu_3')$	$S(\mu_2,-\mu_1')$	$S(\mu_2,-\mu_2')$	$S(\mu_2,-\mu_3')$
0.7	0.7597	2.5877	0.6439	0.4786	0.3606	0.2603
1.0	0.6848	2.6950	0.5870	0.3507	0.1823	0.1188
4.0	0.9347	1.7692	0.9556	0.6881	0.4839	0.3217
10.0	0.8981	1.1406	0.7711	0.8401	0.8245	0.7265
13.0	0.9567	1.2408	1.0336	0.8314	0.6953	0.5914
λ	$S(\mu_3,\mu_1')$	$S(\mu_3,\mu_2')$	$S(\mu_3,\mu_3')$	$S(\mu_3,-\mu_1')$	$S(\mu_3,-\mu_2')$	$S(\mu_3,-\mu_3')$
0.7	0.2958	0.6439	4.7780	0.2505	0.2603	0.4261
1.0	0.1785	0.5870	4.9828	0.1361	0.1188	0.1601
4.0	0.4574	0.9556	3.2709	0.3483	0.3217	0.4908
10.0	0.5653	0.7711	1.7295	0.5683	0.7263	1.1506
13.0	0.7306	1.0336	1.9070	0.6411	0.5914	0.7728

TABLE III

$$1/2[\sum_{n=1}^{3} a_j \; S(\mu_i, \pm\mu_j)]$$

MATERIAL: ALUMINUM

FOR DISCRETE POSITIONS OF INCIDENT RAY AND WAVE LENGTHS (λ) BASED ON EXPERIMENTAL DATA

WAVE LENGTH	DIRECTION OF INCIDENT RAY		
λ	μ_1	μ_2	μ_3
0.6	0.706	0.762	0.806
0.7	0.622	0.892	0.971
0.8	0.886	0.845	1.202
0.9	0.727	0.975	0.964
1.0	0.766	0.949	1.069
1.2	0.583	0.807	0.905
1.4	0.358	0.481	0.521
2.0	0.574	0.637	0.663
2.5	0.728	0.810	0.876
3.0	0.647	0.770	0.832
4.0	0.676	0.705	0.674
5.0	0.783	0.822	0.922
6.0	0.966	0.993	0.997
7.0	1.385	0.887	0.816
8.0	0.592	0.600	0.605
9.0	0.831	0.836	0.838
10.0	0.894	0.900	0.897
11.0	0.911	0.914	0.915
12.0	0.881	0.944	0.888
13.0	0.970	0.850	0.848
14.0	0.679	0.682	0.682
15.0	0.986	0.992	0.993

TABLE III - Continued

$$1/2\left[\sum_{n=1}^{3} a_j S(\mu_i, \pm\mu_i)\right]$$

FOR DISCRETE POSITIONS OF INCIDENT RAY AND WAVE LENGTHS (λ) BASED ON EXPERIMENTAL DATA

MATERIAL: CARBON

WAVE LENGTH λ	DIRECTION OF INCIDENT RAY μ_1	μ_2	μ_3
1.0	0.669	0.921	1.107
4.0	0.240	0.372	0.409
10.0	0.698	0.767	0.830
12.0	0.920	0.995	1.032

MATERIAL: GLASS BEADS

0.8	0.919	0.931	0.935
1.0	0.991	1.016	1.027
4.0	0.351	0.441	0.499

MATERIAL: IRON

0.6	0.904	0.972	1.021
0.9	1.041	1.190	1.291
4.0	0.609	0.610	0.610
10.0	0.918	0.921	0.920
14.0	0.950	0.957	0.954

TABLE III - Continued

$$1/2\left[\sum_{n=1}^{3} a_j S(\mu_i, \pm\mu_j)\right]$$

MATERIAL: SILICA

0.7	0.869	0.951	1.000
1.0	0.775	0.881	0.915
4.0	0.876	0.903	0.918
10.0	0.847	0.886	0.890
13.0	0.894	0.904	0.924

APPENDIX C

1. PROGRAM FOR EIGENVALUES AND EIGENVECTORS CALCULATION
2. PROGRAM FOR DIMENSIONLESS PARAMETERS M, N, AND Q CALCULATION

PROGRAM I

Program Symbol	Meaning
W	Gaussian Quadrature Weight Factor
U	Gaussian Quadrature coordinates
X	Initial iteration value
Lamda	Wavelength
Albedo	σ/β
MM	A test: MM > 1 is for isotropic cases MM < 1 is for anisotropic cases
ABDI	σ/β, for isotropic cases
ABD2	σ/β, for anisotropic cases
E	Eigenvalue
X3	Eigenvector
S	The matrix

```
C      THIS PROGRAM WAS RUN ON OSAGE COMPUTER.
C      EIGENVALUES AND EIGENVECTORS OF A 6X6 MATRIX
C      S ARE THE MATRIX. EI ARE THE EIGENVALUES.
C      X3 ARE THE EIGENVECTORS. MM GREATER THAN 1 IS FOR ISOTROPIC CASE.
C      X ARE THE ITERATION FACTOR WITH A STARTING VALUE OF 1.
C      THIS IS A MODIFIED PROGRAM FROM THE WORK BY HSIA.
       DIMENSION S(6,6),X(6),Y(6),XNO(6),T(6),EI(6),SMO(6,6),
      1SC(6,6),E(6),Z(5,5),X1(5),X2(6),X3(6,6),S1(6),U(6),W(6)
       READ 1,(W(J),J=1,6), (U(J),J=1,6),(X(J),J=1,6)
     1 FORMAT(6E12.6)
    99 READ 101,LAMDA
   101 FORMAT(7HLAMDA =, I3/)
       READ 102, ALBEDO
   102 FORMAT(8HALBEDO =, F5.3/)
       READ 2, MM,ADB1, ADB2, SUM
     2 FORMAT(I2, 3E12.6)
       READ 1, ((S(I,J),J=1,6),I=1,3)
       PRINT 1, (W(J),J=1,6), (U(J),J=1,6), (X(J),J=1,6)
       PRINT 101, LAMDA
       PRINT 102, ALBEDO
       PRINT 2, MM, ADB1, ADB2, SUM
       PRINT 1, ((S(I,J), J=1,6), I=1,3)
C      THE SCATTERING FUNCTIONS AND THE MATRIX
       IF(MM-1)55,55,66
    55 DO 38 M=1,3
       DO 38 J=1,6
    38 S(M,J)=0.5*ADB1*W(J)/U(M)*S(M,J)
       GO TO 445
    66 DO 44 M=1,3
       DO 44 J=1,6
    44 S(M,J)=0.5*ADB2*W(J)/U(M)
   445 DO 39 M=1,3
    39 S(M,M)=S(M,M)-1./U(M)
       DO 440 M=4,6
       DO 440 J=1,3
```

```
440 S(M,J)=-S(M-3,J+3)
    DO 441 M=4,6
    DO 441 J=4,6
441 S(M,J)=-S(M-3, J-3)
    PRINT 442, ((S(M,J), J=1,6), M=1,6)
442 FORMAT(///(6E12.6))
    DO 3 I=1,6
    DO 3 J=1,6
    SC(I,J)=0.0
    DO 3 K=1,6
  3 SC(I,J)=SC(I,J)+S(I,K)*S(K,J)
    KK=0
 15 KK=KK+1
  9 DO 4 N=KK,6
    Y(N)=0.0
    DO 4 J=KK,6
  4 Y(N)=Y(N)+SC(N,J)*X(J)
    DO 5 J=KK,6
  5 XNO(J)=Y(J)/Y(KK)
    DO 6 J=KK,6
    T(J)=ABSF(XNO(J)-X(J))
    IF(T(J)-SUM)6,6,7
  7 DO 8 M=KK,6
  8 X(M)=XNO(M)
    GO TO 9
  6 CONTINUE
    EI(KK)=0.0
    DO 10 J=KK,6
 10 EI(KK)=EI(KK)+SC(KK,J)*XNO(J)
    DO 12 J=KK,6
    DO 12 M=KK,6
 12 SMO(J,M)=SC(J,M)-SC(KK,M)*XNO(J)
    DO 13 J=KK,6
    DO 13 M=KK,6
 13 SC(J,M)=SMO(J,M)
```

```
      DO 14 J=KK,6
   14 X(J)=1.
      IF(KK-5)15,15,16
   16 DO 17 I=1,6
   17 EI(I)=SQRTF(EI(I))
      DO 18 I=1,3
   18 E(I)=-EI(2*I-1)
      DO 19 I=1,3
   19 E(I+3)=EI(2*I-1)
      PRINT 45, (E(I), I=1,6)
   45 FORMAT(1X,29HEIGENVALUES OF THE MATRIX ARE,//6E12.6)
      NN=0
   25 NN=NN+1
      IF(NN-1)41,41,42
   41 DO 40 I=1,6
   40 S1(I)=S(I,I)
   42 DO 20 I=1,6
   20 S(I,I)=S1(I)-E(NN)
      DO 21 I=1,5
      DO 21 J=1,5
   21 Z(I,J)=S(I,J+1)
      CALL INVERT(Z,5)
      DO 22 I=1,5
      X1(I)=0.0
      DO 22 J=1,5
   22 X1(I)=X1(I)-Z(I,J)*S(J,1)
      X2(1)=1.
      DO 23 I=1,5
   23 X2(I+1)=X1(I)
      JJ=0
   30 JJ=JJ+1
      DO 27 I=1,6
   27 X3(I,NN)=X2(I)/X2(JJ)
      DO 28 I=1,6
      IF(ABSF(X3(I,NN))-1.)28,28,30
```

```
 28 CONTINUE
    IF(NN-5)25,25,200
200 PRINT 727
727 FORMAT(1X,22HTHE EIGENVECTOR MATRIX)
    PRINT 1,((X3(I,NN),NN=1,6),I=1,6)
    PRINT 707
707 FORMAT(//)
    GO TO 99
 26 STOP
    END
```

PROGRAM II

Program Symbol	Meaning
GMA	Eigenvalue
X	Eigenvector
W	Gaussian Quadrature weight factor
U	Gaussian Quadrature coordinate
TE	Optical Spacing
FL1	Reflectance of Wall 1
FL2	Reflectance of Wall 2
Lamda	λ , Wavelength
Albedo	σ/β
XM, XXM	Dimensionless Parameter M
XN, XXN	Dimensionless Parameter N
Q, XQ	Dimensionless Parameter Q

```
C       THIS PROGRAM WAS RUN ON OSAGE COMPUTER.
C       THIS CALCULATION IS FOR THE PARAMETERS M,N,Q OF HEAT FLUX
C       IN ISOTHERMAL SCATTERING MEDIUM.
C       GMA ARE THE EIGENVALUES. X ARE THE EIGENVECTORS.
C       W ARE THE WEIGHT FACTORS. U ARE GAUSSIAN COORDINATES.
C       TE IS THE OPTICAL DEPTH.
C       FL1,FL2 ARE THE REFLECTIVITIES OF SURFACE 1,2 RESPECTIVELY.
C       PROGRAM M N Q
        DIMENSION  GMA(6),X(6,6),A(6,6),B(6,6),W(3),U(3),TE(10),
       1FL1(9),FL2(9),SUMLA(6),SUMLB(6),SUMDG(6),SUMEH(6),SUMIDF(6),
       2SUM1(3),SUM2(3),SUM3(3),SUM4(3),Y(3,3),XM(10),XN(10),Q(10)
        READ 1,(W(J),J=1,3),(U(J),J=1,3)
      1 FORMAT(3E12.6)
        READ 77,(TE(KK),KK=1,10)
     77 FORMAT(5F4.1)
        READ 2,(FL1(LL),LL=1,9),(FL2(LL),LL=1,9)
      2 FORMAT(9F5.1)
     99 READ 3, LAMDA
      3 FORMAT(I3)
        READ 4, ALBEDO
      4 FORMAT(F5.3)
        READ 66,(GMA(J),J=1,6),((X(I,J),J=1,6),I=1,6)
     66 FORMAT(6E12.6)
        LL=0
      5 LL=LL+1
        DO 6 J=1,6
        SUM1(J)=0.
        DO 6 I=1,3
      6 SUM1(J)=SUM1(J)+W(I)*U(I)*X(3+I,J)
        DO 71 J=1,6
        DO 71 I=1,3
     71 A(I,J)=X(I,J)-2.*FL1(LL)*SUM1(J)
        KK=0
      7 KK=KK+1
        DO 8 J=1,6
```

```
      SUM2(J)=0.
      DO 8 I=1,3
    8 SUM2(J)=SUM2(J)+W(I)*U(I)*X(I,J)*EXPF(GAM(J)*TE(KK))
      DO 73 J=1,6
      DO 73 I=1,3
   73 A(3+I,J)=X(3+I,J)*EXPF(GMA(J)*TE(KK))-2.*FL2(LL)*SUM2(J)
      DO 9 I=1,6
      DO 9 J=1,6
    9 B(I,J)=A(I,J)
      CALL INVERT(B,6)
      DO 11 I=1,6
      SUMLA(I)=0.
      DO 11 K=1,3
   11 SUMLA(I)=SUMLA(I)+B(I,K)
      DO 12 I=1,6
      SUMLB(I)=0.
      DO 12 K=4,6
   12 SUMLB(I)=SUMLB(I)+B(I,K)
      DO 100 I=1,6
      SUMDG(I)=0.
      DO 100 K=1,6
  100 SUMDG(I)=SUMDG(I)+SUMLA(K)*X(I,K)
      DO 101 I=1,6
      SUMEH(I)=0.
      DO 101 K=1,6
  101 SUMEH(I)=SUMEH(I)+SUMLB(K)*X(I,K)
      SUMM=0.
      DO 67 J=1,3
   67 SUMM=SUMM+W(J)*U(J)*(1.-FL1(LL))*(SUMDG(J)-SUMDG(J+3))
      XM(KK)=6.2832*SUMM
      SUMN=0.
      DO 23 J=1,3
   23 SUMN=SUMN+W(J)*U(J)*(1.-FL2(LL))*(SUMEH(J)-SUMEH(J+3))
      XN(KK)=-6.2832*SUMN
      Q(KK)=XM(KK)-XN(KK)
```

```
   33 IF(KK-10)7,31,31
   31 PRINT 555
  555 FORMAT(19X,44HRADIANT HEAT TRANSFER BETWEEN PARALLEL WALLS//////)
      PRINT 37, LAMDA
   37 FORMAT(6X,27HALUMINUM ---- WAVE LENGTH =,F5.1,7H MICRON//)
      PRINT 38, ALBEDO
   38 FORMAT(6X,27HTHE ALBEDO ---- SIGMA/BETA =,F5.3//)
      PRINT 25, FL1(LL)
   25 FORMAT(6X,24HREFLECTIVITY OF WALL 1 =,F3.1//)
      PRINT 96, FL2(LL)
   96 FORMAT(6X,24HREFLECTIVITY OF WALL 2 =,F3.1/////)
      PRINT 27
   27 FORMAT(6X,7HOPTICAL,/6X,7HSPACING,14X,1HM,18X,1HN,19X,1HQ//)
   34 DO 28 KK=1,10
   28 PRINT 29,TE(KK),XM(KK),XN(KK),Q(KK)
   29 FORMAT(6X,F4.1,3F20.4/)
C     THIS IS THE M N Q PRORAM FOR INFINITIVE OPTICAL SPACING.
      DO 404 J=1,3
      SUM3(J)=0.
      DO 403 I=1,3
  403 SUM3(J)=SUM3(J)+W(I)*U(I)*X(3+I,J)
      DO 404 I=1,3
  404 Y(I,J)=X(I,J)-2.*FL1(LL)*SUM3(J)
      CALL INVERT(Y,3)
      DO 407 I=1,3
      SUM4(I)=0.
      DO 407 J=1,3
  407 SUM4(I)=SUM4(I)+Y(I,J)
      DO 408 I=1,6
      SUMIDF(I)=0.
      DO 408 J=1,3
  408 SUMIDF(I)=SUMIDF(I)+SUM4(J)*X(I,J)
      SUMIFM=0.
     DO 412 I=1,3
  412 SUMIFM=SUMIFM+W(I)*U(I)*(1.-FL1(LL))*(SUMIDF(I)-SUMIDF(I+3))
```

```
      XXM=6.2832*SUMIFM
      XXN=0.
      XQ=XXM
      PRINT 413, XXM,XXN,XQ
  413 FORMAT(6X,4HIFNT, 3F20.4/)
      IF(LL-9)5,32,32
   32 GO TO 99
   30 STOP
      END
```

APPENDIX D

PROGRAM FOR EQUATION (41)

EAS MEDIA

WALL REFLECTIVITY = 0.5

RESULTS

Program Symbol	Meaning
C	Constant
AJ	A_j (page 19)
SPCG	Optical Spacing
T	Temperature
RHOA	Density of the Medium
RHO	Density of the Particle
DIA	Diameter of particle in Micron
EPS	ε, Pre-determined Accuracy
VEL	Free Stream Velocity
DSTY	Density
CP	C_p, Specific Heat
XK	Conductivity
REF	Reflectance, of the Wall
XNU	Viscosity
XD, XXD	Distance from leading edge of Plate
ALPHA	Particle Parameter
TKE	K^e, Mass Distinction Coefficient
XM, XXM	Dimensionless Parameter M
XN, XXN	Dimensionless Parameter N
XQ, XXQ	Dimensionless Parameter Q
QNETR	Radiative Heat Flux
XQNETR, RAD	Radiative Heat Flux of Wall 1
XXQNTR	Radiative Heat Flux of Wall 2
QNETCD, CON	Conductive Heat Flux at the Wall

```
C      THIS IS THE BOUNDARY LAYER THICKNESS ITERATION CALCULATION
C      M,N,Q VALUES ARE COMPUTED FROM THE EQUATION FITTED BY
C      ORNOR CURVE FITTING PROGRAM.
C      THIS PROGRAM IS FOR WALL REFLECTIVITY = 0.5.
       DIMENSION ALPHA(3,5),C(5),TKE(3,5),BETA(5),TE(6,10),FX(6),XM(3,5),
      1XN(3,5),XQ(3,5),XXM(3,5),XXN(3,5),XXQ(3,5),AJ(5),SPCG(3),
      2XQNETR(3),XXQNTR(3),QNETC(3),QNETR(3),T(5),D(15),DELT(15),
      3XXD(15),RATIO(15),RAD(15),COND(15),QNETCD(3),ADD(15),ADDA(15)
       READ(1,98)(C(J), J=1,5)
    98 FORMAT(5E12.6)
    97 FORMAT(5F12.5)
       READ(1,97)(AJ(J),J=1,5)
       READ(1,97)(SPCG(I),I=1,3)
    99 READ(1,97)(T(L),L=1,3)
       READ(1,97)RHOA,RHO,DIA,EPS,VEL
       READ(1,97)DSTY,CP,XK,REF
       READ(1,98)XNU
       FCL=7.0
       I=0
       XD=0.
   888 XD=XD+.1
       RE=SQRT(VEL*XD*DSTY/XNU)
       DEL=5.*XD/RE
       I=I+1
       XXD(I)=XD
       D(I)=DEL
   666 IF(I-1)124,124,125
   124 SPCG(1)=D(I)
       GO TO 126
   125 SPCG(1)=DELT(I-1)
   126 SPCG(2)=FCL*D(I)
       SPCG(3)=(SPCG(1)+SPCG(2))/2.
   887 DO 605 M=1,3
       L=0
   999 L=L+1
       DO 1000 J=1,5
```

```
1000 ALPHA(L,J)=C(J)*DIA*T(L)
     DO 150 J=1,5
     IF(ALPHA(L,J)-5.999)110,110,140
 110 TKE(L,J)=-.05245204507+4.917661615*ALPHA(L,J)
    1-2.909426676*ALPHA(L,J)*ALPHA(L,J)+.7760694133*ALPHA(L,J)
    2*ALPHA(L,J)*ALPHA(L,J)-.09776202625*ALPHA(L,J)*ALPHA(L,J)
    3*ALPHA(L,J)*ALPHA(L,J)+.004731505485*ALPHA(L,J)*ALPHA(L,J)
    4*ALPHA(L,J)*ALPHA(L,J)*ALPHA(L,J)
     GO TO 150
 140 TKE(L,J)=2.44
 150 CONTINUE
     DO 160 J=1,5
 160 TE(L,J)=RHOA*SPCG(M)*(457200./DIA/RHO)*TKE(L,J)
     KK=0
   7 KK=KK+1
     IF(TE(L,KK)-2.)200,200,201
 200 XM(L,KK)=1.564164332-.137654*TE(L,KK)+.0828503893
    1*TE(L,KK)*TE(L,KK)-.02014180485*TE(L,KK)*TE(L,KK)*TE(L,KK)
    2+.001692504166*TE(L,KK)*TE(L,KK)*TE(L,KK)*TE(L,KK)
     XXM(L,KK)=1.663934828+2.086270658*TE(L,KK)-1.263094039*
    1TE(L,KK)*TE(L,KK)+.3079682682*TE(L,KK)*TE(L,KK)*TE(L,KK)
    2-.0259186626*TE(L,KK)*TE(L,KK)*TE(L,KK)*TE(L,KK)
     GO TO 170
 201 XM(L,KK)=1.4865
     XXM(L,KK)=2.8262
 170 XN(L,KK)=EXP(.353326-1.097372*TE(L,KK))
     XQ(L,KK)=XM(L,KK)-XN(L,KK)
     XXN(L,KK)=XN(L,KK)
     XXQ(L,KK)=XXM(L,KK)-XXN(L,KK)
     IF(KK-5)7,31,31
  31 IF(L-3)999,32,32
  32 SUMAM=0.
     DO 600 J=1,5
 600 SUMAM=SUMAM+AJ(J)*XM(1,J)
     SUMAN=0.
     DO 601 J=1,5
```

```
601 SUMAN=SUMAN+AJ(J)*XN(2,J)
    SUMAQ=0.
    DO 602 J=1,5
602 SUMAQ=SUMAQ+AJ(J)*XQ(3,J)
    XQNETR(M)=1.0E-11*((T(1)*T(1)*T(1)*T(1)*SUMAM)-(T(2)*T(2)*
   1T(2)*T(2)*SUMAN)-(T(3)*T(3)*T(3)*T(3)*SUMAQ))
    XSUMAM=0.
    DO 700 J=1,5
700 XSUMAM=XSUMAM+AJ(J)*XXM(2,J)
    XSUMAN=0.
    DO 701 J=1,5
701 XSUMAN=XSUMAN+AJ(J)*XXN(1,J)
    XSUMAQ=0.
    DO 702 J=1,5
702 XSUMAQ=XSUMAQ+AJ(J)*XXQ(3,J)
    XXQNTR(M)=1.0E-11*((T(2)*T(2)*T(2)*T(2)*XSUMAM)-(T(1)*T(1)*
   1T(1)*T(1)*XSUMAN)-(T(3)*T(3)*T(3)*T(3)*XSUMAQ))
    QNETR(M)=XQNETR(M)+XXQNTR(M)
    IF(I-1)779,779,778
779 QNETCD(M)=1.5*(T(1)-T(2))*XK/SPCG(M)
    QNETC(M)=36000.*DSTY*CP*VEL*(T(1)-T(2))*(.375*(SPCG(M)-DEL)+
   1.15*DEL*DEL/SPCG(M)-3./280.*DEL*DEL*DEL*DEL/(SPCG(M)*SPCG(M)*
   2SPCG(M)))
    GO TO 776
778 QNETCD(M)=3.*XK*(T(1)-T(2))/(SPCG(M)+DELT(I-1))
    QNETC(M)=36000.*DSTY*CP*VEL*(T(1)-T(2))*(.375*(SPCG(M)-D(I)
   1-DELT(I-1)+D(I-1))+.15*(D(I)*D(I)/SPCG(M)-D(I-1)*D(I-1)/DELT(I-1))
   2-3./280.*(D(I)*D(I)*D(I)*D(I)/(SPCG(M)*SPCG(M)*SPCG(M))-
   3D(I-1)*D(I-1)*D(I-1)*D(I-1)/(DELT(I-1)*DELT(I-1)*DELT(I-1))))
776 FX(M)=QNETC(M)-QNETR(M)-QNETCD(M)
605 CONTINUE
    IF(FX(1)*FX(2))611,111,111
111 FCL=FCL-.1
    SPCG(M)=D(I)
    SPCG(2)=FCL*D(I)
    SPCG(3)=(SPCG(1)+SPCG(2))/2.0
```

```
      GO TO 887
  611 IF(FX(3))606,30,607
  606 IF(FX(3)+EPS)608,30,30
  607 IF(FX(3)-EPS)30,30,608
  608 IF(FX(3)*FX(1))609,30,610
  609 SPCG(2)=SPCG(3)
      FX(2)=FX(3)
      SPCG(3)=(SPCG(1)+SPCG(2))/2.0
      GO TO 887
  610 SPCG(1)=SPCG(3)
      FX(1)=FX(3)
      SPCG(3)=(SPCG(1)+SPCG(2))/2.0
      GO TO 887
   30 RATIO(I)=XQNETR(3)/QNETCD(3)
      RAD(I)=XQNETR(3)
      COND(I)=QNETCD(3)
      DELT(I)=SPCG(3)
      ADD(I)=RAD(I)+COND(I)
      ADDA(I)=ADD(I)/3600.
      IF(XD-1.4999)889,997,997
  889 SPCG(1)=SPCG(3)
      SPCG(2)=7.*D(I)
      SPCG(3)=(SPCG(1)+SPCG(2))/2.0
      GO TO 888
  997 WRITE(3,613)T(1),T(2),RHOA
      WRITE(2,613)T(1),T(2),RHOA
  613 FORMAT(1H1,//////12X,18HWALL TEMPERATURE =,F10.1,1X,1HR,//
     112X,25HFREE STREAM TEMPERATURE =,F7.1,1X,1HR,//12X,
     231HREFLECTIVITY OF THE WALL =  0.5//12X,
     334HAPPARENT DENSITY OF THE PARTICLE =,F5.2//////13X,1HX,6X,
     48HRAD.HEAT,5X,8HCON.HEAT,5X,8HRAD/CON.,4X,4HVBLT,5X,4HTBLT/
     524X,13HBTU/SQ.FT.HR.,22X,3HFT.6X,3HFT.//)
      DO 614 I=1,15
      WRITE(2,615)XXD(I),RAD(I),COND(I),RATIO(I),D(I),DELT(I)
  614 WRITE(3,615)XXD(I),RAD(I),COND(I),RATIO(I),D(I),DELT(I)
```

```
 615 FORMAT(11X,F4.1,2F13.2,F12.3,2F9.4/)
     WRITE(3,9999)
9999 FORMAT(1H1,//////12X,1HX,29X,15HTOTAL HEAT FLUX///
    130X,13HBTU/SQ.FT.HR.,11X,14HBTU/SQ.FT.SEC.//)
     DO 616 I=1,15
 616 WRITE(3,617)XXD(I),ADD(I),ADDA(I)
 617 FORMAT(10X,F4.1,F25.1,F25.3/)
     GO TO 99
 998 STOP
     END
```

WALL TEMPERATURE = 1000.0 R

FREE STREAM TEMPERATURE = 500.0 R

REFLECTIVITY OF THE WALL = 0.5

APPARENT DENSITY OF THE PARTICLE = 0.10

X	RAD.HEAT	CON.HEAT	RAD/CON.	VBLT	TBLT
	BTU/SQ.FT.HR.			FT.	FT.
0.1	759.94	21035.05	0.036	0.0007	0.0007
0.2	749.65	16188.84	0.046	0.0010	0.0011
0.3	742.48	11576.58	0.064	0.0012	0.0015
0.4	736.74	9490.60	0.078	0.0014	0.0017
0.5	731.91	8235.05	0.089	0.0016	0.0019
0.6	727.66	7373.54	0.099	0.0018	0.0021
0.7	723.89	6735.37	0.107	0.0019	0.0023
0.8	720.45	6238.31	0.115	0.0020	0.0025
0.9	717.30	5836.14	0.123	0.0022	0.0027
1.0	714.38	5502.59	0.130	0.0023	0.0028
1.1	711.66	5220.02	0.136	0.0024	0.0029
1.2	709.11	4976.84	0.142	0.0025	0.0031
1.3	706.68	4763.54	0.148	0.0026	0.0032
1.4	704.39	4574.72	0.154	0.0027	0.0033
1.5	702.25	4408.13	0.159	0.0028	0.0035

WALL TEMPERATURE = 2000.0 R

FREE STREAM TEMPERATURE = 500.0 R

REFLECTIVITY OF THE WALL = 0.5

APPARENT DENSITY OF THE PARTICLE = 0.10

X	RAD.HEAT	CON.HEAT	RAD/CON.	VBLT	TBLT
	BTU/SQ.FT.HR.			FT.	FT.
0.1	13050.82	70109.94	0.186	0.0009	0.0010
0.2	12872.46	53821.97	0.239	0.0013	0.0016
0.3	12750.95	38368.67	0.332	0.0016	0.0020
0.4	12655.15	31372.13	0.403	0.0018	0.0023
0.5	12574.98	27137.91	0.463	0.0021	0.0027
0.6	12505.62	24223.04	0.516	0.0023	0.0029
0.7	12444.22	22058.97	0.564	0.0024	0.0032
0.8	12389.26	20373.05	0.608	0.0026	0.0035
0.9	12339.14	19010.43	0.649	0.0028	0.0037
1.0	12293.24	17878.26	0.688	0.0029	0.0039
1.1	12250.77	16918.86	0.724	0.0031	0.0041
1.2	12211.19	16090.41	0.759	0.0032	0.0043
1.3	12174.29	15366.50	0.792	0.0033	0.0045
1.4	12139.56	14726.79	0.824	0.0035	0.0047
1.5	12106.93	14156.04	0.855	0.0036	0.0049

WALL TEMPERATURE = 4000.0 R

FREE STREAM TEMPERATURE = 500.0 R

REFLECTIVITY OF THE WALL = 0.5

APPARENT DENSITY OF THE PARTICLE = 0.10

X	RAD.HEAT	CON.HEAT	RAD/CON.	VBLT	TBLT
	BTU/SQ.FT.HR.			FT.	FT.
0.1	209934.69	176923.81	1.187	0.0012	0.0013
0.2	206698.69	133732.88	1.546	0.0016	0.0022
0.3	204427.81	93068.88	2.197	0.0020	0.0029
0.4	202605.25	74262.19	2.728	0.0023	0.0035
0.5	201063.50	62763.44	3.204	0.0026	0.0041
0.6	199721.88	54793.64	3.645	0.0028	0.0046
0.7	198533.25	48847.27	4.064	0.0031	0.0051
0.8	197469.00	44190.25	4.469	0.0033	0.0056
0.9	196509.88	40417.78	4.862	0.0035	0.0061
1.0	195641.69	37284.41	5.247	0.0037	0.0066
1.1	194853.50	34630.10	5.627	0.0039	0.0071
1.2	194136.94	32346.24	6.002	0.0040	0.0076
1.3	193484.50	30355.70	6.374	0.0042	0.0081
1.4	192891.19	28602.75	6.744	0.0044	0.0086
1.5	192351.56	27045.44	7.112	0.0045	0.0090

WALL TEMPERATURE = 3000.0 R

FREE STREAM TEMPERATURE = 500.0 R

REFLECTIVITY OF THE WALL = 0.5

APPARENT DENSITY OF THE PARTICLE = 0.10

X	RAD.HEAT	CON.HEAT	RAD/CON.	VBLT	TBLT
	BTU/SQ.FT.HR.			FT.	FT.
0.1	66401.56	123848.38	0.536	0.0011	0.0012
0.2	65452.77	94563.69	0.692	0.0015	0.0019
0.3	64803.02	66853.13	0.969	0.0018	0.0024
0.4	64289.73	54209.15	1.186	0.0021	0.0029
0.5	63859.55	46524.32	1.373	0.0024	0.0033
0.6	63486.83	41213.16	1.540	0.0026	0.0037
0.7	63156.46	37254.23	1.695	0.0028	0.0040
0.8	62860.20	34155.75	1.840	0.0030	0.0044
0.9	62590.90	31644.57	1.978	0.0032	0.0047
1.0	62344.71	29554.78	2.109	0.0033	0.0050
1.1	62117.42	27779.01	2.236	0.0035	0.0053
1.2	61907.23	26245.46	2.359	0.0037	0.0056
1.3	61711.85	24904.70	2.478	0.0038	0.0059
1.4	61529.83	23719.21	2.594	0.0040	0.0062
1.5	61359.66	22661.62	2.708	0.0041	0.0065

WALL TEMPERATURE = 5000.0 R

FREE STREAM TEMPERATURE = 500.0 R

REFLECTIVITY OF THE WALL = 0.5

APPARENT DENSITY OF THE PARTICLE = 0.10

X	RAD.HEAT BTU/SQ.FT.HR.	CON.HEAT BTU/SQ.FT.HR.	RAD/CON.	VBLT FT.	TBLT FT.
0.1	511828.94	224505.19	2.280	0.0012	0.0016
0.2	502964.31	166890.31	3.014	0.0018	0.0026
0.3	496509.63	113210.81	4.386	0.0022	0.0035
0.4	491246.38	88043.44	5.580	0.0025	0.0044
0.5	486784.75	72636.19	6.702	0.0028	0.0052
0.6	482940.38	61994.77	7.790	0.0031	0.0060
0.7	479610.31	54111.32	8.863	0.0033	0.0069
0.8	476724.31	47995.55	9.933	0.0035	0.0077
0.9	474233.13	43094.09	11.005	0.0037	0.0085
1.0	472093.94	39068.86	12.084	0.0039	0.0093
1.1	470272.63	35700.69	13.173	0.0041	0.0102
1.2	468734.88	32839.37	14.274	0.0043	0.0110
1.3	467450.63	30378.38	15.388	0.0045	0.0119
1.4	466390.13	28240.16	16.515	0.0047	0.0128
1.5	465524.31	26365.66	17.656	0.0048	0.0137

WALL TEMPERATURE = 500.0 R

FREE STREAM TEMPERATURE = 1000.0 R

REFLECTIVITY OF THE WALL = 0.5

APPARENT DENSITY OF THE PARTICLE = 0.10

X	RAD.HEAT BTU/SQ.FT.HR.	CON.HEAT	RAD/CON.	VBLT FT.	TBLT FT.
0.1	-699.81	-21125.41	0.033	0.0007	0.0007
0.2	-674.36	-16258.18	0.041	0.0010	0.0011
0.3	-656.89	-11645.22	0.056	0.0012	0.0014
0.4	-643.04	-9574.07	0.067	0.0014	0.0017
0.5	-631.28	-8321.60	0.076	0.0016	0.0019
0.6	-621.11	-7461.34	0.083	0.0018	0.0021
0.7	-612.01	-6825.36	0.090	0.0019	0.0023
0.8	-603.75	-6327.91	0.095	0.0020	0.0025
0.9	-596.22	-5926.29	0.101	0.0022	0.0026
1.0	-589.26	-5593.92	0.105	0.0023	0.0028
1.1	-582.80	-5312.90	0.110	0.0024	0.0029
1.2	-576.77	-5071.53	0.114	0.0025	0.0030
1.3	-571.06	-4860.15	0.117	0.0026	0.0031
1.4	-565.69	-4673.34	0.121	0.0027	0.0033
1.5	-560.53	-4506.36	0.124	0.0028	0.0034

WALL TEMPERATURE = 500.0 R

FREE STREAM TEMPERATURE = 2000.0 R

REFLECTIVITY OF THE WALL = 0.5

APPARENT DENSITY OF THE PARTICLE = 0.10

X	RAD.HEAT	CON.HEAT	RAD/CON.	VBLT	TBLT
	BTU/SQ.FT.HR.			FT.	FT.
0.1	-11220.47	-72201.31	0.155	0.0009	0.0009
0.2	-10533.77	-55877.93	0.189	0.0013	0.0015
0.3	-10084.13	-40368.31	0.250	0.0016	0.0019
0.4	-9742.23	-33488.62	0.291	0.0018	0.0022
0.5	-9464.48	-29385.66	0.322	0.0021	0.0024
0.6	-9229.62	-26587.45	0.347	0.0023	0.0027
0.7	-9028.20	-24533.58	0.368	0.0024	0.0029
0.8	-8850.98	-22950.03	0.386	0.0026	0.0031
0.9	-8693.36	-21680.17	0.401	0.0028	0.0032
1.0	-8552.64	-20638.57	0.414	0.0029	0.0034
1.1	-8425.19	-19766.45	0.426	0.0031	0.0035
1.2	-8309.52	-19023.18	0.437	0.0032	0.0036
1.3	-8203.74	-18381.95	0.446	0.0033	0.0038
1.4	-8106.62	-17822.12	0.455	0.0035	0.0039
1.5	-8016.75	-17328.00	0.463	0.0036	0.0040

WALL TEMPERATURE = 500.0 R

FREE STREAM TEMPERATURE = 3000.0 R

REFLECTIVITY OF THE WALL = 0.5

APPARENT DENSITY OF THE PARTICLE = 0.10

X	RAD.HEAT	CON.HEAT	RAD/CON.	VBLT	TBLT
	BTU/SQ.FT.HR.			FT.	FT.
0.1	-55871.16	-136457.63	0.409	0.0011	0.0011
0.2	-52194.84	-107185.94	0.487	0.0015	0.0016
0.3	-50003.34	-79340.31	0.630	0.0018	0.0020
0.4	-48472.23	-67540.00	0.718	0.0021	0.0023
0.5	-47333.20	-60793.62	0.779	0.0024	0.0025
0.6	-46458.32	-56415.70	0.823	0.0026	0.0026
0.7	-45770.52	-53364.20	0.858	0.0028	0.0028
0.8	-45229.01	-51147.63	0.884	0.0030	0.0029
0.9	-44796.91	-49495.16	0.905	0.0032	0.0029
1.0	-44455.16	-48241.69	0.922	0.0033	0.0030
1.1	-44184.38	-47284.85	0.934	0.0035	0.0031
1.2	-43973.51	-46553.39	0.945	0.0037	0.0031
1.3	-43815.38	-46004.89	0.952	0.0038	0.0031
1.4	-43697.26	-45600.84	0.958	0.0040	0.0032
1.5	-43611.75	-45306.54	0.963	0.0041	0.0032

WALL TEMPERATURE = 500.0 R

FREE STREAM TEMPERATURE = 4000.0 R

REFLECTIVITY OF THE WALL = 0.5

APPARENT DENSITY OF THE PARTICLE = 0.10

X	RAD.HEAT BTU/SQ.FT.HR.	CON.HEAT BTU/SQ.FT.HR.	RAD/CON.	VBLT FT.	TBLT FT.
0.1	-176094.13	-220884.69	0.797	0.0012	0.0011
0.2	-165561.06	-177639.50	0.932	0.0016	0.0016
0.3	-160695.81	-137589.13	1.168	0.0020	0.0019
0.4	-158105.81	-123490.13	1.280	0.0023	0.0020
0.5	-156743.50	-116992.00	1.340	0.0026	0.0021
0.6	-156094.25	-113905.75	1.370	0.0028	0.0021
0.7	-155888.19	-112634.25	1.384	0.0031	0.0021
0.8	-155928.69	-112391.06	1.387	0.0033	0.0021
0.9	-156099.13	-112701.50	1.385	0.0035	0.0021
1.0	-156325.88	-113289.69	1.380	0.0037	0.0021
1.1	-156559.31	-113977.69	1.374	0.0039	0.0021
1.2	-156783.81	-114669.44	1.367	0.0040	0.0021
1.3	-156978.38	-115309.19	1.361	0.0042	0.0021
1.4	-157136.44	-115852.25	1.356	0.0044	0.0020
1.5	-157277.38	-116316.06	1.352	0.0045	0.0020

WALL TEMPERATURE = 500.0 R

FREE STREAM TEMPERATURE = 5000.0 R

REFLECTIVITY OF THE WALL = 0.5

APPARENT DENSITY OF THE PARTICLE = 0.10

X	RAD.HEAT	CON.HEAT	RAD/CON.	VBLT	TBLT
	BTU/SQ.FT.HR.			FT.	FT.
0.1	-432330.19	-340313.31	1.270	0.0012	0.0010
0.2	-412976.69	-286068.69	1.444	0.0018	0.0014
0.3	-408074.38	-238169.63	1.713	0.0022	0.0015
0.4	-407363.25	-229051.38	1.778	0.0025	0.0015
0.5	-407913.81	-228799.31	1.783	0.0028	0.0015
0.6	-408659.19	-230849.38	1.770	0.0031	0.0015
0.7	-409237.44	-232978.38	1.757	0.0033	0.0015
0.8	-409648.25	-234592.75	1.746	0.0035	0.0015
0.9	-409917.75	-235714.81	1.739	0.0037	0.0015
1.0	-410137.44	-236527.50	1.734	0.0039	0.0015
1.1	-410267.13	-237111.00	1.730	0.0041	0.0015
1.2	-410396.44	-237545.25	1.728	0.0043	0.0015
1.3	-410483.88	-237909.88	1.725	0.0045	0.0015
1.4	-410531.69	-238137.69	1.724	0.0047	0.0015
1.5	-410610.94	-238352.19	1.723	0.0048	0.0015

APPENDIX E

PROGRAM FOR EQUATION (41)

NON-SCATTERING MEDIA

WALL REFLECTIVITY = 0.5

```
C      NON-SCATTERING PROGRAM
C      THIS IS THE BOUNDARY LAYER THICKNESS ITERATION CALCULATION
C      M,N,Q VALUES ARE COMPUTED FROM THE EQUATION FITTED BY
C      ORNOR CURVE FITTING PROGRAM.
C      THIS PROGRAM IS FOR WALL REFLECTIVITY = 0.5.
       DIMENSION ALPHA(3,5),C(5),TKE(3,5),BETA(5),TE(6,10),FX(6),XM(3,5),
      1XN(3,5),XQ(3,5),XXM(3,5),XXN(3,5),XXQ(3,5),AJ(5),SPCG(3),
      2XQNETR(3),XXQNTR(3),QNETC(3),QNETR(3),T(5),D(15),DELT(15),
      3XXD(15),RATIO(15),RAD(15),COND(15),QNETCD(3),ADD(15),ADDA(15)
       READ(1,98)(C(J), J=1,5)
    98 FORMAT(5E12.6)
    97 FORMAT(5F12.5)
       READ(1,97)(AJ(J),J=1,5)
       READ(1,97)(SPCG(I),I=1,3)
    99 READ(1,97)(T(L),L=1,3)
       READ(1,97)RHOA,RHO,DIA,EPS,VEL
       READ(1,97)DSTY,CP,XK,REF
       READ(1,98)XNU
       FCL=7.0
       I=0
       XD=0.
   888 XD=XD+.1
       RE=SQRT(VEL*XD*DSTY/XNU)
       DEL=5.*XD/RE
       I=I+1
       XXD(I)=XD
       D(I)=DEL
   887 DO 605 M=1,3
       L=0
   999 L=L+1
       DO 1000 J=1,5
  1000 ALPHA(L,J)=C(J)*DIA*T(L)
       DO 150 J=1,5
       IF(ALPHA(L,J)-5.999)110,110,140
   110 TKE(L,J)=-.05245204507+4.917661615*ALPHA(L,J)
      1-2.909426676*ALPHA(L,J)*ALPHA(L,J)+.7760694133*ALPHA(L,J)
```

```
   2*ALPHA(L,J)*ALPHA(L,J)-.09776202625*ALPHA(L,J)*ALPHA(L,J)
   3*ALPHA(L,J)*ALPHA(L,J)+.004731505485*ALPHA(L,J)*ALPHA(L,J)
   4*ALPHA(L,J)*ALPHA(L,J)*ALPHA(L,J)
    GO TO 150
140 TKE(L,J)=2.44
150 CONTINUE
    DO 160 J=1,5
160 TE(L,J)=RHOA*SPCG(M)*(457200./DIA/RHO)*TKE(L,J)
    KK=0
  7 KK=KK+1
200 XM(L,KK)=1.5708
    IF(TE(L,KK)-5.)201,201,170
201 XN(L,KK)=EXP(.4396745786-1.718898383*TE(L,KK)+.2706370292
   1*TE(L,KK)*TE(L,KK)-.06571344943*TE(L,KK)*TE(L,KK)*TE(L,KK)
   2+.00595999853*TE(L,KK)*TE(L,KK)*TE(L,KK)*TE(L,KK))
    XXM(L,KK)=1.759999704+1.848052789*TE(L,KK)-1.015429689
   1*TE(L,KK)*TE(L,KK)+.2434419505*TE(L,KK)*TE(L,KK)*TE(L,KK)
   2-.02066605507*TE(L,KK)*TE(L,KK)*TE(L,KK)*TE(L,KK)
    GO TO 171
170 XN(L,KK)=0.
    XXM(L,KK)=3.1416
171 XQ(L,KK)=XM(L,KK)-XN(L,KK)
    XXN(L,KK)=XN(L,KK)
    XXQ(L,KK)=XXM(L,KK)-XXN(L,KK)
    IF(KK-5)7,31,31
 31 IF(L-3)999,32,32
 32 SUMAM=0.
    DO 600 J=1,5
600 SUMAM=SUMAM+AJ(J)*XM(1,J)
    SUMAN=0.
    DO 601 J=1,5
601 SUMAN=SUMAN+AJ(J)*XN(2,J)
    SUMAQ=0.
    DO 602 J=1,5
602 SUMAQ=SUMAQ+AJ(J)*XQ(3,J)
    XQNETR(M)=1.0E-11*((T(1)*T(1)*T(1)*T(1)*SUMAM)-(T(2)*T(2)*
```

```
   1T(2)*T(2)*SUMAN)-(T(3)*T(3)*T(3)*T(3)*SUMAQ))
    XSUMAM=0.
    DO 700 J=1,5
700 XSUMAM=XSUMAM+AJ(J)*XXM(2,J)
    XSUMAN=0.
    DO 701 J=1,5
701 XSUMAN=XSUMAN+AJ(J)*XXN(1,J)
    XSUMAQ=0.
    DO 702 J=1,5
702 XSUMAQ=XSUMAQ+AJ(J)*XXQ(3,J)
    XXQNTR(M)=1.0E-11*((T(2)*T(2)*T(2)*T(2)*XSUMAM)-(T(1)*T(1)*
   1T(1)*T(1)*XSUMAN)-(T(3)*T(3)*T(3)*T(3)*XSUMAQ))
    QNETR(M)=XQNETR(M)+XXQNTR(M)
    IF(I-1)779,779,778
779 QNETCD(M)=1.5*(T(1)-T(2))*XK/SPCG(M)
    QNETC(M)=36000.*DSTY*CP*VEL*(T(1)-T(2))*(.375*(SPCG(M)-DEL)+
   1.15*DEL*DEL/SPCG(M)-3./280.*DEL*DEL*DEL*DEL/(SPCG(M)*SPCG(M)*
   2SPCG(M)))
    GO TO 776
778 QNETCD(M)=3.*XK*(T(1)-T(2))/(SPCG(M)+DELT(I-1))
    QNETC(M)=36000.*DSTY*CP*VEL*(T(1)-T(2))*(.375*(SPCG(M)-D(I)
   1-DELT(I-1)+D(I-1))+.15*(D(I)*D(I)/SPCG(M)-D(I-1)*D(I-1)/DELT(I-1))
   2-3./280.*(D(I)*D(I)*D(I)*D(I)/(SPCG(M)*SPCG(M)*SPCG(M))-
   3D(I-1)*D(I-1)*D(I-1)*D(I-1)/(DELT(I-1)*DELT(I-1)*DELT(I-1))))
776 FX(M)=QNETC(M)-QNETR(M)-QNETCD(M)
605 CONTINUE
    IF(FX(1)*FX(2))611,111,111
111 FCL=FCL-.1
    SPCG(M)=D(I)
    SPCG(2)=FCL*D(I)
    SPCG(3)=(SPCG(1)+SPCG(2))/2.0
    GO TO 887
611 IF(FX(3))606,30,607
606 IF(FX(3)+EPS)608,30,30
607 IF(FX(3)-EPS)30,30,608
608 IF(FX(3)*FX(1))609,30,610
```

```
  609 SPCG(2)=SPCG(3)
      FX(2)=FX(3)
      SPCG(3)=(SPCG(1)+SPCG(2))/2.0
      GO TO 887
  610 SPCG(1)=SPCG(3)
      FX(1)=FX(3)
      SPCG(3)=(SPCG(1)+SPCG(2))/2.0
      GO TO 887
   30 RATIO(I)=XQNETR(3)/QNETCD(3)
      RAD(I)=XQNETR(3)
      COND(I)=QNETCD(3)
      DELT(I)=SPCG(3)
      ADD(I)=RAD(I)+COND(I)
      ADDA(I)=ADD(I)/3600.
      IF(XD-1.4999)889,997,997
  889 SPCG(1)=SPCG(3)
      SPCG(2)=7.*D(I)
      SPCG(3)=(SPCG(1)+SPCG(2))/2.0
      GO TO 888
  997 WRITE(3,613)T(1),T(2),RHOA
      WRITE(2,613)T(1),T(2),RHOA
  613 FORMAT(1H1,//////12X,14HNON-SCATTERING//
     112X,18HWALL TEMPERATURE =,F10.1,1X,1HR,//
     212X,25HFREE STREAM TEMPERATURE =,F7.1,1X,1HR,//12X,
     331HREFLECTIVITY OF THE WALL =  0.5//12X,
     434HAPPARENT DENSITY OF THE PARTICLE =,F5.2//////13X,1HX,6X,
     58HRAD.HEAT,5X,8HCON.HEAT,5X,8HRAD/CON.,4X,4HVBLT,5X,4HTBLT/
     624X,13HBTU/SQ.FT.HR.,22X,3HFT.6X,3HFT.//)
      DO 614 I=1,15
      WRITE(2,615)XXD(I),RAD(I),COND(I),RATIO(I),D(I),DELT(I)
  614 WRITE(3,615)XXD(I),RAD(I),COND(I),RATIO(I),D(I),DELT(I)
  615 FORMAT(11X,F4.1,2F13.2,F12.3,2F9.4/)
      WRITE(3,9999)
 9999 FORMAT(1H1,//////12X,1HX,29X,15HTOTAL HEAT FLUX///
     130X,13HBTU/SQ.FT.HR.,11X,14HBTU/SQ.FT.SEC.//)
      DO 616 I=1,15
```

```
616 WRITE(3,617)XXD(I),ADD(I),ADDA(I)
617 FORMAT(10X,F4.1,F25.1,F25.3/)
    GO TO 99
998 STOP
    END
```

APPENDIX F

PROGRAM FOR EQUATION (41)

EAS MEDIA

WALL REFLECTIVITY = 0.1

```
C      THIS IS THE BOUNDARY LAYER THICKNESS ITERATION CALCULATION
C      M,N,Q VALUES ARE COMPUTED FROM THE EQUATION FITTED BY
C      ORNOR CURVE FITTING PROGRAM.
C      THIS PROGRAM IS FOR WALL REFLECTIVITY = 0.1.
       DIMENSION ALPHA(3,5),C(5),TKE(3,5),BETA(5),TE(6,10),FX(6),XM(3,5),
      1XN(3,5),XQ(3,5),XXM(3,5),XXN(3,5),XXQ(3,5),AJ(5),SPCG(3),
      2XQNETR(3),XXQNTR(3),QNETC(3),QNETR(3),T(5),D(15),DELT(15),
      3XXD(15),RATIO(15),RAD(15),COND(15),QNETCD(3),ADD(15),ADDA(15)
       READ(1,98)(C(J), J=1,5)
       READ(1,97)(SPCG(I),I=1,3)
    98 FORMAT(5E12.6)
    97 FORMAT(5F12.5)
       READ(1,97)(AJ(J),J=1,5)
       READ(1,97)(SPCG(I),I=1,3)
    99 READ(1,97)(T(L),L=1,3)
       READ(1,97)RHOA,RHO,DIA,EPS,VEL
       READ(1,97)DSTY,CP,XK,REF
       READ(1,98)XNU
       FCL=7.0
       I=0
       XD=0.
   888 XD=XD+.1
       RE=SQRT(VEL*XD*DSTY/XNU)
       DEL=5.*XD/RE
       I=I+1
       XXD(I)=XD
       D(I)=DEL
   887 DO 605 M=1,3
       L=0
   999 L=L+1
       DO 1000 J=1,5
  1000 ALPHA(L,J)=C(J)*DIA*T(L)
       DO 150 J=1,5
       IF(ALPHA(L,J)-5.999)110,110,140
   110 TKE(L,J)=-.05245204507+4.917661615*ALPHA(L,J)
      1-2.909426676*ALPHA(L,J)*ALPHA(L,J)+.7760694133*ALPHA(L,J)
```

```
   2*ALPHA(L,J)*ALPHA(L,J)-.09776202625*ALPHA(L,J)*ALPHA(L,J)
   3*ALPHA(L,J)*ALPHA(L,J)+.004731505485*ALPHA(L,J)*ALPHA(L,J)
   4*ALPHA(L,J)*ALPHA(L,J)*ALPHA(L,J)
    GO TO 150
140 TKE(L,J)=2.44
150 CONTINUE
    DO 160 J=1,5
160 TE(L,J)=RHOA*SPCG(M)*(457200./DIA/RHO)*TKE(L,J)
    KK=0
  7 KK=KK+1
    IF(TE(L,KK)-2.)200,200,201
200 XM(L,KK)=2.82716292-.8336357822*TE(L,KK)+1.661862051*
   1TE(L,KK)*TE(L,KK)-2.316992595*TE(L,KK)*TE(L,KK)*TE(L,KK)
   2+2.143686456*TE(L,KK)*TE(L,KK)*TE(L,KK)*TE(L,KK)
   3-1.271848788*TE(L,KK)*TE(L,KK)*TE(L,KK)*TE(L,KK)*TE(L,KK)
   4+.4730205502*TE(L,KK)*TE(L,KK)*TE(L,KK)*TE(L,KK)*TE(L,KK)
   5*TE(L,KK)-.1058776539*TE(L,KK)*TE(L,KK)*TE(L,KK)*TE(L,KK)
   6*TE(L,KK)*TE(L,KK)*TE(L,KK)+.01296319017*TE(L,KK)*TE(L,KK)
   7*TE(L,KK)*TE(L,KK)*TE(L,KK)*TE(L,KK)*TE(L,KK)*TE(L,KK)
   8-.0006637004158*TE(L,KK)*TE(L,KK)*TE(L,KK)*TE(L,KK)*TE(L,KK)
   9*TE(L,KK)*TE(L,KK)*TE(L,KK)*TE(L,KK)
    GO TO 170
201 XM(L,KK)=2.5687
170 XN(L,KK)=EXP(.92069-1.10612*TE(L,KK))
    XQ(L,KK)=XM(L,KK)-XN(L,KK)
    XXM(L,KK)=2.8274
    XXN(L,KK)=XN(L,KK)
    XXQ(L,KK)=2.8274-XXN(L,KK)
    IF(KK-5)7,31,31
 31 IF(L-3)999,32,32
 32 SUMAM=0.
    DO 600 J=1,5
600 SUMAM=SUMAM+AJ(J)*XM(1,J)
    SUMAN=0.
    DO 601 J=1,5
601 SUMAN=SUMAN+AJ(J)*XN(2,J)
```

```
      SUMAQ=0.
      DO 602 J=1,5
  602 SUMAQ=SUMAQ+AJ(J)*XQ(3,J)
      XQNETR(M)=1.0E-11*((T(1)*T(1)*T(1)*T(1)*SUMAM)-(T(2)*T(2)*
     1T(2)*T(2)*SUMAN)-(T(3)*T(3)*T(3)*T(3)*SUMAQ))
      XSUMAM=0.
      DO 700 J=1,5
  700 XSUMAM=XSUMAM+AJ(J)*XXM(2,J)
      XSUMAN=0.
      DO 701 J=1,5
  701 XSUMAN=XSUMAN+AJ(J)*XXN(1,J)
      XSUMAQ=0.
      DO 702 J=1,5
  702 XSUMAQ=XSUMAQ+AJ(J)*XXQ(3,J)
      XXQNTR(M)=1.0E-11*((T(2)*T(2)*T(2)*T(2)*XSUMAM)-(T(1)*T(1)*
     1T(1)*T(1)*XSUMAN)-(T(3)*T(3)*T(3)*T(3)*XSUMAQ))
      QNETR(M)=XQNETR(M)+XXQNTR(M)
      IF(I-1)779,779,778
  779 QNETCD(M)=1.5*(T(1)-T(2))*XK/SPCG(M)
      QNETC(M)=36000.*DSTY*CP*VEL*(T(1)-T(2))*(.375*(SPCG(M)-DEL)+
     1.15*DEL*DEL/SPCG(M)-3./280.*DEL*DEL*DEL*DEL/(SPCG(M)*SPCG(M)*
     2SPCG(M)))
      GO TO 776
  778 QNETCD(M)=3.*XK*(T(1)-T(2))/(SPCG(M)+DELT(I-1))
      QNETC(M)=36000.*DSTY*CP*VEL*(T(1)-T(2))*(.375*(SPCG(M)-D(I)
     1-DELT(I-1)+D(I-1))+.15*(D(I)*D(I)/SPCG(M)-D(I-1)*D(I-1)/DELT(I-1))
     2-3./280.*(D(I)*D(I)*D(I)*D(I)/(SPCG(M)*SPCG(M)*SPCG(M))-
     3D(I-1)*D(I-1)*D(I-1)*D(I-1)/(DELT(I-1)*DELT(I-1)*DELT(I-1))))
  776 FX(M)=QNETC(M)-QNETR(M)-QNETCD(M)
  605 CONTINUE
      IF(FX(1)*FX(2))611,111,111
  111 FCL=FCL-.1
      SPCG(M)=D(I)
      SPCG(2)=FCL*D(I)
      SPCG(3)=(SPCG(1)+SPCG(2))/2.0
      GO TO 887
```

```
611 IF(FX(3))606,30,607
606 IF(FX(3)+EPS)608,30,30
607 IF(FX(3)-EPS)30,30,608
608 IF(FX(3)*FX(1))609,30,610
609 SPCG(2)=SPCG(3)
    FX(2)=FX(3)
    SPCG(3)=(SPCG(1)+SPCG(2))/2.0
    GO TO 887
610 SPCG(1)=SPCG(3)
    FX(1)=FX(3)
    SPCG(3)=(SPCG(1)+SPCG(2))/2.0
    GO TO 887
 30 RATIO(I)=XQNETR(3)/QNETCD(3)
    RAD(I)=XQNETR(3)
    COND(I)=QNETCD(3)
    DELT(I)=SPCG(3)
    ADD(I)=RAD(I)+COND(I)
    ADDA(I)=ADD(I)/3600.
    IF(XD-1.4999)889,997,997
889 SPCG(1)=SPCG(3)
    SPCG(2)=7.*D(I)
    SPCG(3)=(SPCG(1D+SPCGU2)D/2C0
    GO TO 888
997 WRITE(3,613)T(1),T(2),RHOA
    WRITE(2,613)T(1),T(2),RHOA
613 FORMAT(1H1,//////12X,18HWALL TEMPERATURE =,F10.1,1X,1HR,//
   112X,25HFREE STREAM TEMPERATURE =,F7.1,1X,1HR,//12X,
   231HREFLECTIVITY OF THE WALL =  0.1//12X,
   334HAPPARENT DENSITY OF THE PARTICLE =,F5.2//////13X,1HX,6X,
   48HRAD.HEAT,5X,8HCON.HEAT,5X,8HRAD/CON.,4X,4HVBLT,5X,4HTBLT/
   524X,13HBTU/SQ.FT.HR.,22X,3HFT.6X,3HFT.//)
    DO 614 I=1,15
    WRITE(2,615)XXD(I),RAD(I),COND(I),RATIO(I),D(I),DELT(I)
614 WRITE(3,615)XXD(I),RAD(I),COND(I),RATIO(I),D(I),DELT(I)
615 FORMAT(11X,F4.1,2F13.2,F12.3,2F9.4/)
    WRITE(3,9999)
```

```
9999 FORMAT(1H1,//////12X,1HX,29X,15HTOTAL HEAT FLUX///
    130X,13HBTU/SQ.FT.HR.,11X,14HBTU/SQ.FT.SEC.//)
     DO 616 I=1,15
 616 WRITE(3,617)XXD(I),ADD(I),ADDA(I)
 617 FORMAT(10X,F4.1,F25.1,F25.3/)
     GO TO 99
 998 STOP
     END
```

APPENDIX G

PROGRAM FOR EQUATION (41).

NON-SCATTERING MEDIA

WALL REFLECTIVITY = 0.1

```
C      NON-SCATTERING PROGRAM
C      THIS IS THE BOUNDARY LAYER THICKNESS ITERATION CALCULATION
C      M,N,Q VALUES ARE COMPUTED FROM THE EQUATION FITTED BY
C      ORNOR CURVE FITTING PROGRAM.
C      THIS PROGRAM IS FOR WALL REFLECTIVITY = 0.1.
       DIMENSION ALPHA(3,5),C(5),TKE(3,5),BETA(5),TE(6,10),FX(6),XM(3,5),
      1XN(3,5),XQ(3,5),XXM(3,5),XXN(3,5),XXQ(3,5),AJ(5),SPCG(3),
      2XQNETR(3),XXQNTR(3),QNETC(3),QNETR(3),T(5),D(15),DELT(15),
      3XXD(15),RATIO(15),RAD(15),COND(15),QNETCD(3),ADD(15),ADDA(15)
       READ(1,98)(C(J), J=1,5)
    98 FORMAT(5E12.6)
    97 FORMAT(5F12.5)
       READ(1,97)(AJ(J),J=1,5)
       READ(1,97)(SPCG(I),I=1,3)
    99 READ(1,97)(T(L),L=1,3)
       READ(1,97)RHOA,RHO,DIA,EPS,VEL
       READ(1,97)DSTY,CP,XK,REF
       READ(1,98)XNU
       FCL=7.0
       I=0
       XD=0.
   888 XD=XD+.1
       RE=SQRT(VEL*XD*DSTY/XNU)
       DEL=5.*XD/RE
       I=I+1
       XXD(I)=XD
       D(I)=DEL
   887 DO 605 M=1,3
       L=0
   999 L=L+1
       DO 1000 J=1,5
  1000 ALPHA(L,J)=C(J)*DIA*T(L)
       DO 150 J=1,5
       IF(ALPHA(L,J)-5.999)110,110,140
   110 TKE(L,J)=-.05245204507+4.917661615*ALPHA(L,J)
      1-2.909426676*ALPHA(L,J)*ALPHA(L,J)+.7760694133*ALPHA(L,J)
```

```
    2*ALPHA(L,J)*ALPHA(L,J)-.09776202625*ALPHA(L,J)*ALPHA(L,J)
    3*ALPHA(L,J)*ALPHA(L,J)+.004731505485*ALPHA(L,J)*ALPHA(L,J)
    4*ALPHA(L,J)*ALPHA(L,J)*ALPHA(L,J)
     GO TO 150
140  TKE(L,J)=2.44
150  CONTINUE
     DO 160 J=1,5
160  TE(L,J)=RHOA*SPCG(M)*(457200./DIA/RHO)*TKE(L,J)
     KK=0
  7  KK=KK+1
200  XM(L,KK)=2.8274
     IF(TE(L,KK)-5.)201,201,170
201  XN(L,KK)=EXP(1.024575454-1.66591357*TE(L,KK)+.1915077488
    1*TE(L,KK)*TE(L,KK)-.03431782127*TE(L,KK)*TE(L,KK)*TE(L,KK)
    2+.00241589551*TE(L,KK)*TE(L,KK)*TE(L,KK)*TE(L,KK))
     XXM(L,KK)=2.849825486+.708873456*TE(L,KK)-.5793956635*TE(L,KK)*
    1TE(L,KK)+.178309771*TE(L,KK)*TE(L,KK)*TE(L,KK)-.0176050074*
    2TE(L,KK)*TE(L,KK)*TE(L,KK)*TE(L,KK)
     GO TO 171
170  XN(L,KK)=0.
     XXM(L,KK)=3.1416
171  XQ(L,KK)=XM(L,KK)-XN(L,KK)
     XXN(L,KK)=XN(L,KK)
     XXQ(L,KK)=XXM(L,KK)-XXN(L,KK)
     IF(KK-5)7,31,31
 31  IF(L-3)999,32,32
 32  SUMAM=0.
     DO 600 J=1,5
600  SUMAM=SUMAM+AJ(J)*XM(1,J)
     SUMAN=0.
     DO 601 J=1,5
601  SUMAN=SUMAN+AJ(J)*XN(2,J)
     SUMAQ=0.
     DO 602 J=1,5
602  SUMAQ=SUMAQ+AJ(J)*XQ(3,J)
     XQNETR(M)=1.0E-11*((T(1)*T(1)*T(1)*T(1)*SUMAM)-(T(2)*T(2)*
```

```
     1T(2)*T(2)*SUMAN)-(T(3)*T(3)*T(3)*T(3)*SUMAQ))
      XSUMAM=0.
      DO 700 J=1,5
  700 XSUMAM=XSUMAM+AJ(J)*XXM(2,J)
      XSUMAN=0.
      DO 701 J=1,5
  701 XSUMAN=XSUMAN+AJ(J)*XXN(1,J)
      XSUMAQ=0.
      DO 702 J=1,5
  702 XSUMAQ=XSUMAQ+AJ(J)*XXQ(3,J)
      XXQNTR(M)=1.0E-11*((T(2)*T(2)*T(2)*T(2)*XSUMAM)-(T(1)*T(1)*
     1T(1)*T(1)*XSUMAN)-(T(3)*T(3)*T(3)*T(3)*XSUMAQ))
      QNETR(M)=XQNETR(M)+XXQNTR(M)
      IF(I-1)779,779,778
  779 QNETCD(M)=1.5*(T(1)-T(2))*XK/SPCG(M)
      QNETC(M)=36000.*DSTY*CP*VEL*(T(1)-T(2))*(.375*(SPCG(M)-DEL)+
     1.15*DEL*DEL/SPCG(M)-3./280.*DEL*DEL*DEL*DEL/(SPCG(M)*SPCG(M)*
     2SPCG(M)))
      GO TO 776
  778 QNETCD(M)=3.*XK*(T(1)-T(2))/(SPCG(M)+DELT(I-1))
      QNETC(M)=36000.*DSTY*CP*VEL*(T(1)-T(2))*(.375*(SPCG(M)-D(I)
     1-DELT(I-1)+D(I-1))+.15*(D(I)*D(I)/SPCG(M)-D(I-1)*D(I-1)/DELT(I-1))
     2-3./280.*(D(I)*D(I)*D(I)*D(I)/(SPCG(M)*SPCG(M)*SPCG(M))-
     3D(I-1)*D(I-1)*D(I-1)*D(I-1)/(DELT(I-1)*DELT(I-1)*DELT(I-1))))
  776 FX(M)=QNETC(M)-QNETR(M)-QNETCD(M)
  605 CONTINUE
      IF(FX(1)*FX(2))611,111,111
  111 FCL=FCL-.1
      SPCG(M)=D(I)
      SPCG(2)=FCL*D(I)
      SPCG(3)=(SPCG(1)+SPCG(2))/2.0
      GO TO 887
  611 IF(FX(3))606,30,607
  606 IF(FX(3)+EPS)608,30,30
  607 IF(FX(3)-EPS)30,30,608
  608 IF(FX(3)*FX(1))609,30,610
```

```
 609 SPCG(2)=SPCG(3)
     FX(2)=FX(3)
     SPCG(3)=(SPCG(1)+SPCG(2))/2.0
     GO TO 887
 610 SPCG(1)=SPCG(3)
     FX(1)=FX(3)
     SPCG(3)=(SPCG(1)+SPCG(2))/2.0
     GO TO 887
  30 RATIO(I)=XQNETR(3)/QNETCD(3)
     RAD(I)=XQNETR(3)
     COND(I)=QNETCD(3)
     DELT(I)=SPCG(3)
     ADD(I)=RAD(I)+COND(I)
     ADDA(I)=ADD(I)/3600.
     IF(XD-1.4999)889,997,997
 889 SPCG(1)=SPCG(3)
     SPCG(2)=7.*D(I)
     SPCG(3)=(SPCG(1)+SPCG(2))/2.0
     GO TO 888
 997 WRITE(3,613)T(1),T(2),RHOA
     WRITE(2,613)T(1),T(2),RHOA
 613 FORMAT(1H1,//////12X,14HNON-SCATTERING//
    112X,18HWALL TEMPERATURE =,F10.1,1X,1HR,//
    212X,25HFREE STREAM TEMPERATURE =,F7.1,1X,1HR,//12X,
    331HREFLECTIVITY OF THE WALL =  0.1//12X,
    434HAPPARENT DENSITY OF THE PARTICLE =,F5.2//////13X,1HX,6X,
    58HRAD.HEAT,5X,8HCON.HEAT,5X,8HRAD/CON.,4X,4HVBLT,5X,4HTBLT/
    624X,13HBTU/SQ.FT.HR.,22X,3HFT.6X,3HFT.//)
     DO 614 I=1,15
     WRITE(2,615)XXD(I),RAD(I),COND(I),RATIO(I),D(I),DELT(I)
 614 WRITE(3,615)XXD(I),RAD(I),COND(I),RATIO(I),D(I),DELT(I)
 615 FORMAT(11X,F4.1,2F13.2,F12.3,2F9.4/)
     WRITE(3,9999)
9999 FORMAT(1H1,//////12X,1HX,29X,15HTOTAL HEAT FLUX///
    130X,13HBTU/SQ.FT.HR.,11X,14HBTU/SQ.FT.SEC.//)
     DO 616 I=1,15
```

```
616 WRITE(3,617)XXD(I),ADD(I),ADDA(I)
617 FORMAT(10X,F4.1,F25.1,F25.3/)
    GO TO 99
998 STOP
    END
```

APPENDIX H

PROGRAM FOR THE EQUATION (46)

```
C      THIS IS THE THERMAL BOUNDARY LAYER THICKNESS
C      ITERATION CALCULATION
       DIMENSION T(5),SPCG(3),QNETC(3),QNETCD(3),XXD(15),
      1D(15),DELT(15),FX(3),COND(15),RATIO(15)
   99 READ(1,98)(T(L),L=1,2)
      READ(1,98)(SPCG(I),I=1,3),EPS,VEL,DSTY,CP,XK
   98 FORMAT(3F20.4)
      READ(1,97)XNU
   97 FORMAT(E12.6)
      WRITE(3,1011)
 1011 FORMAT(1H1//////)
      FCL=7.0
      PR=3600.*XNU*CP/XK
      WRITE(3,1000)PR,DSTY,CP,XK,XNU
 1000 FORMAT(6X,16HPRANDTL NUMBER =,F10.3//6X,9HDENSITY =,F15.4//
     16X,10HSP. HEAT =,F15.4//6X,14HCONDUCTIVITY =,F15.4//
     26X,11HVISCOSITY =,E15.6)
      I=0
      XD=0.
  888 XD=XD+.1
      REY=VEL*XD*DSTY/XNU
      RE=SQRT(REY)
      DEL=5.*XD/RE
      I=I+1
      XXD(I)=XD
      D(I)=DEL
  887 DO 605 M=1,3
      IF(I-1)779,779,778
  779 QNETCD(M)=1.5*(T(1)-T(2))*XK/SPCG(M)
      QNETC(M)=36000.*DSTY*CP*VEL*(T(1)-T(2))*(.375*(SPCG(M)-DEL)+
     1.15*DEL*DEL/SPCG(M)-3./280.*DEL*DEL*DEL*DEL/(SPCG(M)*SPCG(M)*
     2SPCG(M)))
      GO TO 776
  778 QNETCD(M)=3.*XK*(T(1)-T(2))/(SPCG(M)+DELT(I-1))
      QNETC(M)=36000.*DSTY*CP*VEL*(T(1)-T(2))*(.375*(SPCG(M)-D(I)
```

```
     1-DELT(I-1)+D(I-1))+.15*(D(I)*D(I)/SPCG(M)-D(I-1)*D(I-1)/DELT(I-1))
     2-3./280.*(D(I)*D(I)*D(I)*D(I)/(SPCG(M)*SPCG(M)*SPCG(M))-
     3D(I-1)*D(I-1)*D(I-1)*D(I-1)/(DELT(I-1)*DELT(I-1)*DELT(I-1))))
 776 FX(M)=QNETC(M)-QNETCD(M)
 605 CONTINUE
     IF(FX(1)*FX(2))611,111,111
 111 FCL=FCL-.1
     SPCG(1)=DELT(I-1)
     SPCG(2)=FCL*D(I)
     SPCG(3)=(SPCG(1)+SPCG(2))/2.0
     GO TO 887
 611 IF(FX(3))606,30,607
 606 IF(FX(3)+EPS)608,30,30
 607 IF(FX(3)-EPS)30,30,608
 608 IF(FX(3)*FX(1))609,30,610
 609 SPCG(2)=SPCG(3)
     FX(2)=FX(3)
     SPCG(3)=(SPCG(1)+SPCG(2))/2.0
     GO TO 887
 610 SPCG(1)=SPCG(3)
     FX(1)=FX(3)
     SPCG(3)=(SPCG(1)+SPCG(2))/2.0
     GO TO 887
  30 DELT(I)=SPCG(3)
     COND(I)=QNETCD(3)
     RATIO(I)=DELT(I)/D(I)
     IF(XD-1.4999)889,997,997
 889 SPCG(1)=SPCG(3)
     SPCG(2)=7.*D(I)
     SPCG(3)=(SPCG(1)+SPCG(2))/2.0
     GO TO 888
 997 WRITE(3,613)PR,T(1),T(2)
     WRITE(2,613)PR,T(1),T(2)
 613 FORMAT(1H1,//////6X,16HPRANDTL NUMBER =,F10.3//
     16X,18HWALL TEMPERATURE =,F10.1,1X,1HR//
```

```
   26X,25HFREE STREAM TEMPERATURE =,F10.1,1X,1HR//
   3///10X,1HX,11X,8HHT.TRANS,10X,4HVBLT,4X,4HTBLT,3X,
   45HRATIO//21X,13HBTU/SQ.FT.HR.,10X,3HFT.,5X,3HFT.///)
    DO 614 I=1,15
    WRITE(2,615)XXD(I),COND(I),D(I),DELT(I),RATIO(I)
614 WRITE(3,615)XXD(I),COND(I),D(I),DELT(I),RATIO(I)
615 FORMAT(7X,F4.1,6X,F13.2,6X,3F8.4/)
    GO TO 99
998 STOP
    END
```

APPENDIX I

PROGRAM FOR PARAMETERS M, N, AND Q FOR NON SCATTERING MEDIUM

```
C       THE M, N AND Q CALCULATION FOR ZERO SCATTERING CASE.
C       THIS PROGRAM WAS RUN ON OSAGE COMPUTER.
        DIMENSION W(3),U(3),TE(11),XM(11),XN(11),XQ(11),
       1XXM(11),XXN(11),XXQ(11),XL(11),DEN(11)
        READ 1, (W(J), J=1,3)
        READ 1, (U(J), J=1,3)
        READ 1, (TE(KK), KK=1,10)
      1 FORMAT(5F12.6)
     99 READ 2, FL1, FL2
      2 FORMAT(2F5.2)
        DO 97 KK=1,10
        XL(KK)=0.0
        DO 98 J=1,3
     98 XL(KK)=XL(KK)+W(J)*U(J)*EXPF(-TE(KK)/U(J))
        XL(KK)=2.*XL(KK)
        DEN(KK)=1.-FL1*FL2*XL(KK)*XL(KK)
        XM(KK)=3.1416*(1.-FL1)*(1.-FL2*XL(KK)*XL(KK))/DEN(KK)
        XN(KK)=3.1416*XL(KK)*(1.-FL2)*(1.-FL1)/DEN(KK)
        XQ(KK)=XM(KK)-XN(KK)
        XXM(KK)=3.1416*(1.-FL2)*(1.-FL1*XL(KK)*XL(KK))/DEN(KK)
        XXN(KK)=XN(KK)
     97 XXQ(KK)=XXM(KK)-XXN(KK)
        XM(11)=3.1416*(1.-FL1)
        XN(11)=0.
        XQ(11)=XM(11)
        XXM(11)=3.1416*(1.-FL2)
        XXN(11)=0.
        XXQ(11)=XXM(11)
        PRINT 96, FL1, FL2
     96 FORMAT(1H1,//////6X,,15HZERO SCATTER9N7//6X,
       124HREFLECTANCE OF WALL 1  =,F4.1//6X,
       224HREFLECTANCE OF WALL 2  =,F4.1////)
        PRINT 95
     95 FORMAT(6X,7HOPTICAL/6X,7HSPACING,14X,1HM,18X,1HN,19X,1HQ//)
        DO 94 KK=1,11
     94 PRINT 93,TE(KK),XM(KK),XN(KK),XQ(KK)
```

```
93 FORMAT(6X,F4.1,3F20.4/)
   PRINT 96, FL2, FL1
   PRINT 95
   DO 91 KK=1,11
91 PRINT 93, TE(KK),XXM(KK), XXN(KK),XXQ(KK)
   GO TO 99
   STOP
   END
```